学　位　論　文

# Enzymatic Synthesis of Artificial Metallo-DNAs Utilizing Template-independent DNA Polymerases

(鋳型非依存性 DNA ポリメラーゼを活用した金属錯体型人工 DNA の酵素合成)

平成 27 年 12 月博士（理学）申請

東京大学大学院理学系研究科
化学専攻

小　林　輝　樹

# Abstract

## 1. Introduction

DNA molecules self-assemble precisely to form two or three-dimensional structures (e.g. DNA origami, DNA polyhedra) through complementary hydrogen bonding. Consequently, DNA has gained a great interest as one of the promising materials in terms of nanotechnology. Incorporation of metal complex into DNA structures allows for the construction of high-ordered nanostructures that show higher thermal stability. Such artificial metallo-DNAs possess ligand-bearing artificial nucleobases (e.g. hydroxypyridone, **H**), which form metal-mediated base pairs (e.g. **H**–$Cu^{II}$–**H**) in the presence of metal ions (Fig. 1). Due to their unique geometry, dynamics and high thermal stability, metallo-DNAs have recently attracted broad interest as scaffolds to build DNA-based molecular nanomachines and devices.

In this study, I have developed a novel synthetic method of metallo-DNAs using DNA polymerases (Fig. 1). Compared with conventional chemical synthetic methods, enzymatic synthetic methods have characteristics that the reaction proceeds with high efficiency and enzymes undergo post-synthetic, site-selective modification of DNA hybridized structures. Here, among various kinds of polymerases, template-independent DNA polymerases (terminal deoxynucleotidyl transferase, TdT) were chosen. In high contrast to the other polymerases, TdT polymerases can accept unnatural substrates to selectively elongate single-stranded DNAs and thus have been extensively used to incorporate functional building blocks into desired positions of DNA architectures.

To synthesize artificial metallo-DNAs by utilizing TdT polymerase, a hydroxypyridone ligand-bearing artificial nucleotide triphosphates (d**H**TP) was synthesized as a substrate. Subsequently, it was investigated that TdT polymerized d**H**TPs to provide ligand-bearing artificial DNAs and the artificial DNAs formed metallo-DNAs in the presence of $Cu^{II}$ ions. Furthermore, in order to validate the usability of the enzymatic synthesis, post-synthetic and site-selective modification of DNA duplexes was demonstrated.

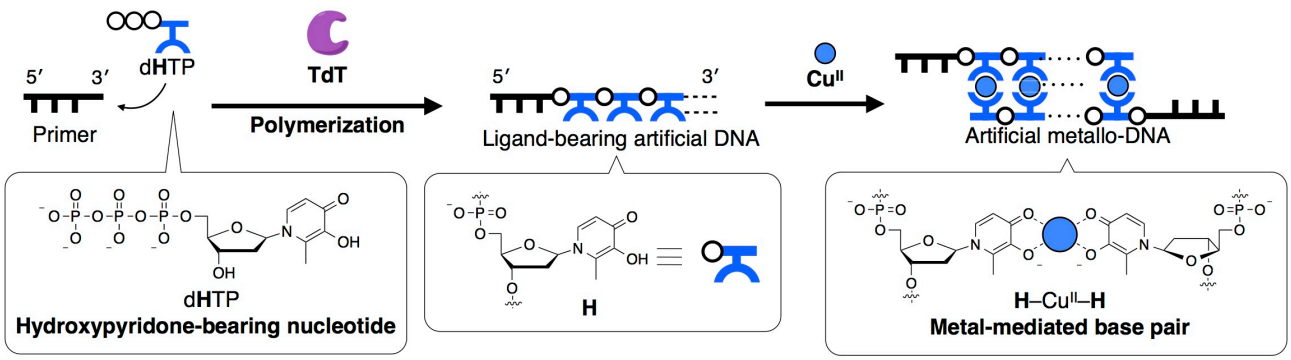


**Fig. 1** Schematic representation for enzymatic synthesis of artificial metallo-DNAs.

## 2. Synthesis of an Enzymatic Substrate (dHTP)

As a substrate for the TdT, the triphosphate derivative of the **H** nucleotide (d**H**TP) was prepared by the conventional Eckstein method for selective 5′-phosphorylation (Scheme 1). DMTr-protected nucleoside **1** was prepared according to the previous report and then benzoylated and detritylated to provide a protected nucleoside **2**. Subsequently, the bis-benzoylated nucleoside **2** was selectively phosphorylated at the 5′-position to yield the desired triphosphate d**H**TP as a triethylammonium salt. Although by-products were generated including a nucleotide monophosphate, they were successfully separated from a desired triphosphate d**H**TP by the

anion-exchange column chromatography. Subsequent reversed-phase HPLC purification afforded d**H**TP that was pure enough for the enzymatic reactions, as characterized by NMR and mass spectrometry (5.3%, 4 steps from **2**).

**Scheme 1** Synthesis of the hydroxypyridone-bearing nucleotide triphosphate (d**H**TP).

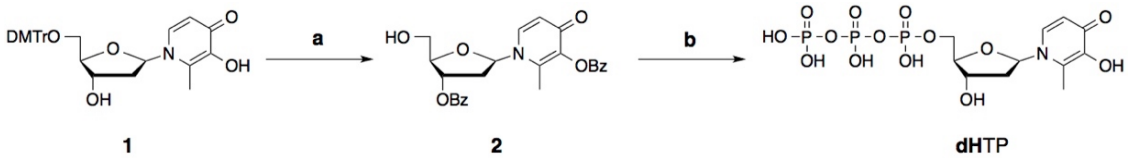


(a) (i) Benzoic anhydride, DMAP, dry pyridine, room temperature; (ii) 2.2% $CCl_3COOH/CH_2Cl_2$, 0 °C; (b) (i) 2-chloro-4*H*-1,3,2-benzodioxaphosphorin-4-one, dioxane, pyridine, room temperature; (ii) bis(tri-*n*-butylammonium)pyrophosphate, *n*-tributylamine in DMF; (iii) 1% $I_2$ in pyridine/$H_2O$; (iv) 1 M NaOH; (v) 0.1 M TEAA buffer (pH 7.0).

## 3. Enzymatic Synthesis of Ligand-bearing Artificial DNAs

Synthesis of ligand-bearing artificial DNAs was investigated with a 6-carboxyfluorescein (FAM) labeled DNA primer (FAM-$dT_{20}$) in the presence of template-independent DNA polymerase (TdT). The primer (5 μM) and **H** nucleotide triphosphate (d**H**TP, 100 μM) were incubated with TdT enzyme (2 U/μM) at 37 °C for 24 h. The resulting products were analyzed by denaturing polyacrylamide gel electrophoresis (PAGE) (Fig. 2). The observed ladder pattern evidenced that TdT enzyme catalyzed the sequential polymerization of d**H**TP, which provided the artificial DNAs tailed with 3–7 **H** nucleotides (5′-FAM-$dT_{20}$-$\mathbf{H}_n$-3′ ($n$ = 3–7)). This result was consistent with the result of MALDI-TOF mass spectmetiric analysis that showed a series of signals with intervals of $m/z$ = 303 which was ascribed as an **H** nucleotide monophosphate ($C_{12}H_{14}NO_7P$).

One of the main products possessing five **H** nucleotides (5′-FAM-$dT_{20}$-$\mathbf{H}_5$-3′, **ODN-1**) was isolated and characterized by MALDI-TOF mass spectrometry. The detected $m/z$ value was 8077.5, which was consistent with the calculated value 8075.4. UV absorption spectral analysis was further conducted as shown in Fig. 3A. The difference spectrum (red line) between **ODN-1** and the primer had an absorption maximum at 282 nm, which was consistent with the spectrum of fivefold **H** nucleoside monomers (blue line, $\lambda_{max}$ = 282 nm). This result confirmed that the **H** nucleotides were polymerized with their ligand moiety intact. Thus, it was concluded that the ligand-bearing artificial DNAs possessing **H** nucleotides were successfully synthesized by TdT polymerase.

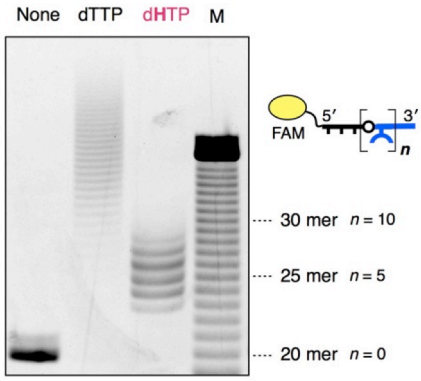


**Fig. 2** Characterization of the reaction products obtained by the TdT-aided extension of a FAM-labeled primer strand using d**H**TP. Denaturing polyacrylamide gel electrophoresis (PAGE) analysis. The bands were detected by FAM fluorescence. [FAM-$dT_{20}$] = 5.0 $\mu$M (primer), [d**H**TP] = 100 $\mu$M, [TdT] = 2 U/$\mu$L in 20 mM Tris-acetate buffer (pH 7.9), 10 mM $Mg(OAc)_2$, 50 mM KOAc, 37 °C, 24 h.

Subsequently, in order to prove metal complexation ability of **ODN-1**, complexation of **ODN-1** with $Cu^{II}$ ions was elucidated by UV absorption spectral analysis. **ODN-1** was combined with $Cu^{II}$ ions (i.e. 0.5 equiv. per **H** nucleotide) in a neutral buffer. As shown in Fig. 3B, a difference spectrum (red line) between the complexation product and the primer was well fitted with a spectrum of the **H**–$Cu^{II}$–**H** complex (blue line, $\lambda_{max}$ = 303 nm). This result confirmed that artificial metallo-DNA duplexes, which have metal-mediated base pairs, was successfully constructed with the enzymatically-synthesized DNA strands in the same manner as conventional chemical DNA synthesis.

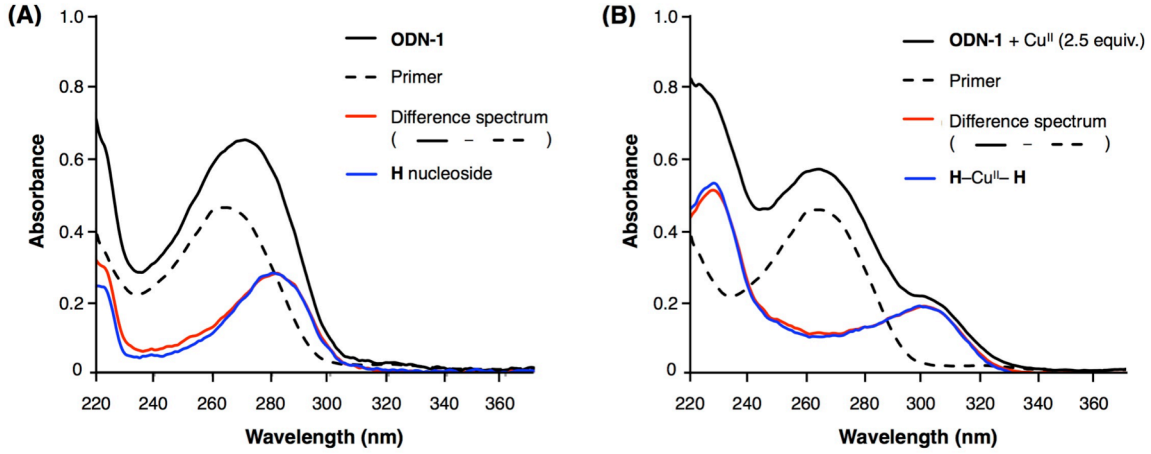


**Fig. 3** UV absorption spectra of the isolated product, 5′-FAM-dT$_{20}$-**H**$_5$-3′ (**ODN-1**) (36 $\mu$M) in the absence **(A)** and presence **(B)** of $Cu^{II}$ ions (90 $\mu$M, 2.5 equiv.) (black solid lines). A spectrum of the primer (36 $\mu$M) (black broken lines), difference spectra (red lines), a spectrum of **H** nucleoside (180 $\mu$M) (A, blue line) and that of **H**–$Cu^{II}$–**H** complex (90 $\mu$M) (B, blue line) are overlaid. In 100 mM HEPES buffer (pH 7.0), 500 mM NaCl, $l$ = 0.1 cm, at room temperature. Concentrations of the DNAs were determined based on the absorbance of the FAM moiety at $\lambda$ = 495 nm.

It was revealed that the enzymatic DNA synthesis stalled when about five **H** nucleotides were incorporated by TdT enzyme. Actually, TdT incorporated neither dTTP nor d**H**TP when **H**-tailed **ODN-1** was used as the primer. This result implied that artificial DNAs possessing several **H** nucleotides have a low affinity to the enzyme and thus did not act as a primer for further elongation. It should be noted that the TdT-catalyzed reaction further proceeded in the presence of the high concentration of DNAs to yield DNA oligomers tailed with about 10 **H** nucleotides. It is most likely that increasing the concentration forced the DNA to bind the enzyme and consequently facilitated the reaction progress. Thus, the limitation in the length of the product was overcome and so the synthesis of much longer ligand-bearing artificial DNAs would be realized by the synthetic method developed here.

## 4. Post-synthetic modification of the DNA duplexes by TdT and metal-mediated assembly of the modified duplexes

One of the practical advantages of the enzymatic reaction is to allow for post-synthetic modification of DNA nanostructures. Consequently, the post-synthetic incorporation of artificial ligand-bearing nucleotides by TdT enzyme would be a powerful tool to construct DNA-based materials with metal-mediated base pairs. Herein, post-synthetic modification of simple DNA duplexes was investigated as a model for DNA-based nanoarchitectures (Fig. 4A).

In the presence of d**H**TP and TdT enzyme, DNA duplex (**ODN-2**·**ODN-3**) with 3′-protruding end was tailed with about five **H** nucleotides in the same manner as single-stranded DNA primer. In contrast, the reaction of 3′-blunt DNA duplex did not proceeded at all. Accordingly, it is expected that the enzymatic DNA synthesis developed here will be usable for site-selective modification of 3′-protruding end of DNA nanostructures.

Subsequently, the metal complexation behavior of **H**-modified duplex was elucidated (Fig. 4A). The modified DNA duplex possessing five **H** nucleotides on average was mixed with $Cu^{II}$ ions (i.e. 0.5 equiv. per **H** nucleotide). The band on the gel image shifted to the position of a higher molecular weight (Fig. 4B, lane 3), which approximately corresponded to twofold molecular weight of the metal-free monomeric duplex. This result indicated that a dimeric complexation structure was constructed by formation of artificial metallo-DNA duplex through metal-mediated **H**–$Cu^{II}$–**H** base pairing. The formation of metallo-DNA duplexes was also confirmed by UV absorption spectroscopy. Furthermore, $Cu^{II}$ titration experiments with PAGE analysis showed that the dimeric structure was formed quantitatively and this structure was stable in the presence of excess amounts of $Cu^{II}$ (i.e. 1.0

equiv. per **H** nucleotide). Subsequent addition of EDTA to remove $Cu^{II}$ ions regenerated the monomeric duplex (lane 4). These results confirmed that the enzymatically modified duplexes can assemble and disassemble in response to addition and removal of $Cu^{II}$.

Taken together, it is expected that the modification method established here will be further applied for the metal-responsive assembly of DNA-based nanomaterials such as DNA origami architectures, DNA-modified proteins and DNA-coated nanoparticles.

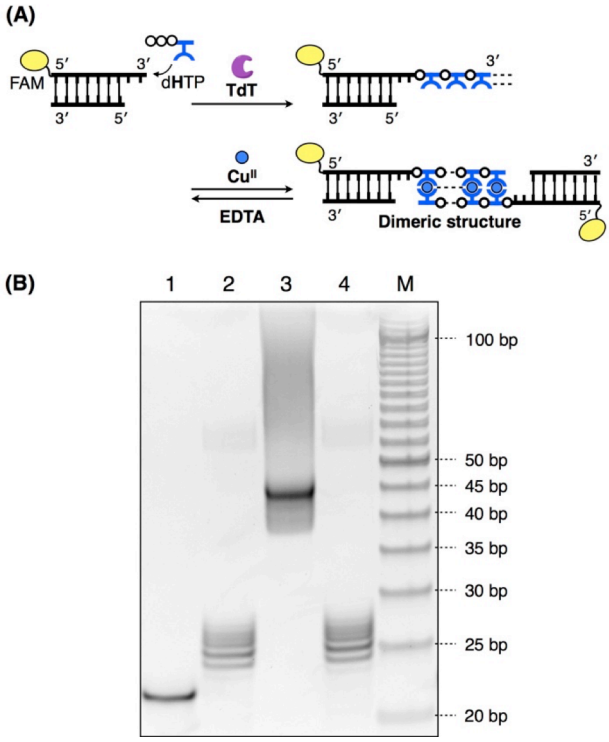


**Fig. 4 (A)** Schematic illustration of enzymatic modification of a DNA duplex and metal-mediated assembly of the duplexes. **(B)** Native PAGE analysis of the resulting structures. (Lane 1) the starting duplex (**ODN-2**·**ODN-3**) (32 $\mu$M), (lane 2) after the enzymatic reaction, (lane 3) after addition of $Cu^{II}$ ions (90 $\mu$M), (lane 4) after subsequent addition of EDTA (1 mM), (M) double-stranded DNA markers. The bands were detected by FAM fluorescence. **ODN-2**: FAM-5′-GAA GGA ACG TAC ACT CGC AGT T-3′ (22 mer), **ODN-3**: 5′-CTG CGA GTG TAC GTT CCT TC-3′ (20 mer). The condition of the enzymatic reaction was the same as that for Fig. 2.

## 4. Conclusion

In this study, a hydroxypyridone ligand-bearing artificial nucleotide triphosphate (d**H**TP) was synthesized as a substrate of TdT polymerase. By chemical and bio-related analytical methods, it was revealed that TdT are useful to sequentially polymerize d**H**TP for synthesis of ligand-bearing artificial DNAs. It was found that ligand moieties of the artificial DNA remained intact. The enzymatically-synthesized DNAs formed **H**–$Cu^{II}$–**H** base pair quantitatively to construct the metallo-DNAs as was the case of chemically synthesized DNA. In addition, the enzymatic DNA synthesis was stalled when about five **H** nucleotides were polymerized, probably because the elongated artificial DNA had a low affinity with the enzyme. It was revealed that further polymerization reaction was facilitated with the high concentration of DNAs by forcing DNAs to bind to the enzyme. Furthermore, in order to reveal the usability of the enzymatic synthesis, post-synthetic and site-selective modification of DNA duplexes was demonstrated. The reaction proceeded only from the 3′-protruding end. Therefore, this strategy can be applied to site-selective modification for the 3′-protruding end on the DNA-based materials. The modified DNA duplex self-assembled in response to formation of complexes with $Cu^{II}$ ions. Consequently, TdT-catalyzed post-synthetic modification would be readily applied for DNA-modified nanomaterials and biomacromolecules. The method established here will allow for the development of DNA-based materials whose structures and functions can be regulated in response to metal coordination.

# Abbreviation

| | | | |
|---|---|---|---|
| Anal. | analysis | Hz | hertz |
| a.u. | arbitrary unit | *i*PrOH | isopropanol |
| AuNP | gold nanoparticle | J | coupling constant |
| bp | base pair | *l* | optical length |
| calcd. | caluclated | M | molar |
| Co | cobalt | M | marker |
| Cu | copper | MALDI | matrix assisted laser desorption/ionization |
| dATP | deoxyadenosine triphosphate | Me | methyl |
| dCTP | deoxycytidine triphosphate | MeCN | acetonitrile |
| dGTP | deoxyguanosine triphosphate | MeOH | methanol |
| d**H** | hydroxypyridone-baring nucleoside | Mg | magnesium |
| d**H**MP | hydroxypyridone-baring nucleotide monophosphate | Mn | manganese |
| d**H**TP | hydroxypyridone-baring nucleotide triphosphate | MOPS | 4-morpholinepropanesulfonic acid |
| dTTP | deoxythymidine triphosphate | MS | mass spectrometry |
| DMF | *N*, *N*-dimethylformamide | *m*/*z* | mass-to-charge ratio |
| DNA | deoxyribonucleic acid | *n*- | normal |
| EDTA | ethylenediaminetetraacetic acid | NMR | nuclear magnetic resonance |
| en | ethylenediamine | P | primer |
| ESI | electron spray ionization | PAGE | polyacrylamide gel electrophoresis |
| Et | ethyl | ppm | parts per million |
| EtOH | ethanol | TdT | terminal deoxynucleotidyl transferase |
| Equiv. | equivalent | Tris | tris(hydroxymethyl)aminomethane |
| FAM | 6-carboxyfluorescein | TMS | tetramethylsilane |
| Fe | iron | TOF | time-of-flight |
| H | hydroxypyridone-baring nucleotide | UV | ultraviolet |
| HEPES | 4-(2-hydroxyethyl)-1-piperazineethanesulfonic acid | Vis | visible |
| HRMS | high resolution mass spectrometry | v/v | volume-to-volume ratio |

# Contents

# Chapter 1

## General Introduction

## 1-1. New era of nanofabrication with DNA molecules

Deoxyribonucleic acid (DNA) is one of the most significant biogenic polymers, which stores genetic information of all living things on the Earth. DNA molecules have been well known to be the blueprint of life, as the accurate and selective DNA-assembly is responsible for recoding genetic codes to make up complicated living-systems. Besides its biological importance, DNA has recently attracted much attention as promising materials for fabricating supramolecular systems with controllable functions on a nanoscale level.

The motivation of my research here is to open the door to a new era of nanofabrication in supramolecular chemistry by utilizing DNA as materials through a bottom-up strategy.

## 1-2. Structure of DNA and DNA self-assembly

DNA is a structurally sophisticated, but quite a simple polymer, which consists of only four kinds of building blocks, nucleotides (Fig. 1-2-1A). Each nucleotide is composed of three primary units: a 2′-deoxyribose, a phosphodiester group and a nucleobase moiety. 2′-Deoxyribose is a five-membered sugar, which is connected with the two neighboring nucleotides through phosphodiester bonds between the 3′ and the 5′-positions. There are four kinds of nucleobases, adenine (A), thymidine (T), guanine (G) and cytosine (C), which are nitrogen heterocycles acting as proton donors and accepters to form hydrogen bonds. Watson-Crick hydrogen-bonded base pairs (i.e. A–T and G–C) have high accuracy and selectivity for their binding partnership (Fig. 1-2-1B). This is essential for sequence-specific self-assembly of DNA strands to form duplexes in nature.

Two single-stranded DNAs hybridize to form a typical right-handed B-DNA duplex in an anti-parallel fashion via hydrogen-bonded base pairing. That is, while one strand is in the 3′ to 5′ direction, the complementary strand is in the 5′ to 3′ direction. In the DNA duplex, the base pairs are stacked with the intervals of 3.4 Å to make up a helical structure. The diameter

of the helix is about 2.4 nm and the helical pitch is 3.4 nm on average that involves 10 base pairs (Fig. 1-2-1A).

These DNA duplexes can form various nano-sized structures when single-stranded DNAs hybridized together based on the design of their sequence. The size and shape of the resulting DNA nanostructures are thus programmable and predictable. From a viewpoint of nanotechnology, DNA is a possible versatile building block to construct functional nanomaterials. Details will be discussed in the next section **1-3**.

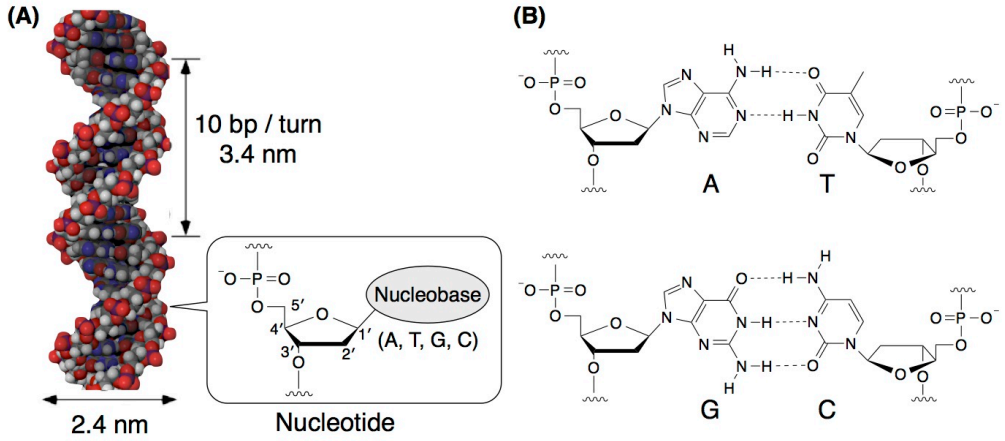


**Fig. 1-2-1** Schematic illustration for structures of **(A)** a DNA duplex and a nucleotide, and **(B)** Watson-Crick hydrogen-bonded base pairs, A-T and G-C.

## 1-3. DNA nanotechnology

"DNA nanotechnology" is an emerging field exponentially developed over the last decade. As described in section **1-2**, due to the programmability and predictability of secondary structures of DNA, deliberate design of DNA sequences promise to make up a bottom-up self-assembly of versatile two- and three-dimensional architectures.

By taking advantage of these natures, DNA molecules can be utilized as promising components (1) to build unique geometric frameworks, (2) to array functional components on the frameworks and (3) to construct nanomachines and nanodevices.

(1) In the 1980s, N. C. Seeman pioneered the nanofabrication of DNA architectures utilizing the sequence-specific DNA self-assembly (Fig. 1-3-1A).[1] Since then, Seeman et al. have designed a variety of DNA sequences to fabricate two- and three-dimensional nanostructures.[2,3] For instance, double crossover DNA motifs (DX motifs) have been widely utilized as one of the significant origins of two-dimensional DNA motifs in DNA nanotechnology (Fig. 1-3-1B).[3]

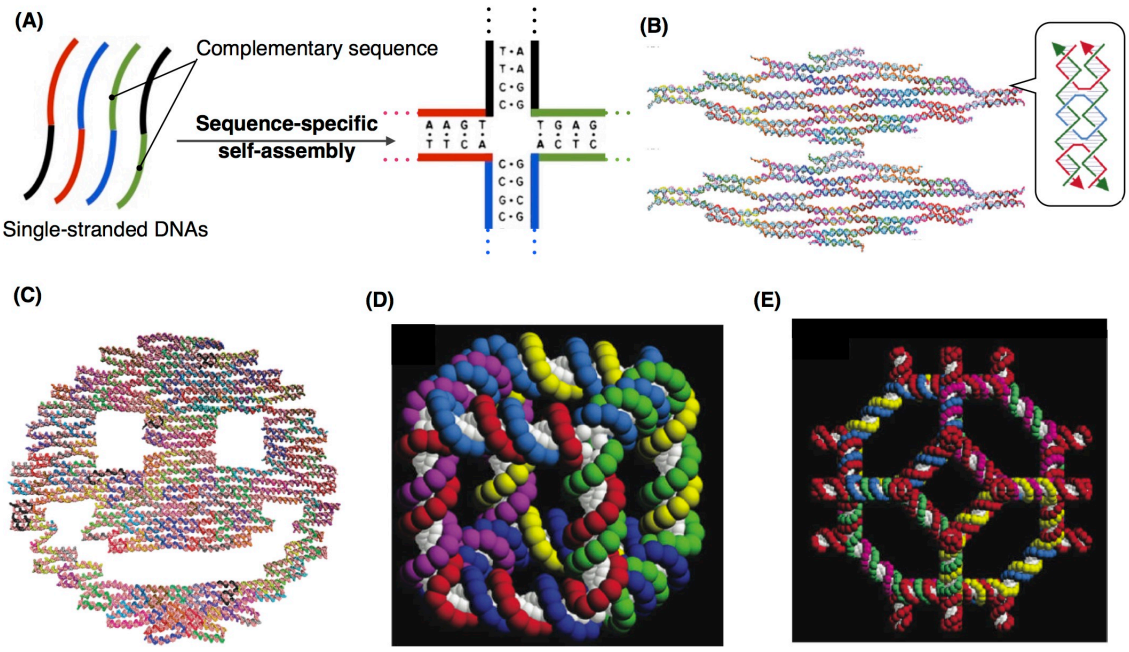


**Fig. 1-3-1**. Schematic representation for **(A)** sequence-specific self-assembly of DNAs (ref. 1), **(B)** double crossover DNA motifs (DX motifs) (ref. 2), **(C)** "smiley face" of DNA origami (ref. 4), **(D)** DNA cube (ref. 5) and **(E)** DNA octahedron (ref. 6). Figure **(A)**, **(D)** and **(E)** are reproduced with permission from ref. 2. Copyright 2010 Annual Reviews.

In 2006, P. W. K. Rothemund established DNA origami, which is one of the distinguished high-dimensional DNA motifs composed of long single-stranded bacteriophage DNAs and various kinds of short staple DNA strands.[4] DNA origami structures show versatile geometries based on the sequences of the staple strands (Fig. 1-3-1C). As shown in Figs. 1-3-1D and E, unique structural motifs such as cube and octahedron have been developed.[5,6]

As described above, the two- and three-dimensional self-assembled structures can be easily constructed in a programmable way.

(2) Recently, DNA nanotechnology has been extensively developed in terms of the size and complexity of the DNA-based nanoarchitectures.[7–9,21] In particular, they have greatly contributed to constructing versatile two- and three-dimensional arrays of functional components such as nanoparticles and biomolecules for functional supramolecular systems (Fig 1-3-2).[10–22]

One typical example is the two- or three-dimensional arrangement of electronic and photonic components for functional metal nanoparticles.[15–21] Fig. 1-3-2A shows DNA-based two-dimensional nanoarrays of gold nanoparticles (AuNPs).[15] 5-nm AuNPs were attached to the edge of a DNA-based triangle structure consisting of DX motifs, and 10-nm AuNPs were embedded on another triangle consisting of different DX motifs. As a result of the self-assembly of DNA triangles, 5- and 10-nm AuNPs were alternately arranged on DX motif scaffolds at regular intervals. A TEM image (Fig. 1-3-2A, gray circle) confirmed that objective two-dimensional arrays of AuNPs were successfully constructed.

Another attention-getting research is the enzyme array, which aimed to observe their reactions at the molecular level and to construct artificial cascade nanoreactors.[16,22] As shown in Fig. 1-3-2B, an artificial multi-enzyme complex has been constructed on DNA scaffolds.[16] in which three components, namely glucose-6-phosphate dehydrogenase (G6pDH), malic dehydrogenase (MDH) and their cofactor $NAD^+$, were conjugated. The activity of the artificial complex was 90-fold higher than the same complex but with freely diffusing $NAD^+$.

The result revealed that the activity depends on the distance between the conjugated components.

Taken together, nanoconjugated DNA scaffolds enable to precisely control the spatial arrangement of functional components within the nanostructures to develop structure-based unique properties.

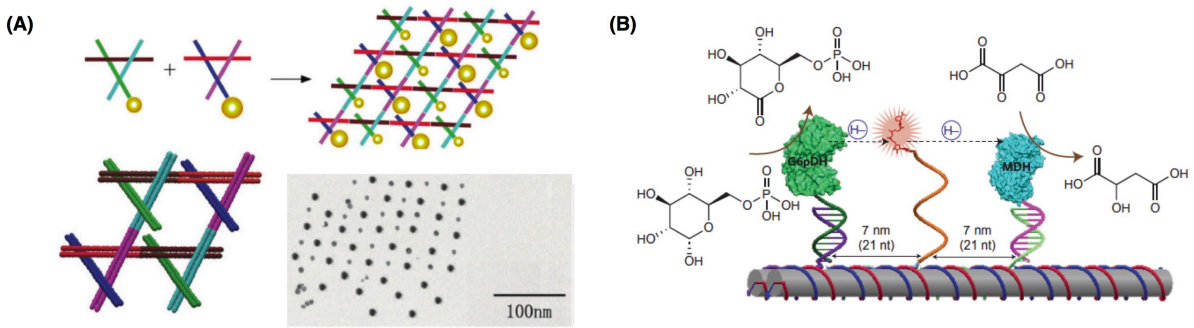


**Fig. 1-3-2**. Schematic representation for arrangement of functional components: **(A)** Two-dimensional nanoarrays of gold nanoparticles on DX motifs (gray circle: TEM image). Reproduced with permission from ref. 3. Copyright 2010 Annual Reviews. **(B)** Construction of an artificial multi-enzyme complex utilizing DNA scaffolds. Reprinted with permission from ref. 16. Copyright 2014 Nature Publishing Group.

(3) Another target of DNA nanotechnology has been to endow the DNA architectures with dynamic properties.[23–30] This molecular system is now called a "DNA machine" or "DNA robot". In this field, strand displacement reaction is often utilized as a driving force of the dynamics, in which pre-hybridized DNA strands are replaced by another DNA strand.

B. Yurke et al. have opened up this field[30] by developing a DNA machine which can reversibly switch between its opened and closed forms. Since then, a great number of DNA machines have been reported. One attractive example is a "DNA walker" (Fig. 1-3-3A). N. A. Pierce et al. reported that a DNA molecule walked on a DNA scaffold by sequence-programmed assembly and disassembly of DNA strands,[27] which took a lead role in the development of other processive movement of DNA-based nanomachines such as a molecular motor and a trailer.[31–34]

The dynamic behaviors were applied to a basket-shaped DNA structure, which enabled encapsulation-release of molecules to delivery drugs and materials (Fig 1-3-3B, C).[35,36] In

2009, E. Andersen et al. demonstrated that a DNA origami-based nanobox was transformed from a closed form to an opened form by the strand displacement mechanism (Fig 1-3-3B).[37] More recently, S. M. Douglas made up a "DNA robot" which was responsible for drug-delivery system to recognize and thereby kill cancer cells (Fig 1-3-3C).[35]

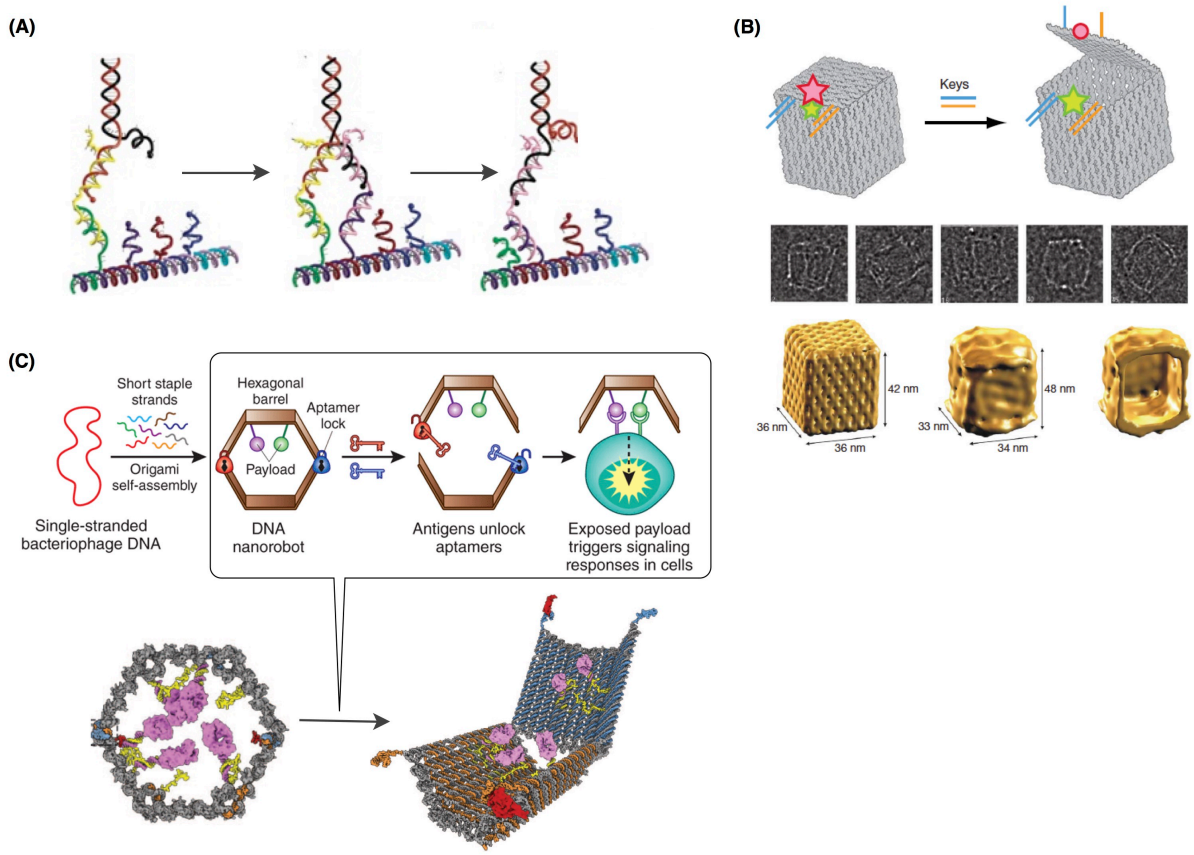


**Fig. 1-3-3**. Schematic representation for **(A)** movement of a "DNA walker". Reproduced with permission from ref. 27. Copyright 2014 American Chemical Society. **(B)** Movement of a "DNA box". Reprinted with permission from ref. 37. Copyright 2009 Nature Publishing Group. **(C)** A "DNA nanorobot" which attacks a cancer cell to induce cell-death by delivered antibodies. Reproduced with permission from ref. 35. Copyright 2012 The American Association for the Advancement of Science.

Moreover, DNA nanostructure have been utilized to construct nanodevices for sensing and even computation,[38–41] although the mechanism is based simply on hydrogen bonding sequence-specific assembly of DNA strands.

Taken together, DNA is considered as a universal attractive molecule to construct functional supramolecular architectures with nanometer-level precision.

## 1-4. Metal-mediated base pairs based self-assembly of DNAs

As hydrogen-bonded base-pairing is a fundamental characteristic of DNA nanoarchitectures, the physicochemical properties of individual DNA molecules are limited to those related to molecular recognition and thermal stability. Noncanonical metal-mediated base pairs have recently attracted broad interest because they append further various functionalities to DNA-based materials.[42] A metal-mediated base pair consists of two ligand-type nucleobases and a central metal ion, which crosslink two DNA strands through metal coordination bonding (Fig. 1-4-1).

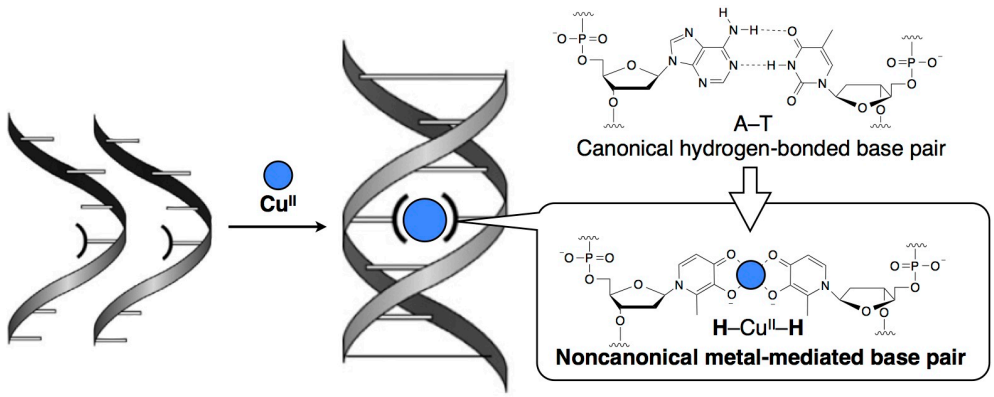


**Fig. 1-4-1** Schematic representation for introduction of a metal-mediated base pair into DNA duplex

Metal-mediated base pairs with natural nucleobases have been extensively explored over the past decades because their preparation is relatively easy compared with artificial base pairs. For instance, a natural thymine (T) base forms an $Hg^{II}$-mediated base pair (T–$Hg^{II}$–T) through a selective binding of an $Hg^{II}$ ion to the N3 atoms.[43,44] A. Ono et al. focused on this unique base pair and reported that $Hg^{II}$ ions drastically stabilize DNA duplex containing T–T mismatch pairs. The formation of T–$Hg^{II}$–T base pairs raised the melting temperature, while a canonical A–T base pairing in the same DNA sequence little stabilized the duplex.[44]

Consequently, the T–$Hg^{II}$–T base pairing has been utilized to hybridize DNA strands to construct stable DNA-based functional systems such as metal ion sensors and molecular machines (Fig. 1-4-2).[42,45,46] As shown in Fig 1-4-2, rotational movement as well as

processive movement have been achieved based on the $Hg^{II}$-mediated assembly and disassembly of DNA strands.

T–$Hg^{II}$–T base pairing is one of the typical metal-mediated base pairs with natural DNA that was applied for DNA nanomachines. However, this base pairing mode cannot be orthogonal to native base-pairing ones, because substitution of hydrogen bonded natural base pairs for metal-coordination bonding breaks the complementarity rule of the canonical base pairing.

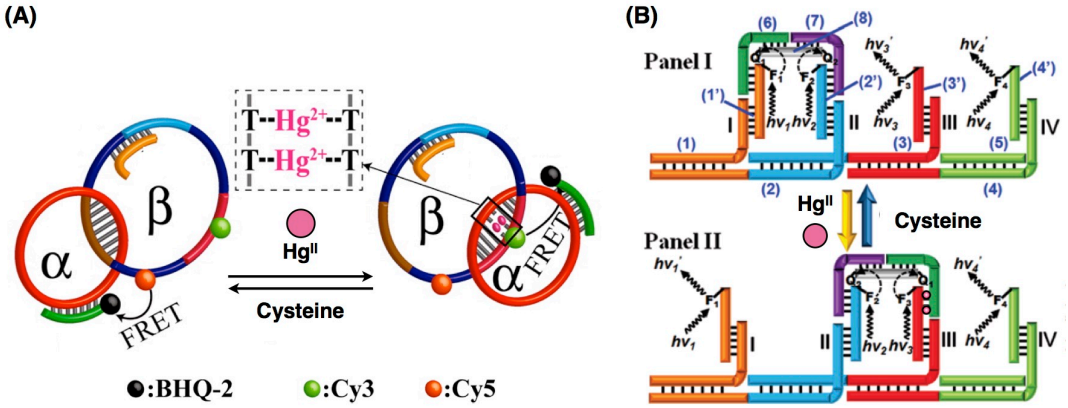


**Fig. 1-4-2** Schematic illustration for molecular systems based on $Hg^{II}$-mediated DNA assembly: **(A)** a molecular machine "DNA rotor". Reproduced with permission from ref. 45a. Copyright 2013 American Chemical Society and **(B)** a molecular machine "DNA walker". Reproduced with permission from ref. 45b. Copyright 2011 American Chemical Society.

Metal-mediated base pairs with unnatural ligand-bearing nucleobases have gained great interest since our first report.[42,47] The first artificial metal-mediated base pair consists of a pair of *o*-phenylendiamine nucleosides and a $Pd^{II}$ ion, which was reported in 1999 by K. Tanaka and M. Shionoya.[47] Since then, various artificial ligand-bearing nucleotides have been established and embedded into DNA sequences by automated DNA chemical synthesizers.

Artificial ligand-type nucleotides form metal-mediated base pairs with various metal ions such as $Cu^{II}$, $Ag^{I}$ and $Gd^{III}$ ions.[42,47-54] Such metal-mediated base pairs have substantial advantages as building blocks of DNA nanoarchitectures because they are fully orthogonal to the natural base paring system and metal complexes exhibit versatile physicochemical properties.

Characteristics of the artificial base pairs are summarized as follows: (1) thermal stabilization of DNA duplexes, (2) introduction of metal-dependent physicochemical properties into DNA and (3) structural control of DNA nanostructures.

A leading example is a $Cu^{II}$-mediated hydroxypyridone base pair (**H**–$Cu^{II}$–**H**, Fig. 1-4-3A ), which is formed through 2:1 complexation of hydroxypyridone-bearing nucleotides (**H**) with a $Cu^{II}$ ion (Fig. 1-4-3A).[49] The **H**–$Cu^{II}$–**H** base pair is formed quantitatively even at a low concentration as low as 50 μM. Moreover, $Cu^{II}$-mediated formation of **H**–$Cu^{II}$–**H** significantly stabilized DNA duplexes containing an **H**–**H** mismatch.[49]

Self-assembly of a given number of $Cu^{II}$ ions in a DNA duplex was successfully achieved.[50] The number of assembled $Cu^{II}$ ions depends on the number of incorporated nucleotides **H** into the DNA strands. DNA strands possessing one to five nucleotides **H** can assemble one to five $Cu^{II}$ ions in the duplexes by the **H**–$Cu^{II}$–**H** formation. The spin-spin interactions[50] and electroconductivity[51] of these $Cu^{II}$-mediated DNA duplexes were also discussed.

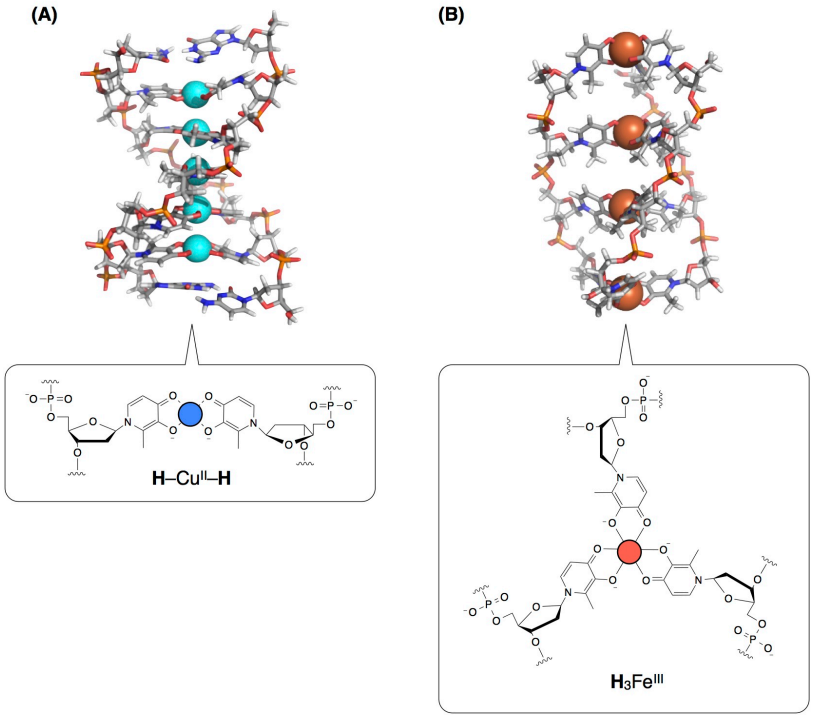


**Fig. 1-4-3** Typical examples of metal-mediated artificial DNAs: **(A)** $Cu^{II}$-mediated duplex. Reprinted with permission from ref. 50. Copyright 2003 The American Association for the Advancement of Science and **(B)** $Fe^{III}$-mediated triplex. Reprinted with permission from ref. 52. Copyright 2009 WILEY-VCH Verlag GmbH & Co. KGaA, Weinheim.

As another structural motif, a DNA triplex was constructed with $\mathbf{H}_3Fe^{III}$ base triplets (Fig. 1-4-3B).[52] Similarly to nucleotides **H**, pyridine-bearing nucleotides (**P**) form not only a linear base pair (**P**–$Ag^I$–**P**) but also a $\mathbf{P}_3Ag^I$ base triplet.[53] Thus, the structural forms of metal-mediated DNA structures can be controlled according to the kinds of metal ions.

One of the distinguished examples of metal-mediated control of DNA self-assembly is the transformation between hairpin structures and duplexes (Fig. 1-4-4). In the absence of transition metal ions, DNA possessing imidazole-bearing nucleotide (**Im**) formed a hairpin structure, while, in the presence of $Ag^I$ ions, metal-mediated base pairs (**Im**–$Ag^I$–**Im**) formed a DNA duplex.[54]

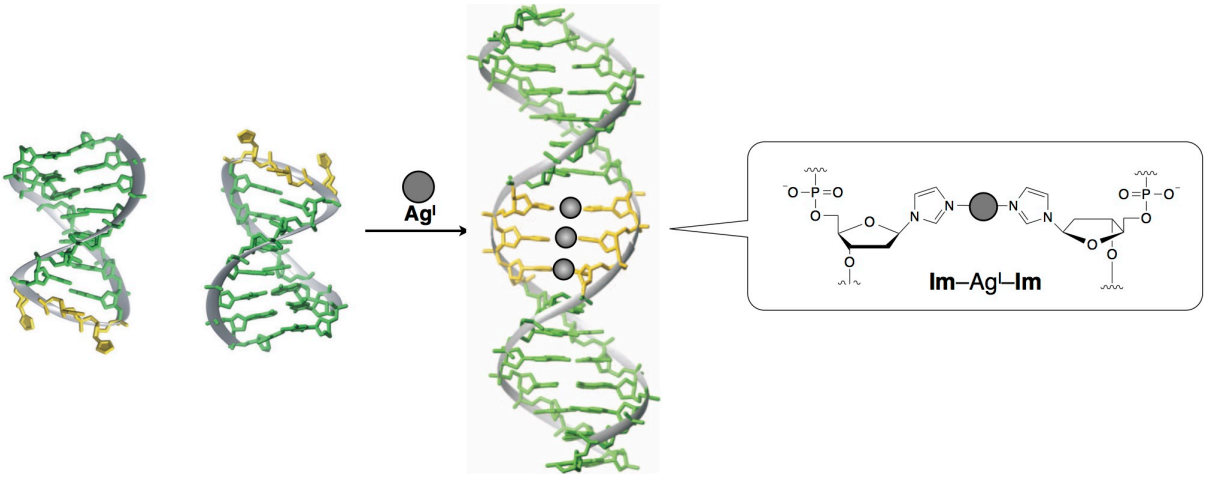


**Fig. 1-4-4** Schematic representation of $Ag^I$-mediated geometrical control of DNA association. Reproduced with permission from ref. 54. Copyright 2010 Nature Publishing Group.

Taking together, due to the orthogonality to natural hydrogen-bonded base pairing and to the possible control of the structures, I expect an artificial **H** nucleotide will be a promising candidate to regulate structural changes and dynamics of DNA nanostructures.

## 1-5. Enzymatic manipulation of DNA nanostructures

In DNA nanotechnology, both natural and synthetic DNA have been prepared with automated chemical DNA synthesizers. Another advantage for constructing DNA-based materials is that some natural DNA synthetic enzymes may possibly accept modified nucleotides as the substrates on DNA templates, while natural enzymes, in general, have high-selectivity in the DNA polymerization.

To construct and regulate synthetic large DNAs, enzymes such as ligase, polymerase and restriction endonuclease provide excellent tools in DNA nanotechnology.[55] For instance, DNA ligases, which covalently couple multiple DNA molecules, are utilized to enlarge DNA nanostructures from nanoscale to even macroscopic scale.[55–57] This enzyme catalyzes cross-linking reactions between the 5′-monophosphate moiety of one strand and the 3′-hydroxy group of the other strand, generating a phosphodiester bond. As shown in Fig. 1-5-1A, X-shaped DNA junction structures self-assembled to form three-dimensional networks with hydrogen bonding followed by a ligase-mediated cross-link reaction. The resulting product was DNA-based hydrogel, which is expected in extensive applications for cell transplant therapy such as drug delivery, cell culture and tissue engineering.[57]

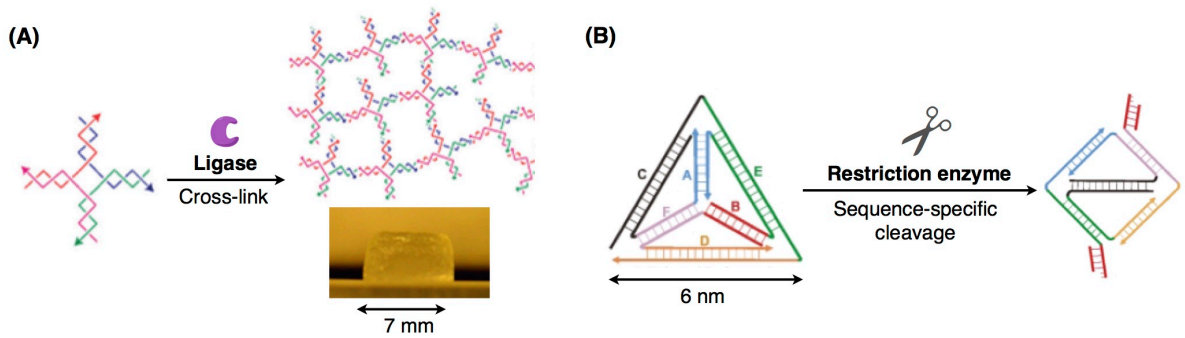


**Fig. 1-5-1 (A)** Construction of macroscopic DNA gels by ligases. Reproduced with permission from ref. 57. Copyright 2006 Nature Publishing Group. **(B)** Sequence-specific cleavage of DNA by restriction enzymes (ref. 59). Reproduced with permission from ref. 59. Copyright 2004 The Royal Society of Chemistry.

Restriction enzymes can cleave phosphodiester bonds of DNAs in a sequence specific manner. This enzyme allows sculpturing DNA materials to modify DNA structures (Fig.

1-5-1B).[58,59,63] Due to the high-specificity of the reaction, only desired sites can be clipped. Thus, this enzyme is a key tool for molecular-level manufacturing with precise control.

As mentioned above, a great number of DNA nanoarchitectures have been developed by enzymatic modification and programed self-assembly of DNA components in a well-defined manner. However, the construction of high-ordered artificial DNA architectures is still limited in terms of the type and number of the building blocks leading to new structural motifs.

DNA polymerase has great potential to overcome this limitation. DNA polymerase is an essential biogenic enzyme and generally responsible for the extension and replication of DNA strands in living cells. Due to its extremely high biological responsibility, DNA polymerase has attracted great interest in terms of its use for duplication and amplification of target DNA structures by polymerase chain reaction (PCR) or rolling circle amplification (RCA) (Fig. 1-5-2).[60–64] In these reactions, the polymerase reads the sequence of an original template DNA and subsequently duplicates the corresponding complementary DNA strand.

H. Yan et al. further demonstrated that Φ29 DNA polymerase repeatedly duplicates a four-way junction nanostructures (Fig. 1-5-2),[63] which can become key components of other two- and three-dimensional DNA nanoarchitectures. After the first RCA reaction, the duplicated junctions as antisense (–) strands were released by a restriction enzyme *Pst*I. On the second RCA reaction, these junctions were duplicated as original sense (+) strands. As a result, the use of DNA polymerases exhibited high potential to amplify DNA nanostructures. They were also successful in the duplication of even tile-shaped two-dimensional DNA motifs.[64] It would be possible to enzymatically duplicate various DNA nanostructures.

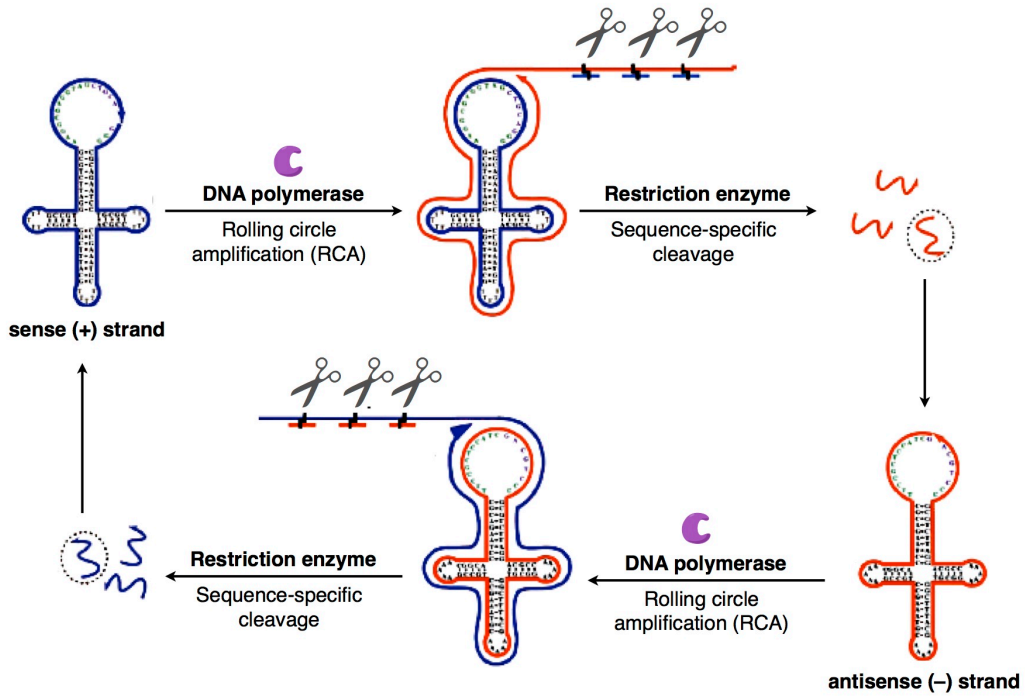


**Fig. 1-5-2** Schematic representation for DNA polymerase-catalyzed duplication of DNA junction nanostructures. Reproduced with permission from ref. 63. Copyright 2006 WILEY-VCH Verlag GmbH & Co. KGaA, Weinheim.

In conclusion, DNA-modifying enzymes are excellent tools for modification of various DNA nanostructures. As the reaction is highly site-selective, the enzymes can be applied to post-synthetic modification for DNA nanostructures.

Consequently, I expect that the artificial metallo-DNA moieties can be introduced into DNA nanoarchitectures by DNA-modifying enzymes, which will endow the DNA nanostructures with metal-responsive functions in a post-synthetic manner.

## 1-6. Template-independent DNA polymerases

In DNA nanotechnology, as mentioned above, DNA polymerase is one of the promising tools to construct DNA nanoarchitectures. Basically, a DNA polymerase incorporates a nucleotide monomer at the 3′-terminus of a DNA primer using a nucleotide triphosphate to synthesize a new DNA strand (Fig. 1-6-1A). This enzyme reads the sequence of a template DNA strand and subsequently replicates a complementary DNA strand in the 5′ to 3′ direction (Fig. 1-6-1B).

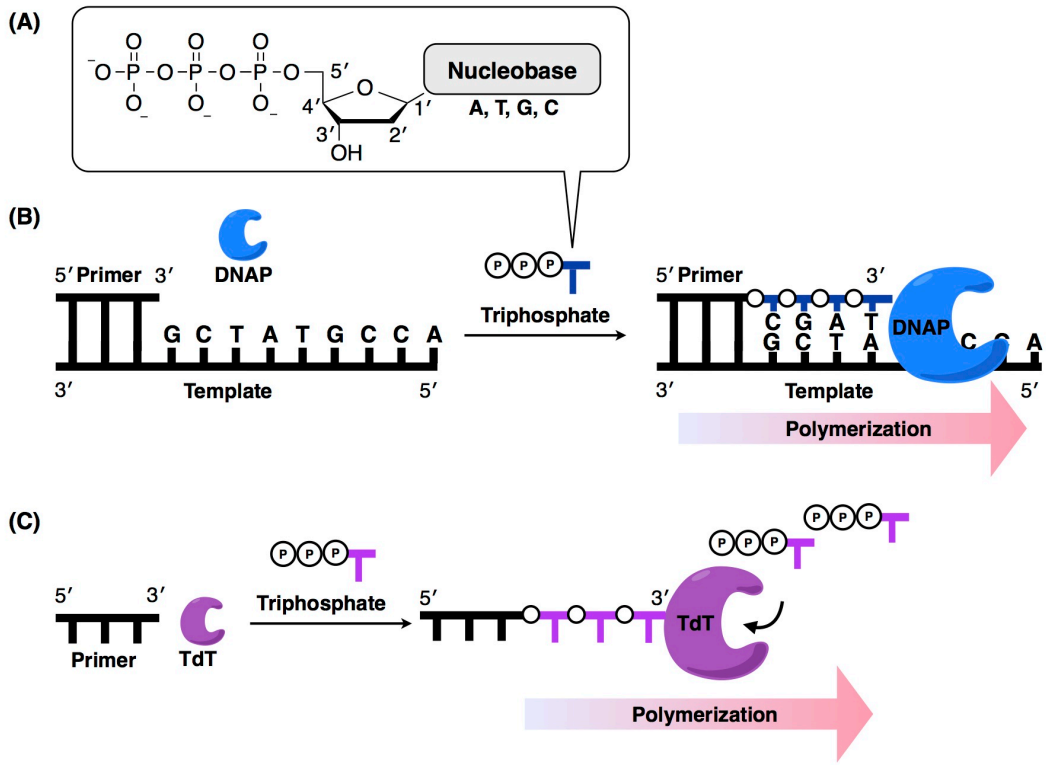


**Fig. 1-6-1** Schematic representation for **(A)** structure of 2′-deoxynucleotide-5′-triphosphates, **(B)** template-dependent polymerization of DNAs and **(C)** template-independent polymerization of DNAs. DNAP: DNA polymerase, TdT: terminal deoxynucleotidyl transferase

All kinds of DNA polymerases require two divalent metal cations such as $Mg^{II}$, $Mn^{II}$ and $Co^{II}$ ions for the catalytic reactions by a two-metal ion mechanism. In this mechanism, two metal ions are located in the center of the active site. The metal ions activate the 3′-hydroxy group of the primer DNA. The ions promote $S_N2$ nucleophilic attack on the α-phosphate of the incoming triphosphate. The ions stabilize a negatively charged transition state and assist

the removal of a pyrophosphate to provide an extended DNA. Consequently, divalent metal cations affect the efficiency and fidelity of enzymatic reactions.

Template-independent DNA polymerase, terminal deoxynucleotidyl transferase (TdT), is one of a multiple of DNA polymerases (Fig. 1-6-1C). In high contrast to the other DNA polymerases, TdT polymerase selectively recognizes a single-stranded DNA and sequentially polymerizes nucleotide triphosphates at the 3′-terminus of the DNA.[65] This enzyme *in vivo* randomly incorporates any natural triphosphates into immunologically-relevant genes and consequently diversifies the immunological responses to antigen.[65]

In the absence of template DNA strands, geometric constraints for incoming substrates are lowered. Consequently, TdT enzyme exhibits high flexibility to accept unnatural nucleotide triphosphates as its substrates (Fig. 1-6-3). For instance, TdT polymerase can accept noncanonical substrates possessing a modified nucleobase (Fig. 1-6-3A)[66–69] as well as even an artificial one (Fig. 1-6-3B)[70,71].

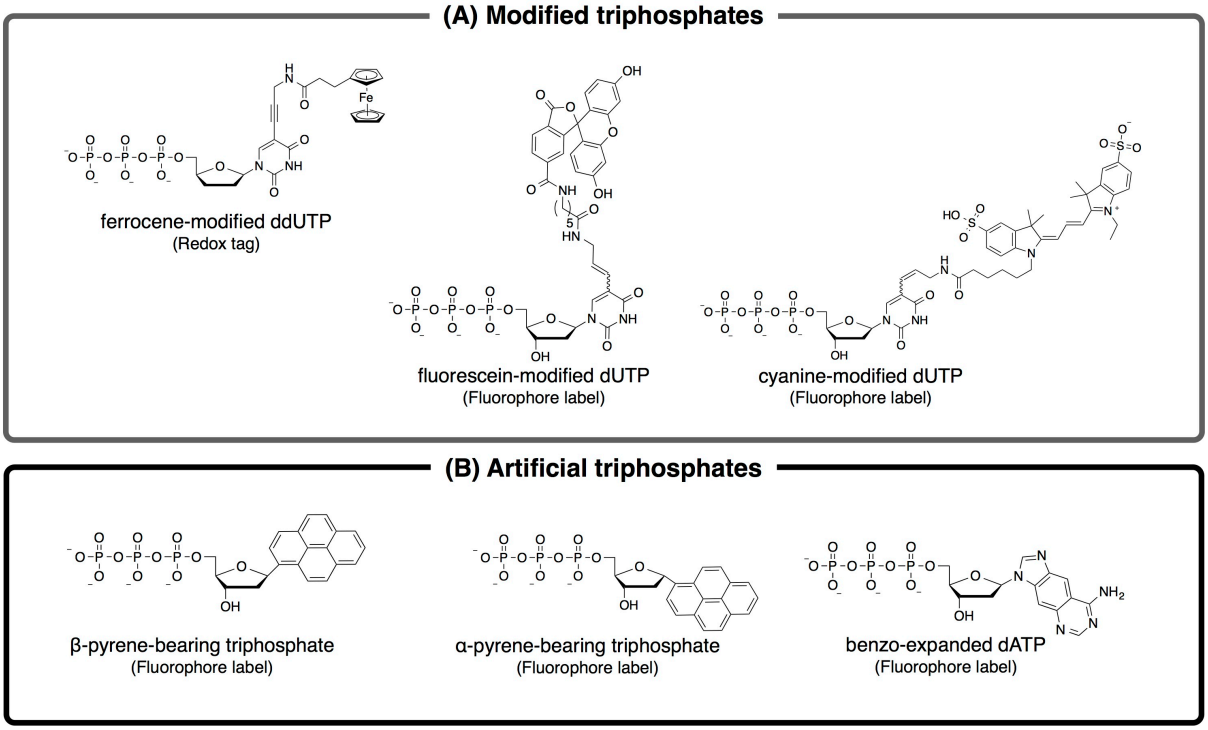


**Fig. 1-6-3** Selected examples of unnatural substrates for TdT

Consequently, TdT has been extensively applied for the 3′-modification of oligonucleotides with fluorophores[67,70] and redox-active functionalities[68] as well as for the

3′-capping to confer exonuclease resistance.[72] Therefore, in biological and medicinal fields, this enzyme has been utilized for single molecule sequencing, TUNEL assay (*in situ* localization of apoptosis) and TdT-dependent PCR, which prove the widespread availability of TdT enzymes.

Moreover, in DNA nanotechnology, TdT-mediated DNA synthesis has been utilized for the modification of DNA: (1) block copolymer nanoparticles[73] and (2) DNA origami nanostructures[74] (Fig. 1-6-4).

(1) F. E. Alemdaroglu et al. demonstrated post-synthetic size control of DNA-based micelles utilizing TdT (Fig. 1-6-4A).[73] The micelles, which were composed of single-stranded DNAs (22 mer) and *b*-polypropylene oxide (PPO), were treated with TdT enzyme in the presence of thymidine triphosphate (dTTP). Over 1–16 hours, TdT incorporated about 60 thymidine nucleotides into the terminus of DNA moieties. With an increase in the reaction time, the diameter of micelles was enlarged.

(2) In 2015, J. Kjems et al. showed enzymatic modification of DNA origami structures (Fig. 1-6-4B).[74] On the DNA origami structures, a single-stranded DNA moiety (12 mer) overhung at the equidistant linear positions, ~24 nm apart. AFM measurements established that TdT embedded dTTP into the overhung DNA terminus at ~1 nm/min. After 20 min, The DNAs were elongated up to 20 nm.

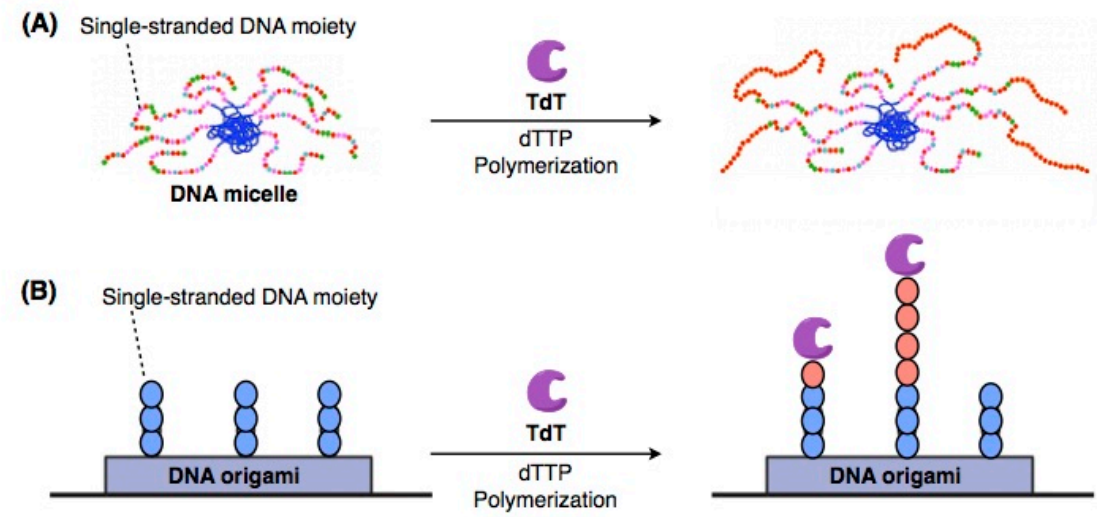


**Fig. 1-6-4** Schematic representation of TdT-catalyzed modification of **(A)** DNA micelles. Reprinted with permission from ref. 73. Copyright 2008 WILEY-VCH Verlag GmbH & Co. KGaA, Weinheim. **(B)** DNA origami nanostructures (ref. 74).

These modification reactions proceed selectively on the single-stranded DNA moieties.

Thus, the post-synthetic incorporation of a nucleotide unit by TdT enzyme using a nucleotide triphosphate would be a powerful tool to endow DNA hybrid materials with unique functionalities. Such reactions would be utilized for site-selective modification of single-stranded DNA moieties in DNA nanostructures with precise control.

## 1-7. The aim of this study

In this study, I have developed a novel synthetic method for artificial metallo-DNAs via an enzymatic DNA polymerization reaction by template-independent DNA polymerase, terminal deoxynucleotidyl transferase (TdT) (Fig. 1-7-1).

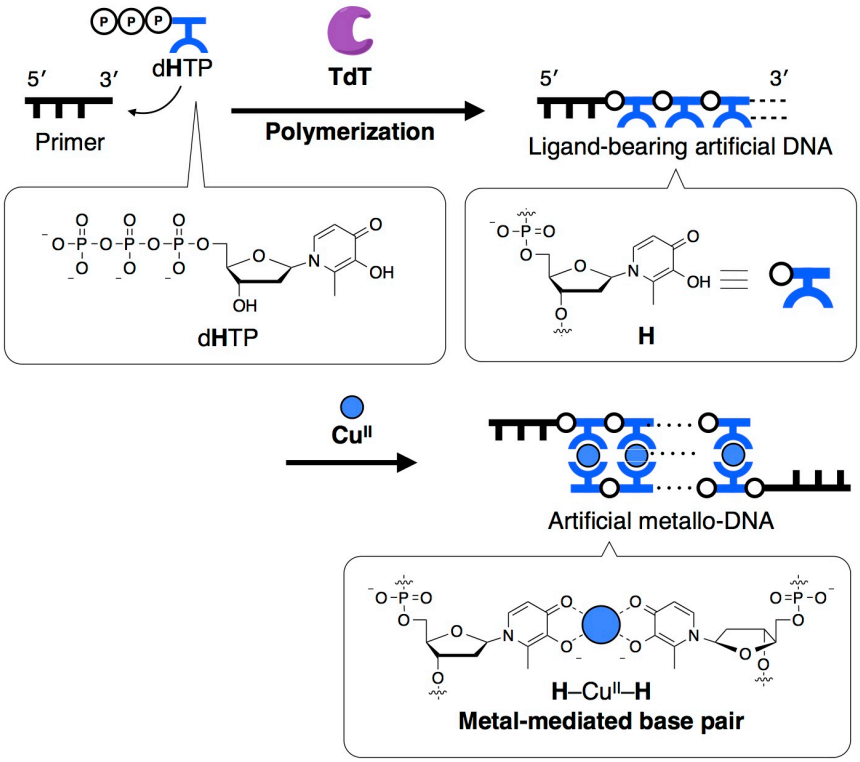


**Fig. 1-7-1** Overview of this work: enzymatic synthesis of artificial-metallo DNAs utilizing template-independent DNA polymerases. TdT: terminal deoxynucleotidyl transferase

Recent DNA nanotechnology has enabled construction of DNA-based functional molecules such as nanomachines and nanodevices. Artificial metallo-DNAs now play a central role in the DNA nanoarchitectures due to their metal-based unique physiochemical properties. In order to embed metallo-DNA components into natural DNA structures, as mentioned in section **1-5**, the use of DNA-modifying enzymes was expected to provide a fundamental and powerful tool to develop DNA-based materials.[55] However, enzymatic synthesis of artificial metallo-DNAs had not been extensively explored yet.[75–77]

Thus, I am working towards developing a new synthetic method for artificial metallo-DNAs by means of natural enzymes to shape a new discipline in DNA nanotechnology.

As described in section **1-6**, TdT catalyzes the polymerization of not only natural nucleotide triphosphates, but also unnatural noncanonical ones at the 3′-terminus of single-stranded primers. Herein, I expect that ligand-type artificial nucleotides may act as a substrate for TdT which would become an excellent tool for the synthesis of artificial metallo-DNAs and subsequent modification of DNA nanoarchitectures.

**Chapter 2** describes the synthesis of a hydroxypyridone-bearing nucleotide triphosphate (d**H**TP) as a substrate for TdT.

In **Chapter 3**, I examined the TdT-catalyzed polymerization of d**H**TP to synthesize ligand-bearing artificial DNA strands and subsequently metal complexation of enzymatically synthesized DNA to produce artificial metallo-DNAs.

Finally in **Chapter 4**, to estimate the usability of the enzymatic synthesis, I investigated post-synthetic modification of DNA duplexes with the TdT-catalyzed reaction and metal-mediated assembly of modified DNA structures.

In the conclusion remarks (**Chapter 5**), the results are summarized and future outline of this study is discussed.

## 1-8. References


1. N. C. Seeman, *J. Theor. Biol.,* 1982, **99**, 237–247.

2. N. C. Seeman, *Annu. Rev. Biochem*., 2010, **79**, 65–87.

3. T. J. Fu and N. C. Seeman, *Biochemistry*, 1993, **32**, 3211–3220.

4. P. W. K. Rothemund, *Nature*, 2006, **440**, 297–302.

5. J . Chen, N. C. Seeman, *Nature*, 1991, **350**, 631–33.

6. Y. Zhang, N. C. Seeman, *J. Am. Chem. Soc.*, 1994, **116**, 1661–69.

7. Y. Ke, J. Sharma, M. Liu, K. Jahn, Y. Liu and H. Yan, *Nano Lett*., 2009, **9**, 2445–2447.

8. S. M. Douglas, H. Dietz, T. Liedl1, B. Högberg, F. Graf and W. M. Shih, *Nature*, 2009, **459**, 414–418.

9. H. Dietz, S. M. Douglas, W. M. Shih, Science, 2009, **325**, 725–730.

10. A. Kuzuya, M. Kimura, K. Numajiri, N. Koshi, T. Ohnishi, F. Okada and M. Komiyama, *ChemBioChem*, 2009, **10**, 1811–1815.

11. N. V. Voigt, T. Tørring, A. Rotaru, M. F. Jacobsen, J. B. Ravnsbæk, R. Subramani, W. Mamdouh, J. Kjems, A. Mokhir, F. Besenbacher and K. V. Gothelf, *Nat. Nanotechnol*., 2010, **5**, 200–203.

12. N. Stephanopoulos, M. H. Liu, G. J. Tong, Z. Li, Y. Liu, H. Yan and M. B. Francis, *Nano Lett*., 2010, **10**, 2714–2720.

13. M. Langecker, V. Arnaut, T. G. Martin, J. List, S. Renner, M. Mayer, H. Dietz and F. C. Simmel, Science, 2012, **338**, 932–936.

14. A. Kuzyk, R. Schreiber, Z. Fan, G. Pardatscher, E.-M. Roller, A. Hogele, F. C. Simmel, A. O. Govorov and T. Liedl, *Nature*, 2012, **483**, 311–314.

15. J. Zheng, P. E. Constantinou, C. Micheel, A. P. Alivisatos, R. A. Kiehl and N. C. Seeman, *NanoLett*., 2006, **6**, 1502–1504.

16. J. Fu, Y. R. Yang, A. Johnson-Buck, M. Liu, Y. Liu, N.G. Walter, N. W. Woodbury, and H. Yan, *Nat. Nanotechnol*., 2014, **9**, 531−536.

17. A. P. Alivisatos, K. P. Johnson, X. G. Peng, T. E. Wilson, C. J. Loweth, M. P. Bruchez, P. G. Schultz, *Nature*, 1996, **382**, 609–611.

18. A. J. Mastroianni, S. A. Claridge, A. P. Alivisatos, *J. Am. Chem. Soc*., 2009, **131**, 8455–8459.

19. H. Y. Li, S. H. Park, J. H. Reif, T. H. LaBean, H. Yan, *J. Am. Chem. Soc*., 2004, **126**, 418–419.

20. Y. Y. Pinto, J. D. Le, N. C. Seeman, K. Musier-Forsyth, T. A. Taton, R. A. Kiehl, *NanoLett*., 2005, **5**, 2399–2402.

21. (a) C. K. McLaughlin, G. D. Hamblin and H. F. Sleiman, *Chem. Soc. Rev*., 2011, **40**, 5647–5656; (b) H. Li, T. H. LaBean and K. W. Leong, *Interface Focus*, 2011, **1**, 702–724; (c) A. Kuzuya and Y. Ohya, *Polymer Journal*, 2012, **44**, 452–460.

22. Y. R. Yang, Y. Liu, and H. Yan*, Bioconjugate Chem.*, 2015, **26**, 1381−1395.

23. R. P. Goodman, R. M. Berry, A. J. Turberfield, *Chem. Commun*., 2004, **12**, 1372–1373.

24. R. P. Goodman, M. Heilemann, S. Doose, C. M. Erben, A. N. Kapanidis, A. J. Turberfield, *Nat. Nanotechnol.*, 2008, **3**, 93–96.

25. R. Jungmann, C. Steinhauer, M. Scheible, A. Kuzyk, P. Tinnefeld, F. C. Simmel, *Nano Lett*., 2010, **10**, 4756–4761.

26. Y. Sannohe, M. Endo, Y. Katsuda, K. Hidaka,H. Sugiyama, *J. Am. Chem. Soc*., 2010, **132**, 16311–16313.

27. J. S. Shin, N. A. Pierce, *J. Am. Chem. Soc*., 2004, **126**, 10834–10835.

28. Z. G.Wang, J. Elbaz, I. Willner, *Nano Lett.*, 2010, **11**, 304–309.

29. P. Yin, H. Yan, X. G. Daniell, A. J. Turberfield, J. H. Reif, *Angew. Chem. Int. Ed.*, 2004, **43**, 4906–4911.

30. B. Yurke, A. J. Turberfield, A. P.Mills, F. C. Simmel and J. L. Neumann, *Nature*, 2000, **406**, 605–608.

31. J. Bath, S. J. Green and A. J. Turberfield, *Angew. Chem. Int. Ed.*, 2005, **44**, 4358–4361.

32. T. Omabegho, R. Sha and N. C. Seeman, *Science*, 2009, **324**, 67–71.

33. W. B. Sherman and N. C. Seeman, *Nano Lett.*, 2004, **4**, 1203–1207.

34. Y. Tian, Y. He, Y. Chen, P. Yin and C. Mao, *Angew. Chem. Int. Ed.*, 2005, **44**, 4355–4358.

35. S. M. Douglas, I. Bachelet and G. M. Church, *Science*, 2012, **335**, 831–834.

36. (a) P. Zhan, Q. Jiang, Z. Wang, N. Li, H. Yu and B. Ding, *ChemMedChem*, 2014, **9**, 2013 – 2020; (b) M. Endo, Y. Yangc and H. Sugiyama, *Biomater. Sci.*, 2013, **1**, 347–360; (c) V. Linko, A. Ora and M. A. Kostiainen, *Trends in Biotechnology*, 2015, **33**, 586–596.

37. E. S. Andersen, M. Dong, M. M. Nielsen, K. Jahn, R. Subramani, W. Mamdouh, M. M. Golas, B. Sander, H. Stark, C. L. P. Oliveira, J. S. Pedersen, V. Birkedal, Flemming Besenbacher, K. V. Gothelf and Jørgen Kjems, *Nature*, 2009, **459**, 73–77

38. M. N. Stojanovic and D. Stefanovic, *Nat. Biotechnol*., 2003, **21**, 1069–1074.

39. G. Seelig, D. Soloveichik, D. Y. Zhang and E. Winfree, *Science*, 2006, **314**, 1585–1588.

40. Y. Benenson, B. Gil, U. Ben-Dor, R. Adar and E. Shapiro, *Nature*, 2004, **429**, 423–429.

41. B. Ding and N. C. Seeman, *Science*, 2006, **314**, 1583–1585.

42. (a) Y. Takezawa and M. Shionoya, *Acc. Chem. Res.*, 2012, **45**, 2066–2076; (b) P. Scharf and J. Müller, *ChemPlusChem*, 2013, **78**, 20–34; (c) G. H. Clever and M. Shionoya *Coord. Chem. Rev*., 2010, **254**, 2391–2402; (d) K. Tanaka and M. Shionoya, *Coord. Chem. Rev.*, 2007, **251**, 2732–2742; (e) G. H. Clever and M. Shionoya, *Metallofoldamers: Supramolecular Architectures from Helicates to Biomimetics,* 2013, Chapter 9, 303–332 ; (f) A. D. Leon, J . Kong, and C. Achim, *Metallofoldamers: Supramolecular Architectures from Helicates to Biomimetics,* 2013, Chapter 10, 333–377.

43. (a) S. Katz, *Biochim. Biophys. Acta*, 1963, **68**, 240–253; (b) Z. Kuklenyik and L. G. Marzilli, *Inorg. Chem*., 1996, **35**, 5654–5662; (c) J. Kondo, T. Yamada, C. Hirose, I. Okamoto, Y. Tanaka and A. Ono, *Angew. Chem., Int. Ed.*, 2014, **53**, 2385–2388.

44. Y. Miyake, H. Togashi, M. Tashiro, H. Yamaguchi, S. Oda, M. Kudo, Y. Tanaka, Y. Kondo, R. Sawa, T. Fujimoto, T. Machinami and A. Ono, *J. Am. Chem. Soc*., 2006, **128**, 2172–2173.

45. (a); C.-H. Lu, A. Cecconello, J. Elbaz, A. Credi and I. Willner, *Nano Lett*., 2013, **13**, 2303–2308; (b) Z. G. Wang, J. Elbaz, I. Willner, *Nano Lett*., 2010, **11**, 304–309.

46. R. Yang, J. Jin, L. Long, Y. Wang, H. Wang, W. Tan, *Chem. Commun*., 2009, **3**, 322–324.

47. K. Tanaka and M. Shionoya, *J. Org. Chem*., 1999, **64**, 5002–5003.

48. Y. Takezawa, K. Nishiyama, T. Mashima, M. Katahira and M. Shionoya, *Chem. – Eur. J.*, 2015, **21**,14713–14716.

49. K. Tanaka, A. Tengeiji, T. Kato, N. Toyama, M. Shiro and M. Shionoya, *J. Am. Chem. Soc*., 2002, **124**, 12494–12498.

50. K. Tanaka, A. Tengeiji, T. Kato, N. Toyama and M. Shionoya, *Science*, 2003, **299**, 1212–1213.

51. S. Liu, G. H. Clever, Y. Takezawa, M. Kaneko, K. Tanaka, X. Guo and M. Shionoya, *Angew. Chem., Int. Ed*., 2011, **123**, 9048–9052.

52. Y. Takezawa, W. Maeda, K. Tanaka and M. Shionoya, *Angew. Chem., Int. Ed.*, 2009, **48**, 1081–1084.

53. K. Tanaka, Y. Yamada and M. Shionoya, *J. Am. Chem. Soc.*, 2002, **124**, 8802-8803.

54. S. Johannsen, N. Megger, D. Bçhme, R. K. O. Sigel, J. Müller, *Nat. Chem*., 2010, **2**, 229–234.

55. (a) S. Keller and A. Marx, *Chem. Soc. Rev*., 2011, **40**, 5690–5697; (b) D. Yang, M. R. Hartman, T. L. Derrien, S. Hamada, D. An, K. G. Yancey, R. Cheng, M. Ma, and D. Luo, *Acc. Chem. Res.*, 2014, **47**, 1902−1911

56. (a) Y. Li, Y. D. Tseng, S. Y. Kwon, L. d'Espaux, J. S. Bunch, P. L. McEuen and D. Luo, *Nature Mater*., 2004, **3**, 38–42; (b) Y. Li, Y. T. Cu and D. Luo, Nature Biotechnol. 2005, **23**, 885–889.

57. S. H. Um, J. B. Lee, N. Park, S. Y. Kwon, C. C. Umbach and D. Luo, *Nat. Mater*., 2006, **5**, 797–801.

58. (a) R. Kaufmann, D. Peled, R. Naaman and S. S. Daube, *ACS Appl. Mater. Interfaces*, 2009, **1**, 2320–2324; (b) A. G. Kanaras, Z. Wang, A. D. Bates, R. Cosstick and M. Brust, *Angew. Chem., Int. Ed*., 2003, **42**, 191–194; (c) A. Kanaras, Z. Wang, M. Brust, R. Cosstick and A. Bates, *Small*, 2007, 3, 590–594.

59. R. P. Goodman, R. M. Berry and A. J. Turberfield, *Chem. Commun.*, 2004, **12**, 1372–1373.

60. S. R. Nicewarner-Pena, S. Raina, G. P. Goodrich, N. V. Fedoroff and C. D. Keating, *J. Am. Chem. Soc*., 2002, **124**, 7314–7323.

61. W. Zhao, Y. Gao, S. A. Kandadai, M. A. Brook and Y. Li, *Angew. Chem., Int. Ed.*, 2006, **45**, 2409–2413.

62. S. Keller, J. Wang, M. Chandra, R. Berger and A. Marx, *J. Am. Chem. Soc.*, 2008, **130**, 13188–13189.

63. C. Lin, M. Xie, J. J. L. Chen, Y. Liu and H. Yan, *Angew. Chem., Int. Ed*., 2006, **45**, 7537–7539.

64. C. Lin, X. Wang, Y. Liu, N. C. Seeman and H. Yan, *J. Am. Chem. Soc*., 2007, **129**, 14475–14481.

65. (a) J. D. Fowler and Z. Suo, *Chem. Rev*., 2006, **106**, 2092–2110; (b) E. A. Motea and A. J. Berdis, *Biochim. Biophys. Acta*, 2010, **1804**, 1151–1166; (c) S. V. Desiderio, G. D. Yancopoulos, M. Paskind, E. Thomas, M. A. Boss and N. Landau, *Nature*, 1984, **311**, 752–755.

66. Y. Gavrieli, Y. Sherman, S. A. Ben-Sasson, *J. Cell Biol.* 1992, **119**, 493–501.

67. V. Tjong, H. Yu, A. Hucknall, S. Rangarajan and A. Chilkoti, *Anal. Chem.* 2011, **83**, 5153–5159.

68. (a) A. Anne, B. Blanc and J. Moiroux, *Bioconjugate Chem.* 2001, **12**, 396-405; (b) A. Anne, C. Bonnaudat, C. Demaille and K. Wang, *J. Am. Chem. Soc.*, 2007, **129**, 2734–2735; (c) P. Horáková, H. Macíčková-Cahová, H. Pivoňková, J. Špaček, L. Havran, M. Hocek and M. Fojta, *Org. Biomol. Chem.*, 2011, **9**, 1366–1371.

69. M. Hollenstein, *Org. Biomol. Chem*., 2013, **11**, 5162–5172.

70. (a) Y. Cho and E. T. Kool, *ChemBioChem*, 2006, **7**, 669–672; (b) S. K. Jarchow-Choy, A. T. Krueger, H. Liu, J. Gao and E. T. Kool, *Nucleic Acids Res*., 2011, **39**, 1586–1594; (c) M. Hollenstein, F. Wojciechowski and C. J. Leumann, *Bioorg. Med. Chem. Lett*., 2012, **22**, 4428–4430.

71. A. J. Berdis and D. McCutcheon, *ChemBioChem*, 2007, **8**, 1399–1408.

72. (a) M. Kuwahara, S. Obika, H. Takeshima, Y. Hagiwara, J. Nagashima, H. Ozaki, H. Sawai and T. Imanishi, *Bioorg. Med. Chem. Lett*., 2009, **19**, 2941–2943; (b) Y. Kasahara, S. Kitadume, K. Morihiro, M. Kuwahara, H. Ozaki, H. Sawai, T Imanishi and S. Obika, *Bioorg. Med. Chem. Lett*., 2010, **20**, 1626–1629.

73. (a) F. E. Alemdaroglu, J. Wang, M. Börsch, R. Berger and A. Herrmann, *Angew. Chem., Int. Ed.*, 2008, **47**, 974–976; (b) J. Wang, F. E. Alemdaroglu, D. K. Prusty, A. Herrmann and R. Berger, *Macromolecules*, 2008, **41**, 2914–2919.

74. A. H. Okholm, H. Aslan, F. Besenbacher, M. Dong and J. Kjems, *Nanoscale*, 2015, **7**, 10970–10973.

75. H. Urata, E. Yamaguchi, T. Funai, Y. Matsumura and S. Wada, *Angew. Chem., Int. Ed.,* 2010, **49**, 6516–6519.

76. C. Kaul, M. Müller, M. Wagner, S. Schneider and T. Carell, *Nat. Chem*., 2011, **3**, 794–800.

77. E. Kim and C. Switzer, *ChemBioChem*, 2013, **14**, 2403–2407.

# Chapter 2

## Synthesis of an Enzymatic Substrate

## 2-1. Introduction

As mentioned in section **1-6** in **Chapter 1**, 2′-deoxynucleotide 5′-triphosphates are substrates for DNA polymerases which provide a significant platform to introduce functionalities into DNA strands. DNA polymerases can incorporate nucleotides in the triphosphate form to elongate DNA strands effectively under physiological conditions both *in vivo* and *in vitro*. Therefore, many types of triphosphates possessing a modified or an artificial nucleobase have been widely used for versatile applications in biochemistry such as DNA labelling,[1] *in vitro* selection of DNAzymes[2] and aptamers,[3] and expansion of genetic codes.[4]

Although enzymatic synthesis of artificial metallo-DNAs has not been extensively explored yet, a few examples of ligand-bearing artificial triphosphates have been reported (Table. 2-1-1, Entry 1, 2).[5,6]

Carell et al. demonstrated enzymatic incorporation of the **Sal**–$Cu^{II}$(en)–**Sal** base pairs into DNA strands (Table. 2-1-1, Entry 1). *Bst* DNA polymerase I can selectively incorporate a salicylaldehyde (**Sal**)-bearing triphosphate into the opposite side of **Sal** on the template DNA in the presence of ethylenediamine (en) and $Cu^{II}$ ions. DNAs possessing **Sal**–$Cu^{II}$(en)–**Sal** base pairs were successfully amplified by PCR without significant errors.

Switzer et al. also reported enzymatic incorporation of the $\mathbf{Pur^{DC}}$–$Cu^{II}$–**3-Py** base pair (Entry 2). An artificial triphosphate possessing purine-2,6-dicarboxylate ($\mathbf{Pur^{DC}}$) was incorporated selectively into the opposite side of **3-Py** on the template DNA in the presence of $Cu^{II}$ ions by several types of DNA polymerases (i.e. Klenow $exo^-$ and Deep Vent $exo^-$). These results suggest that ligand-bearing artificial triphosphates may be acceptable by DNA polymerases in a manner similar to canonical natural triphosphates.

In this chapter, I describe the synthesis of a hydroxypyridone-bearing artificial triphosphate (d**H**TP) as an enzyme substrate, which will be used to construct artificial metallo-DNAs using TdT polymerase (Table. 2-1-1, Fig. 2-1-1).

**Table. 2-1-1** Structures of ligand-bearing artificial nucleotide triphosphates and the resulting metal-mediated base pairs.

| Entry | Ligand-bearing artificial nucleotide triphosphates | Resulting metal-mediated base pairs |
|---|---|---|
| dHTP | 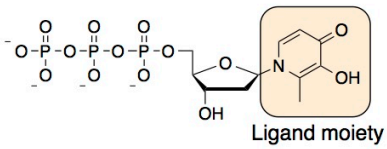  | 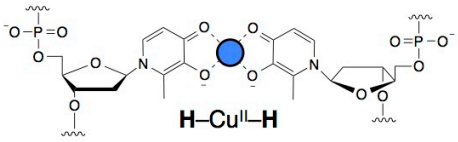  |
| 1 | 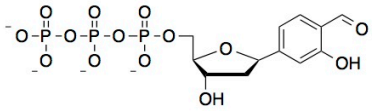 | 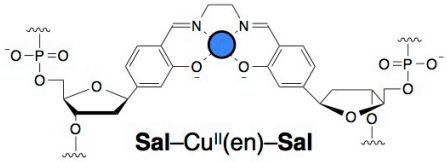  |
| 2 | 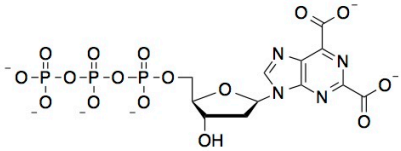 | 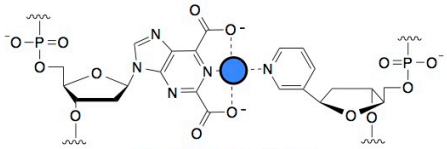  |

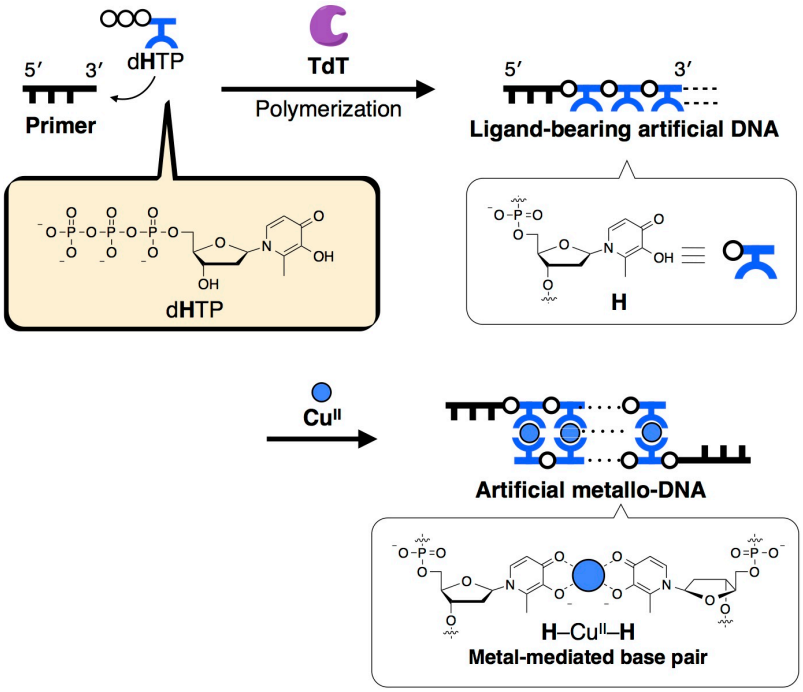


**Fig. 2-1-1** Schematic representation for the enzymatic synthesis of artificial metallo-DNAs

To expand the variation of triphosphates, development of their synthetic routes is critical. So far, there are two typical conventional synthetic methods, namely the Yoshikawa method and Eckestein method.

**Scheme 2-1-1** Yoshikawa method (B = modified or artificial nucleobase).

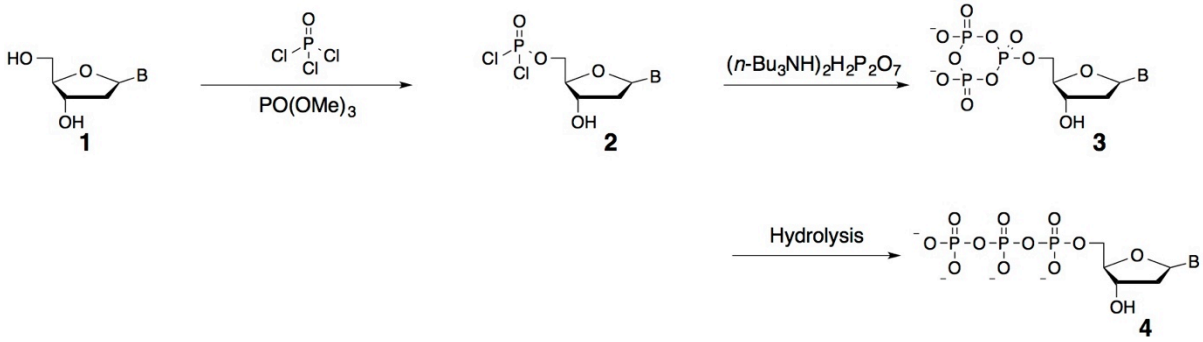


The Yoshikawa method is one of the well-known methods for triphosphate synthesis (Scheme 2-1-1). Nucleoside **1** can be 5′-monophosphorylated selectively at the 5’ position with phosphoryl chloride ($POCl_3$) to generate an activated intermediate **2**. Subsequent reaction of the intermediate with tributylammonium pyrophosphate produces a cyclic triphosphate **3**, followed by hydrolysis to produce 5′-triphosphate **4**.

One of the advantages of this method is its simplicity, which requires no protecting groups and shortens the synthetic route of a desired triphosphate compared with other methods. However, because $POCl_3$ is a strong electrophilic reagent, it is incompatible with all nucleosides and often generates undesirable by-products such as oligo-phosphates.[8,9]

**Scheme 2-1-2** Eckstein method (B = modified or artificial nucleobase, R = protecting group).

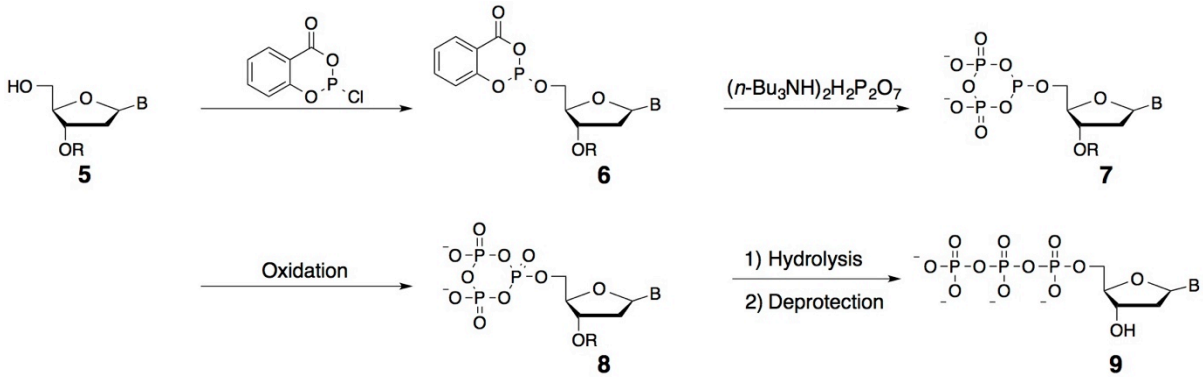


Eckstein method has also been used as a reliable method for the synthesis of a modified triphosphate (Scheme 2-1-2).[10] A reaction between 3′-*O*-protected nucleoside **5** and salicyl chlorophosphite provides a reactive intermediate **6**. This intermediate subsequently reacts with tributylammonium pyrophosphate to provide a cyclic phosphate **7**, which is immediately

converted to cyclic **8** by iodine-mediated oxidation. Finally, the cyclic triphosphate is hydrolyzed and deprotected to produce desired 5′-triphosphate **9**.

In the Eckstein method, all the reactions are generally carried out in one pot. Furthermore, there are less undesired by-products such as oligo-phosphates, which are generated by the Yoshikawa method.[11]

Consequently, by utilizing the Eckstein method, our group has recently achieved the synthesis of a hydroxypyridone-bearing artificial triphosphate (d**H**TP).[12] In the synthetic procedure, the crude product was directly subjected to reverse-phased HPLC to isolate a pure d**H**TP from the reaction mixture containing other nucleoside derivatives such as monophosphates. However, because their retention times were similar to each other, time-consuming repetitive HPLC treatments were required. In this work, I improved our previous purification method to isolate triphosphate d**H**TP.

## 2-2. Synthesis of hydroxypyridone-bearing nucleotide triphosphate (dHTP)

As shown in Scheme 2-2-1, d**H**TP was synthesized by the Eckstein method. Because a salicyl chlorophosphite (essential phosphorylation reagent) is a strong electrophilic reagent, this reagent can react not only at the desired 5′-hydroxy group but also at other undesired hydroxy groups of the nucleoside. Thus, the 3′-hydroxy group of the ribose and the 3-hydroxy group of the hydroxypyridone moiety were site-selectively protected by benzoyl groups prior to the phosphorylation reaction. A DMTr-protected nucleoside **10** was prepared according to a previous literature[13] and then subjected to benzoylation. The reaction with a benzoic anhydride ($Bz_2O$) provided a bis-benzoylated nucleoside which has benzoylated 3′- and 3-hydroxy groups. To ensure the reaction point for 5′-phosphorylation, the nucleoside was detritylated using a trichloroacetic acid ($CCl_3COOH$) to produce a benzoyl-protected nucleoside **11**, whose yield was 50% in 2 steps from the nucleoside **10**.

**Scheme 2-2-1** Synthesis of d**H**TP by Eckstein method.

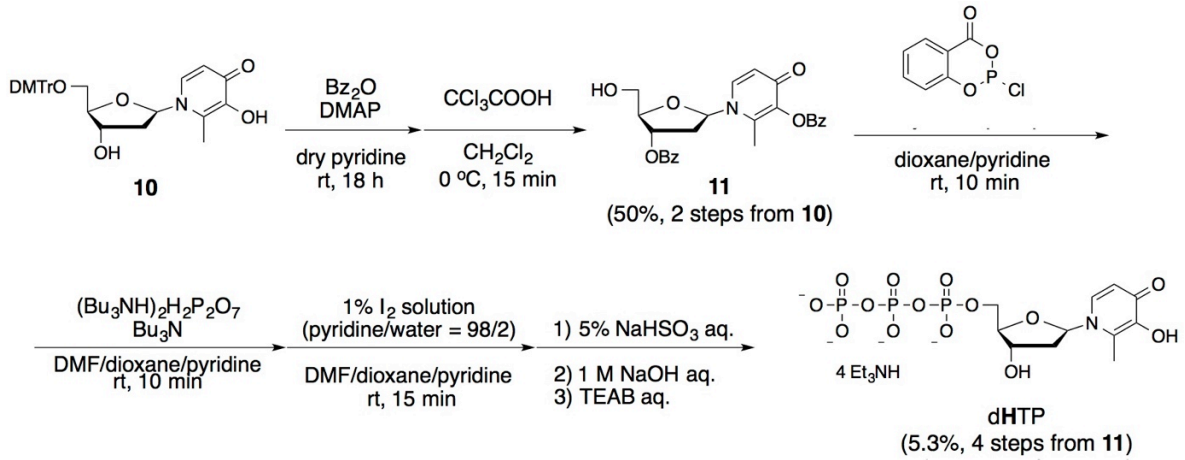


The nucleoside **11** reacted with a salicyl chlorophosphite for 5′-phosphorylation and subsequently reacted with tributylammonium pyrophosphate for displacement of salicylic acid to yield a cyclic intermediate. To produce a cyclic triphosphate, which is a precursor of d**H**TP, the intermediate was subjected to iodine-mediated oxidation of a phosphorus atom. Subsequently, for debenzylation of hydroxy groups and ring-opening the cyclic triphosphate, the nucleoside was subjected to NaOH-mediated hydrolysis to yield desired 5′-triphosphate d**H**TP.

The resulting reaction mixture contained many kinds of by-products (i.e. monophosphates and other nucleoside derivatives) and reagent debris (i.e. pyrophosphates and salicylic acids). Because the desired d**H**TP has a triphosphate moiety, it seemed to be distinguishable from the other compounds by the negative charge difference. Thus, the reaction mixture was immediately applied to an anion-exchange chromatography (DEAE sephadex) to isolate d**H**TP (Fig. 2-2-1). Hydroxypyridone nucleoside has a large absorption band at 282 nm and the extinction coefficient of the unmodified **H** nucleoside was reported as $5.34 \times 10^3$ $M^{-1}$ $cm^{-1}$ at 260 nm.[13] Then, the elution of compounds was monitored based on UV absorbance at 260 nm and 282 nm to detect d**H**TP.

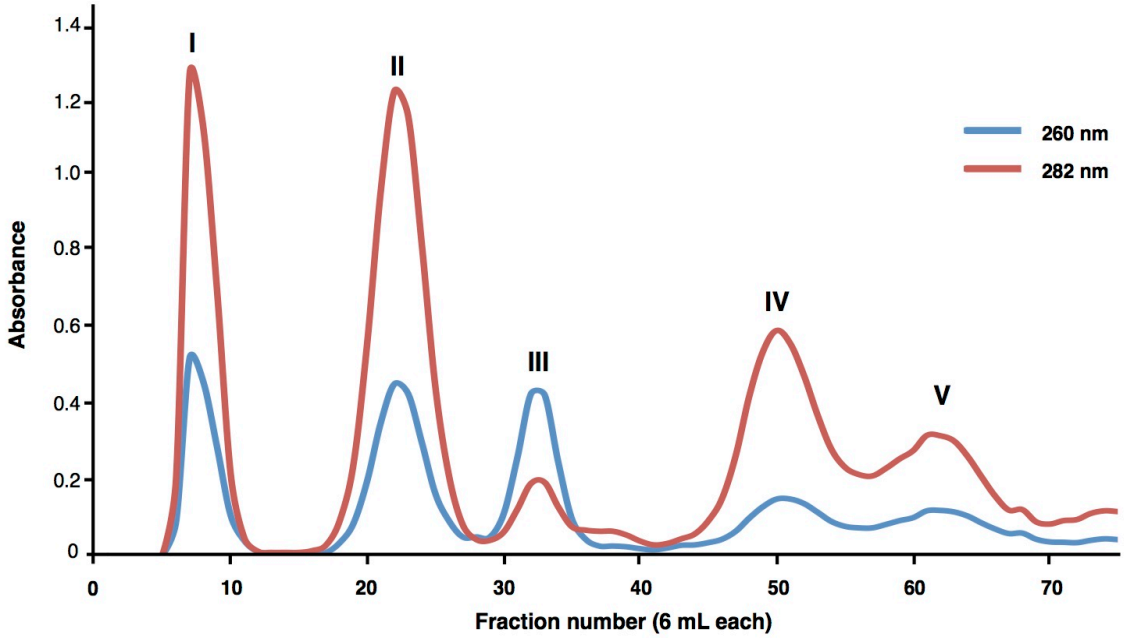


**Fig. 2-2-1** Elution profile of an anion-exchange column chromatography. DEAE Sephadex A-25, buffers: A = 50 mM TEAB, B = 750 mM TEAB (pH 8.5), gradient: 0% A (0 min), 100% A (90 min), flow rate: 5.0 mL/min, temperature: 25 °C.

The elution profile of the anion-exchange chromatography is shown in Fig. 2-2-1. The reaction mixture was distinctly separated into 5 fractions (fraction **I**–**V**). The fractions **III** and **IV** contained reagent debris such as salicylic acids. The fractions **I**, **II** and **V**, which have large absorption band at 282 nm, were expectedly ascribed to hydroxypyridone nucleotide derivatives. $^1$H NMR analysis of each fraction (Fig. 2-2-2) confirmed that the fractions **I, II** and **V** contained a hydroxypyridone-bearing

artificial nucleoside (d**H**),[13] a hydroxypyridone-bearing artificial monophosphate (d**H**MP)[14] and a desired triphosphate (d**H**TP),[12] respectively.

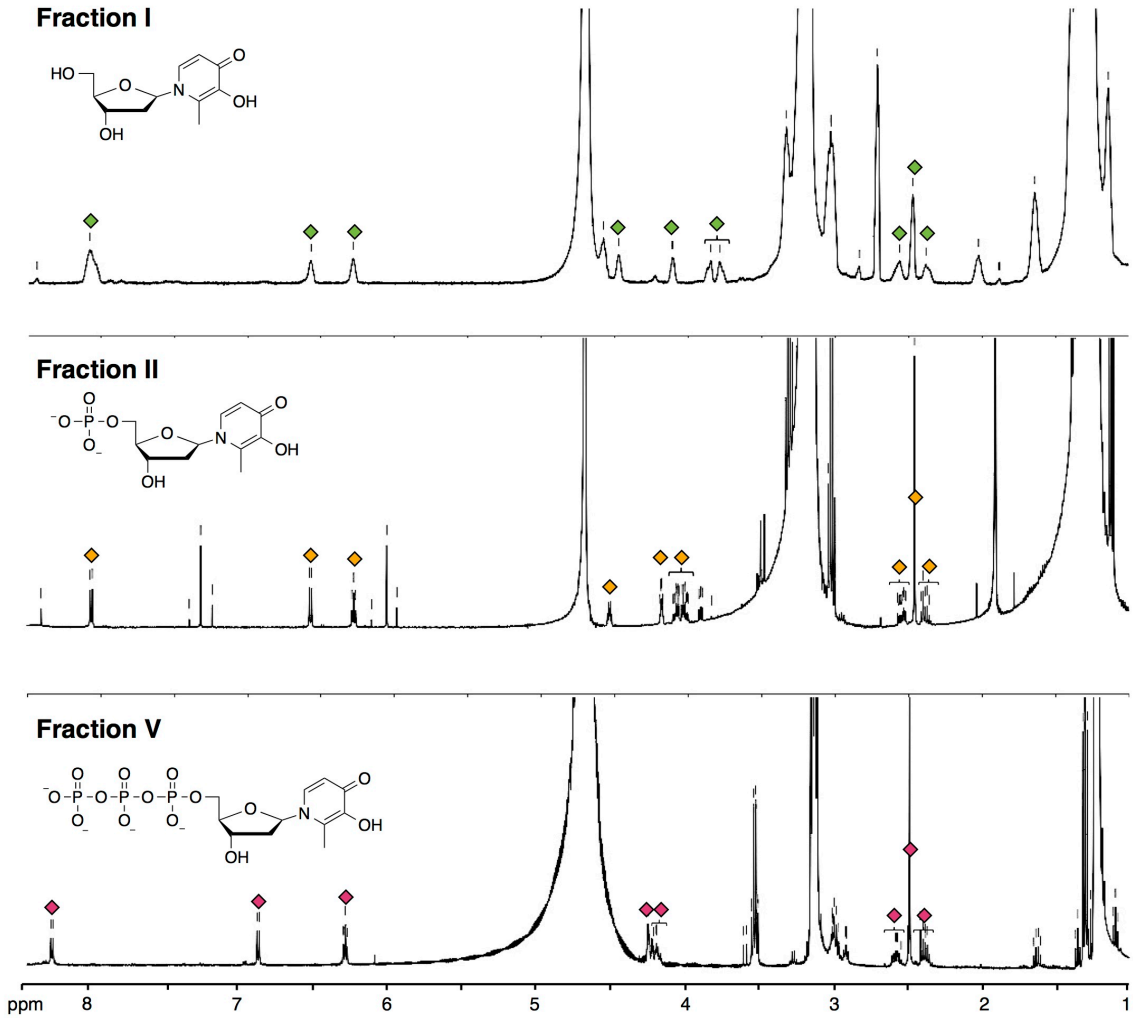


**Fig. 2-2-2** $^1$H NMR spectra of fractions **I**, **II** and **V** after the anion-exchange column chromatography (500 MHz, $D_2O$, 300 K).

Quantification of these nucleoside derivatives was performed based on the UV absorbance at 260 nm by applying the extinction coefficient of the unmodified **H** nucleoside ($\varepsilon_{260}$ = 5.34 × $10^3$ $M^{-1}$ $cm^{-1}$). Each yield was roughly estimated to be d**H** (20%), d**H**MP (30%) and d**H**TP (10%). It was apparent that d**H** was generated by hydrolysis of the unreacted **11** probably because the first phosphorylation with a salicyl chlorophosphite did not proceed efficiently. The generation of d**H**MP implies

that the substitution reactions by tributylammonium pyrophosphate to displace salicylic acid did not proceed completely under this condition.

The fraction **V** was further subjected to reverse-phase HPLC twice to isolate d**H**TP (Fig. 2-2-3). The isolated yield was 5.3% in 4 steps from nucleoside **11**. Purified d**H**TP was characterized by $^{1}$H, $^{13}$C, $^{31}$P NMR (Figs. 2-2-4, 5, 6) and ESI-TOF mass spectra (Fig. 2-2-7; *m/z*: $[M - H]^-$ calcd for $C_{11}H_{17}NO_{14}P_3$ 479.9862, found 479.9879.) and was used in the enzymatic reactions.

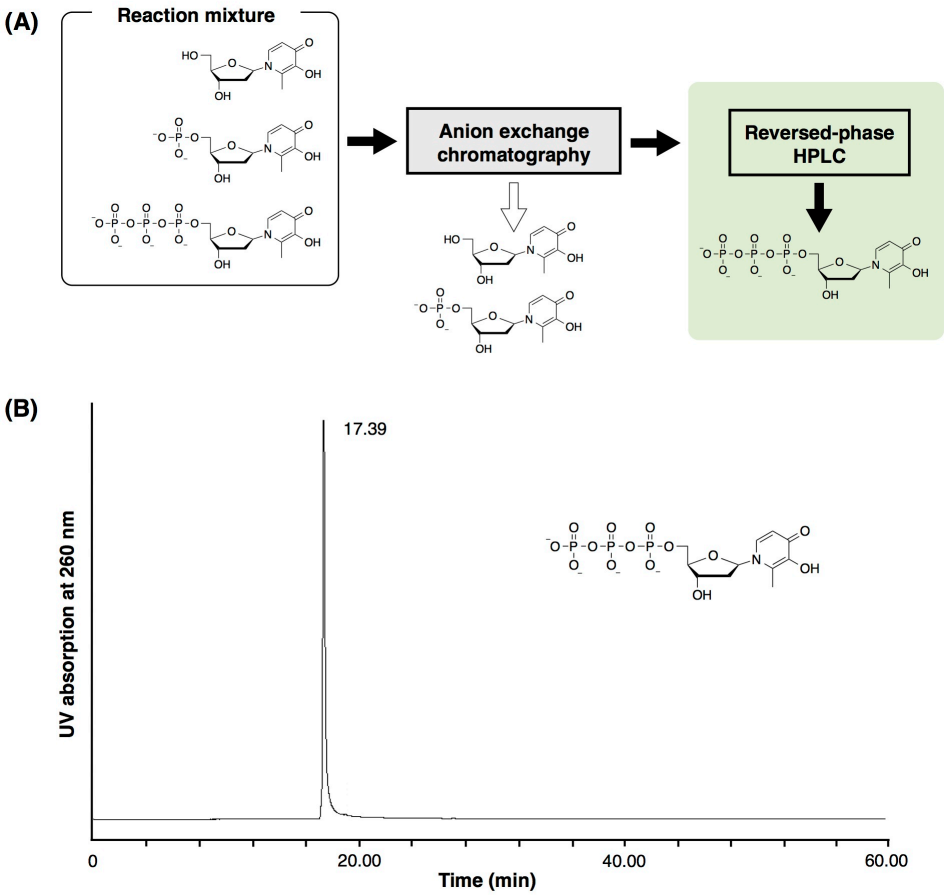


**Fig. 2-2-3** HPLC analysis of d**H**TP. Wako Navi pack C18 column, buffers: A = MeCN, B = 0.1 M TEAA (pH 7.0) + 2% MeCN, gradient: 10% A (0 min), 35% A (30 min), 100% A (45 min), 10% A (60 min), flow rate: 5.0 mL/min, temperature: 25 °C.

An HPLC profile of the purified d**H**TP was shown in Fig. 2-2-3. The result showed that the obtained d**H**TP was pure enough for the enzymatic reactions and the anion-exchange chromatography was effective for the purification of the triphosphate d**H**TP.

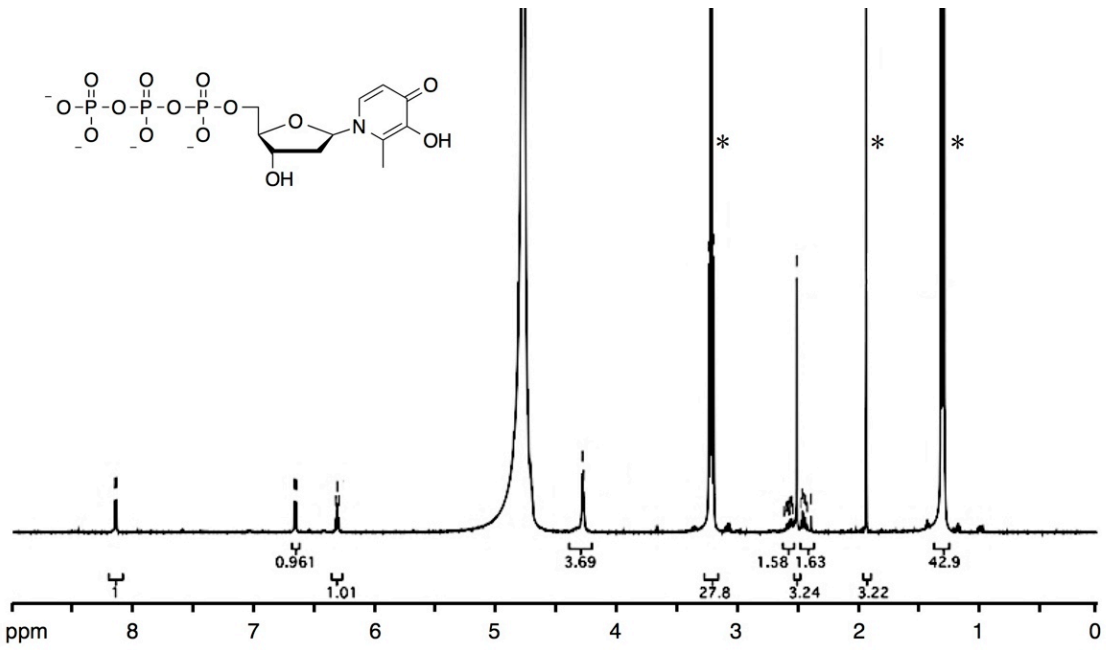


**Fig. 2-2-4** $^{1}$H NMR spectrum of d**H**TP (500 MHz, $D_2O$, 300 K). The asterisks indicate the signals of the residual triethylammonium acetate used in the HPLC purification.

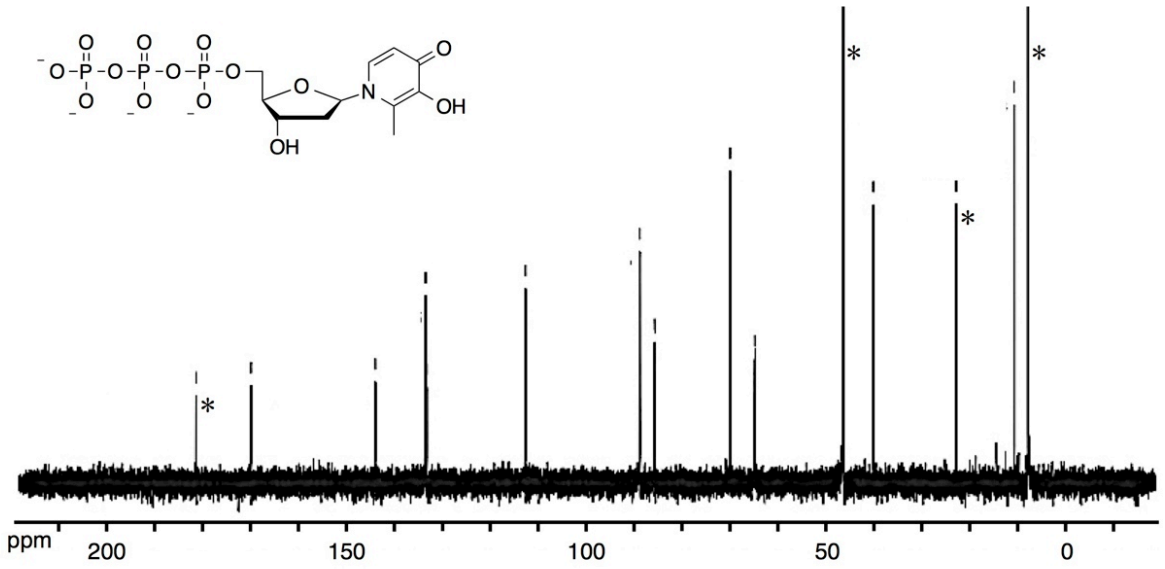


**Fig. 2-2-5** $^{13}$C NMR spectrum of d**H**TP (126 MHz, $D_2O$, 300 K). The asterisks indicate the signals of the residual triethylammonium acetate used in the HPLC purification.

Fig. 2-2-4 and 2-2-5 show $^{1}$H and $^{13}$C NMR spectra of the product. These spectra showed the residual triethylammonium acetate (TEAA) used in the HPLC purification existed. An $^{1}$H NMR spectrum showed that 4 equiv. of triethylamine and 1 equiv. of TEAA coexisted with

d**H**TP. Because residual TEAA does not have any affects on the enzymatic reaction, this sample was subjected to TdT-catalyzed polymerization reaction (**Chapter 3, 4**). In the $^{13}C$ NMR spectrum, carbons on the 4′ and 5′positions were coupled with a neighboring phosphorus atom (δ 85.93 (d, $^{3}J_{CP}$ = 9.1 Hz) and 65.10 (d, $^{2}J_{CP}$ = 5.5 Hz), respectively). These coupling established that the obtained compound has a phosphorus atom on the 5′-position.

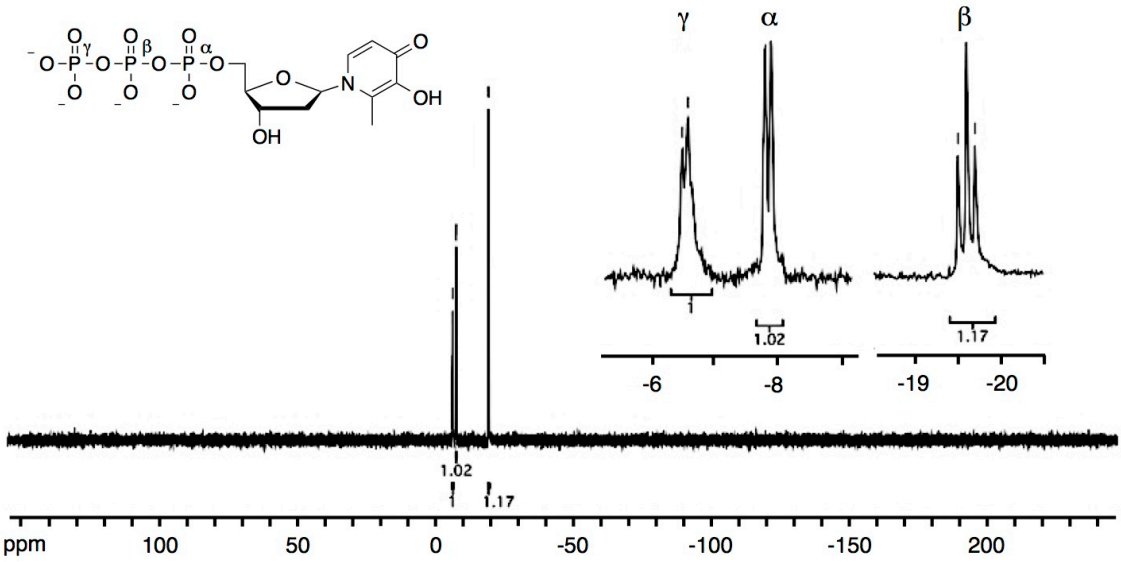


**Fig. 2-2-6** $^{31}P$ NMR spectrum of d**H**TP (202 MHz, $D_2O$, 300 K).

In a $^{31}P$ NMR spectrum (Fig. 2-2-6), three kinds of characteristic signals were observed (δ –6.57 (d, $J$ = 18.0 Hz, 1P), –7.90 (d, $J$ = 19.6 Hz, 1P), –19.64 (t, $J$ = 19.8 Hz, 1P)). This signal pattern is characteristic of nucleoside triphosphates.

Taken together with Fig. 2-2-5, it left no doubt that an obtained triphosphate was nucleoside 5′-triphosphate.

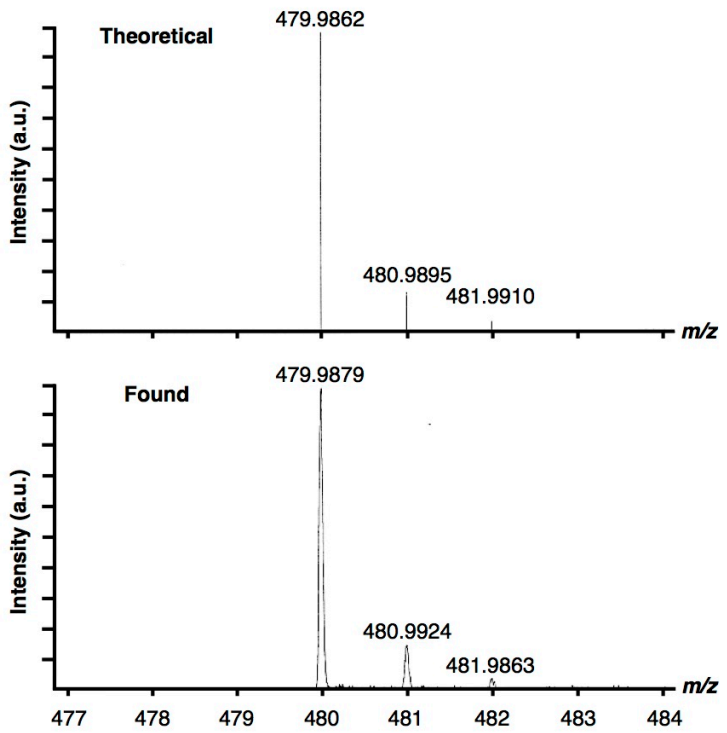


**Fig. 2-2-7** High-resolution ESI mass spectrum of d**H**TP. Negative mode.

## 2-3. Conclusion

To construct artificial metallo-DNAs using TdT enzyme, I synthesized a hydroxypyridone-bearing artificial triphosphate (d**H**TP) as an enzymatic substrate utilizing conventional Eckstein method. Although by-products were generated such as a nucleoside d**H** and monophosphate d**H**MP, they were successfully separated from a desired triphosphate d**H**TP by the anion-exchange column chromatography. Subsequently utilizing reversed-phase HPLC, d**H**TP was highly purified enough for the enzymatic reactions, as characterized by NMR and mass spectrometry.

Compared with the previous work,[12] the isolation and purification methods of d**H**TP developed in this study are simpler and easier to provide highly-purified d**H**TP for enzymatic reactions.

## 2-4. Experimental

### General.

All reactions were carried out under nitrogen atmosphere with commercial dehydrated solvents (Wako Pure Chemical Industries). The reagents for the synthesis were purchased from Wako Pure Chemical Industries, Tokyo Chemical Industry (TCI) and Aldrich. DMTr-protected hydroxypyridone-bearing nucleoside **1** was prepared according to reported procedures.[13] Silica gel column chromatography was performed using silica gel 60 (230–400 mesh, Merck). All NMR spectra were measured on a Bruker AVANCE 500 (500 MHz for $^{1}$H, 126 MHz for $^{13}$C and 202 MHz for $^{31}$P). The spectra were referenced to tetramethylsilane (TMS) in $CDCl_3$ ($\delta$ 0 ppm), or to external 3-(trimethylsilyl)propionic acid sodium salt in $D_2O$ ($\delta$ 0 ppm). Electrospray ionization-time-of-flight (ESI-TOF) mass spectra were recorded on Waters Micromass LCT Premier XE.

### Nucleoside 11.

DMTr-protected nucleoside **10** (0.14 g, 0.26 mmol)[13] was co-evaporated with dry pyridine and then dissolved in dry pyridine (2.0 mL). To the solution were added benzoic anhydride (0.18 g, 0.79 mmol) and DMAP (8.0 mg, 0.07 mmol). After being stirred at room temperature for 18 h, the reaction was quenched with water. The reaction mixture was extracted with AcOEt, dried over $MgSO_4$ and concentrated. The obtained crude bis-benzoylated nucleoside was placed in 2.2% $CCl_3COOH/CH_2Cl_2$ (19 mL) at 0 °C. After being stirred for 15 min, 0.1 M aqueous $NaHCO_3$ (15 mL) was added and the reaction mixture was extracted with AcOEt. The organic layer was dried over $MgSO_4$ and concentrated. The crude product was purified by silica gel column chromatography ($CHCl_3$:MeOH = 100:0–100:4) to give compound **11** as a colorless solid (57.8 mg, 0.13 mmol, 50%). The product was immediately used for the next reaction without further purification because of its lability. $^{1}$H NMR (500 MHz, $CDCl_3$, 300 K): δ 8.48 (br, 1H), 8.19

(br, 2H), 8.03 (br, 2H), 7.60 (br, 2H), 7.46 (br, 4H), 6.67 (br, 1H), 6.14 (br, 1H), 5.65 (br, 1H), 4.36 (br, 1H), 4.02 (br, 1H), 2.62 (br, 1H), 2.40 (s, 3H); HRMS (ESI-TOF) *m*/*z*: $[M + H]^+$ calcd for $C_{25}H_{24}NO_7$ 450.1553, found 450.1507.

**Hydroxypyridone-bearing nucleotide triphosphate (dHTP).**

The nucleoside **11** (0.053 g, 0.11 mmol) was dried by co-evaporation with dry pyridine and then dissolved in a mixture of dry pyridine (0.12 mL) and dry dioxane (0.35 mL). After addition of 1 M solution of 2-chloro-4*H*-1,3,2-benzodioxaphosphorin-4-one in dioxane (0.13 mL), the mixture was stirred at room temperature for 10 min. To the reaction mixture, 0.5 M solution of bis(tri-*n*-butylammonium)pyrophosphate in DMF (0.38 mL) and *n*-butylamine (0.12 mL) were added. After being stirred for 10 min, a 1% solution of iodine in $H_2O$/pyridine (1/1, 2.4 mL) was added. After 15 min, the reaction was quenched with 5% sodium hydrogen sulfite solution (0.90 mL). The mixture was concentrated and dried in vacuo, and then the residue was dissolved in $H_2O$ (3.5 mL) and MeOH (2.3 mL). 1 M aqueous NaOH (1.2 mL) was added and the reaction mixture was stirred at room temperature for 1 h. After addition of 1 M TEAB (pH 8.5, 4 mL) and evaporation, the residue was purified by DEAE Sephadex A-25 ion exchange column chromatography (1.5 x 30 cm, 50 mM to 750 mM TEAB) and by reverse-phase HPLC (Wako Navi pack C-18, 25% to 100% MeCN in 0.1 M TEAA (pH 7.0)) to afford the triphosphate d**H**TP (containing 4 equiv. of triethylamine and 1 equiv. of TEAA, 5.8 μmol, 5.3%). Quantification of the triphosphate was performed based on the UV absorbance at 260 nm under application of the extinction coefficient of the unmodified **H** nucleoside ($\varepsilon_{260} = 5.34 \times 10^3$ $M^{-1}$ $cm^{-1}$).[13]

$^1$H NMR (500 MHz, $D_2O$, 300 K): δ 8.15 (d, *J* = 7.5 Hz, 1H), 6.66 (d, *J* = 7.5 Hz, 1H), 6.31 (dd, *J* = 6.5, 6.5 Hz, 1H), 4.27 (br, 3H), 3.20 (q, *J* = 7.5 Hz, 28H, TEA), 2.60–2.53 (m, 1H), 2.49 (s, 3H), 2.46–2.38 (m, 1H), 1.92 (s, 3H), 1.28 (t, *J* = 7.5 Hz, 43H, TEA).

$^{13}$C NMR (126 MHz, $D_2O$, 300 K): δ 181.37 (C=O, $AcO^-$), 169.96, 144.10, 133.61, 133.38, 112.86, 89.11, 85.93 (d, $^3J_{CP}$ = 9.1 Hz, 4′), 70.30, 65.10 (d, $^2J_{CP}$ = 5.5 Hz, 5′), 46.71 ($CH_2$, TEA), 40.47, 23.24 ($CH_3$, $AcO^-$), 11.18, 8.26 ($CH_3$, TEA)

$^{31}$P NMR (202 MHz, $D_2O$, 300 K): δ –6.57 (d, *J* = 18.0 Hz, 1P), –7.90 (d, *J* = 19.6 Hz, 1P), –19.64 (t, *J* = 19.8 Hz, 1P).

HRMS (ESI-TOF) *m*/*z*: $[M – H]^-$ calcd for $C_{11}H_{17}NO_{14}P_3$ 479.9862, found 479.9879.

## 2-5. References


1. (a) T. Obayashi, M. M. Masud, A. N. Ozaki, H. Ozaki, M. Kuwahara and H. Sawai, *Bioorg. Med. Chem. Lett.*, 2002, **12**, 1167–1170; (b) M. Hocek and M. Fojta, *Chem. Soc. Rev.*, 2011, **40**, 5802–5814; J. Riedl, R. Pohl, N. P. Ernsting, P. Orság, M. Fojta and M. Hocek, *Chem. Sci.*, 2012, **3**, 2797–2806; (c) V. Raindlová, R. Pohl, B. Klepetářová, L. Havran, E. Šimková, P. Horáková, H. Pivoňková, M. Fojta and M. Hocek, *ChemPlusChem*, 2012, **77**, 652–662; (d) Y. J. Seo, D. A. Malyshev, T. Lavergne, P. Ordoukhanian and F. E. Romesberg, *J. Am. Chem. Soc.*, 2011, **133**, 19878–19888; (e) J. Balintová, R. Pohl, P. Horáková, P. Vidláková, L. Havran, M. Fojta and M. Hocek, *Chem. Eur. J.*, 2011, **17**, 14063–14073.

2. (a) C. Tuerk and L. Gold, *Science*, 1990, **249**, 505–510; (b) S. W. Santoro, G. F. Joyce, K. Sakthivel, S. Gramatikova and C. F. Barbas, *J. Am. Chem. Soc.*, 2000, **122**, 2433–2439; (c) D. M. Perrin, T. Garestier and C. Hélène, *J. Am. Chem. Soc.*, 2001, **123**, 1556–1563; (d) A. V. Sidorov, J. A. Grasby and D. M. Williams, *Nucleic Acids Res.*, 2004, **32**, 1591–1601; (e) M. Hollenstein, C. J. Hipolito, C. H. Lam and D. M. Perrin, *Nucleic Acids Res.*, 2009, **37**, 1638–1649; (f) C. J. Hipolito, M. Hollenstein, C. H. Lam and D. M. Perrin, *Org. Biomol. Chem.*, 2011, **9**, 2266–2273.

3. (a) G. F. Joyce, *Annu. Rev. Biochem.*, 2004, **73**, 791–836; (b) T. R. Battersby, D. N Ang, P. Burgstaller, S. C. Jurczyk, M. T. Bowser, D. D. Buchanan, R. T. Kennedy and S. A. Benner, *J. Am. Chem. Soc.*, 1999, **121**, 9781–9789; (c) D. E. Huizenga and J. W. Szostak, *Biochemistry*, 1995, **34**, 656–665; (d) C. H. Lin and D. J. Patel, *Chem. Biol.*, 1997, **4**, 817–832; (e) H. Sawai, A. N. Ozaki, F. Satoh, T. Ohbayashi, M. M. Masud and H. Ozaki, *Chem. Commun.*, 2001, 2604–2605; (f) A. Shoji, M. Kuwahara, H. Ozaki and H. Sawai, *J. Am. Chem. Soc.*, 2007, **129**, 1456–1464; (g) J. A. Latham, R. Johnson and J. J. Toole, *Nucleic Acids Res.*, 1994, **22**, 2817–2822.

4. (a) C. Switzer, S. E. Moroney and S. A. Benner, *J. Am. Chem. Soc.*, 1989, **111**, 8322 – 8323; (b) J. A. Piccirilli, T. Krauch, S. E. Moroney and S. A. Benner, *Nature*,1990, **343**,33–37; (c) D. A. Malyshev and F. E. Romesberg, *Angew. Chem. Int. Ed.*, 2015, **54**, 11930–11944; (b) I. Hirao, M. Kimoto and R. Yamashige, *Acc. Chem. Res.*, 2012, **45**, 2055–2065.

5. C. Kaul, M. Müller, M. Wagner, S. Schneider and T. Carell, *Nat. Chem.*, 2011, **3**, 794–800.

6. E. Kim and C. Switzer, *ChemBioChem*, 2013, **14**, 2403–2407.

7. (a) M. Yoshikawa, T. Kato and T. Takenishi, *Tetrahedron Lett.*, 1967, **50**,5065–5068; (b) M. Yoshikawa, T. Kato and T. Takenishi, *Bull. Chem. Soc. Jpn.*, 1969, **42**, 3505–3508.

8. W. Wu, D. E. Bergstrom and V. J. Davisson, *J. Org. Chem.*, 2003, **68**, 3860–3865.

9. V. Borsenberger, M. Kukwikila and S. Howorka, *Org. Biomol. Chem.*, 2009, **7**, 3826–3835.

10. J. Ludwig, F. Eckstein, *J. Org. Chem.*, 1989, **54**, 631–635.

11. J. C. Williams, L. Lin, M. Smith and Z.Huang, *Chem. Commun.* 2011, **47**, 8142–8144.

12. A. Sakamoto, *Master's thesis (Bioinorganic Chemistry Laboratory, Department of Chemistry, Graduate School of Science, The University of Tokyo)*, 2013

13. K. Tanaka, A. Tengeiji, T. Kato, N. Toyama, M. Shiro and M. Shionoya, *J. Am. Chem. Soc.*, 2002, **124**, 12494–12498.

14. S. Takada, *Master's thesis (Bioinorganic Chemistry Laboratory, Department of Chemistry, Graduate School of Science, The University of Tokyo)*, 2012

# Chapter 3

## Synthesis of Ligand-bearing Artificial DNAs by Template-independent DNA Polymerases

## 3-1. Introduction

As briefly described in section **1-6**, terminal deoxynucleotidyl transferases (TdT) can accept modified and artificial nucleotide triphosphates as enzymatic substrates (Fig. 3-1-1)[1–6,8] even though their nucleobases are significantly different in size and shape comparing with natural nucleobases (Figs. 3-1-1B and C). Therefore, TdT has been extensively utilized for 3′-end modification of DNAs to introduce various kinds of functionalities.

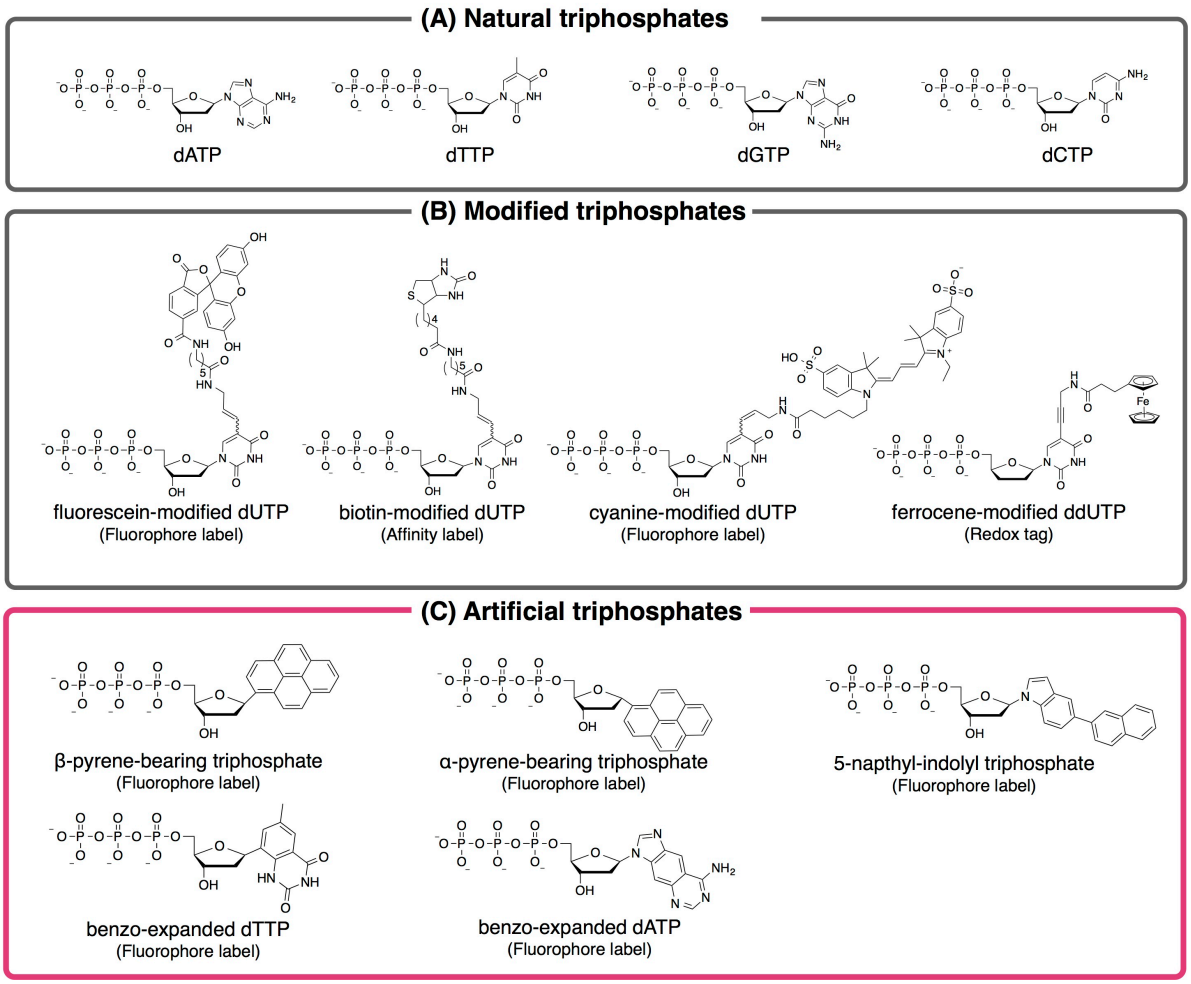


**Fig. 3-1-1** Nucleotide 5′-triphosphates that TdT can polymerize. **(A)** Natural triphosphates, **(B)** modified triphosphates and **(C)** artificial triphosphates possessing unnatural nucleobases.

For example, Kool et al. demonstrated TdT-catalyzed polymerization of fluorescent pyrene-bearing artificial nucleotide triphosphates (Fig. 3-1-1C).[5a] Both anomers (α and β) were found to act as the substrates of the polymerase and the DNA strands were tailed with 3–4 pyrene-bearing nucleotides. While the monomeric nucleotide had a fluorescence

emission maximum at 375 nm, the polymerized nucleotides showed the absorption maximum at 490 nm. This phenomenon suggested the formation of a pyrene excimer between the neighboring pyrenes. The enzymatic synthesis of the pyrene excimer was expected to be applied for biological assays of DNA fragmentation by apoptosis.

Moreover, Kool et al. reported that other fluorescent artificial nucleotide triphosphates were also successfully incorporated by TdT enzyme (Fig.3-1-1C).[5b] These nucleotide analogs include benzo-fused bicyclic or tricyclic unnatural nucleobases. Even though the nucleobases were significantly larger than natural ones, the reaction of the artificial triphosphates showed efficiency similar to those of natural ones.

As described above, TdT accepts artificial nucleotide triphosphates. It is a major advantage to incorporate artificial functionalities into the DNA nanoarchitectures. Therefore, I have been very interested by this unique nature of TdT in order to synthesize an artificial metallo-DNA.

In this **Chapter 3**, I have examined the TdT-catalyzed polymerization of a hydroxypyridone ligand-bearing triphosphate (d**H**TP) to synthesize ligand-bearing artificial DNA strands. The hydroxypyridone has a similar size and shape to those of natural thymine base (Fig. 3-1-2). Thus, it was expected that TdT incorporated d**H**TP efficiently to provide ligand-bearing artificial DNA oligomers. The enzymatically synthesized DNA was subsequently utilized to form metallo-DNA duplexes through the formation of $Cu^{II}$–mediated artificial base pairing (Fig. 3-1-3).

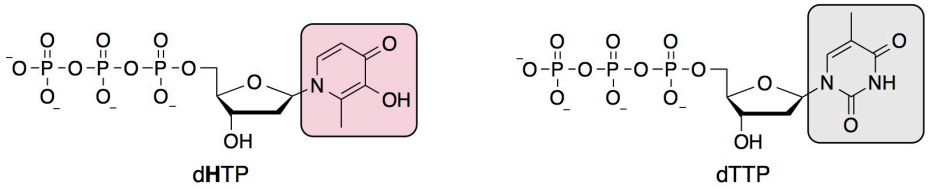


**Fig. 3-1-2** Comparison of the structures between artificial d**H**TP and natural dTTP.

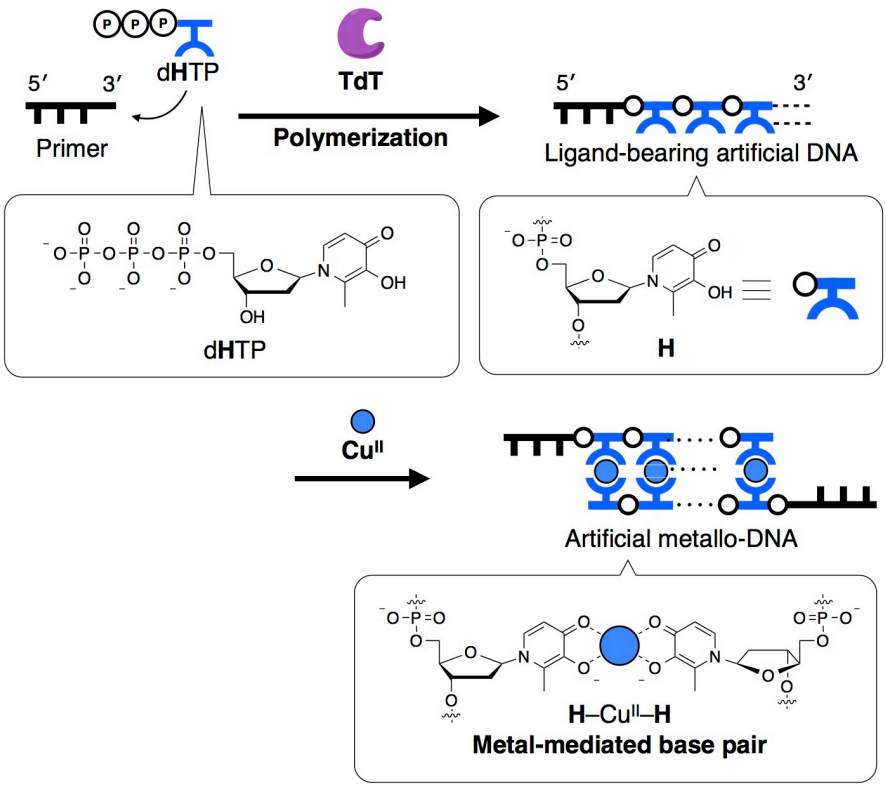


**Fig. 3-1-3** Schematic representation for the synthesis of artificial ligand-bearing artificial DNAs and the construction of metallo-DNA duplexes.

## 3-2. Enzymatic polymerization of dHTP and synthesis of the ligand-bearing artificial DNA possessing H nucleotides

I examined the TdT-catalyzed primer extension reaction with a hydroxypyridone-bearing nucleotides triphosphate (d**H**TP) to synthesize ligand-bearing artificial DNA. The reaction was followed with a 6-carboxyfluorescein (FAM)-labeled primer strand (5′-FAM-$dT_{20}$-3′) (Fig. 3-2-1A). The primer (5 μM) was incubated with 20 equiv. of the triphosphate (100 μM) in the presence of TdT enzyme (2 U/μM) at 37 °C for 24 h. The reaction products were analyzed by denaturing polyacrylamide gel electrophoresis (PAGE) (Fig. 3-2-1B). The gel image exhibited a characteristic ladder pattern, indicating that the TdT catalyzed the polymerization of d**H**TP similarly to natural triphosphate dTTP.

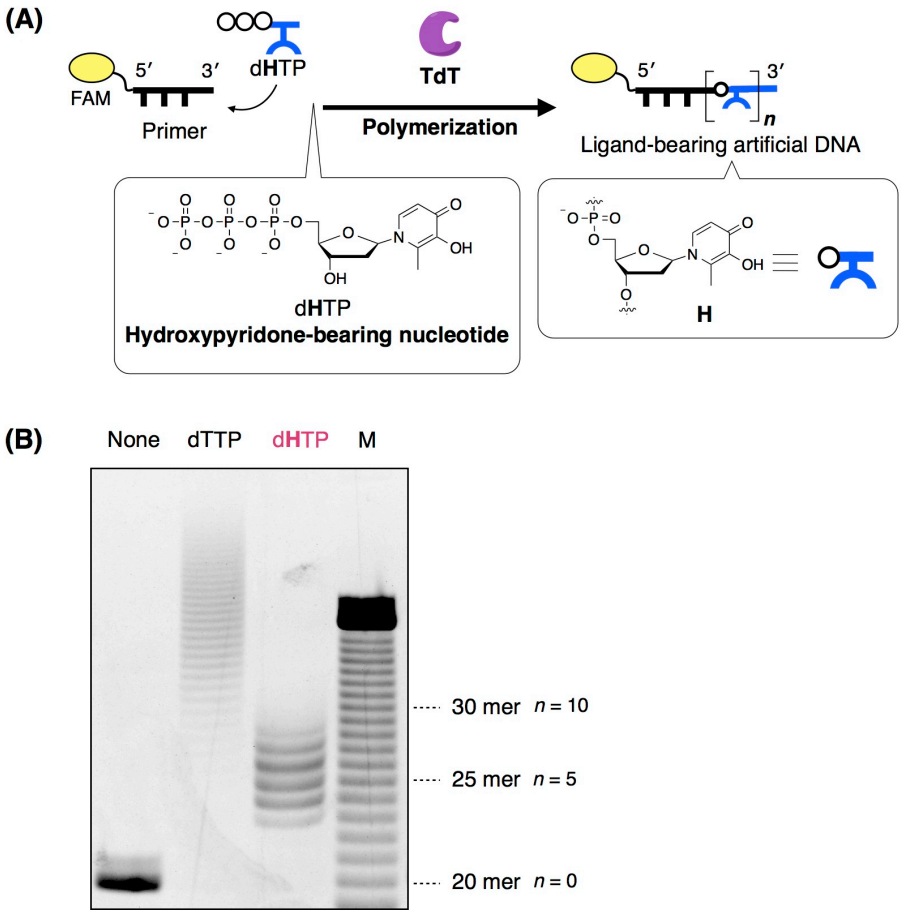


**Fig. 3-2-1 (A)** Schematic representation for TdT-catalyzed polymerization of d**H**TP. **(B)** Denaturing polyacrylamide gel electrophoresis (PAGE) analysis of the reaction products. The bands were detected by FAM fluorescence. [5′-FAM-$dT_{20}$-3′ (primer)] = 5.0 μM, [d**H**TP] = [dTTP] =100 μM, [TdT] = 2 U/μL in 20 mM Tris-acetate buffer (pH 7.9), 10 mM $Mg(OAc)_2$, 50 mM KOAc, 37 °C, 24 h.

Each band was ascribable to the DNA oligomers tailing with 3–7 **H** nucleotides (5′-FAM-$dT_{20}$-$\mathbf{H}_n$-3′ ($n$ = 3–7)). The average extension length of the DNA was roughly estimated to be 5 mer from band intensities. In the case of the reaction with dTTP, ~20 dTTPs were incorporated in average. This result showed that the polymerization of d**H**TP proceeded more slowly than that of natural dTTP, whose mechanism will be discussed in section **3-4**. Collectively, it was confirmed that TdT certainly accepted d**H**TP as a substrate and catalyzed the polymerization reaction.

The reaction products were identified utilizing MALDI-TOF mass spectrometry (Fig. 3-2-2). In the mass spectrum of the reaction mixture, a series of signals with intervals of $m/z$ = 303 were observed. The intervals $m/z$ were ascribable to the molecular weight of a hydroxypyridone-bearing nucleotide monophosphate ($C_{12}H_{14}NO_7P$) (Fig. 3-2-2A). In addition, the detected $m/z$ values were consistent with the calculated values for the DNA oligomers possessing 3–7 **H** nucleotides (5′-FAM-$dT_{20}$-$\mathbf{H}_n$-3′ ($n$ = 3–7), Table 3-2-1). Consequently, the mass spectrometric analysis revealed the sequential polymerization of 3–7 d**H**TP by TdT enzyme.

One of the main products possessing five **H** nucleotides at the 3′-end (5′-FAM-$dT_{20}$-$\mathbf{H}_5$-3′, **ODN-1**) was extracted from the gel and successfully isolated. **ODN-1** was also characterized by MALDI-TOF mass spectrometry (Fig. 3-2-2B). The detected $m/z$ value was 8077.5, which was consistent with the calculated value 8075.4.

**ODN-1** was further characterized by UV absorption spectroscopy (Fig. 3-2-3, 4). As shown in Fig. 3-2-3, the absorbance of **ODN-1** in a pH 7.0 buffer solution (black solid line) was significantly larger than that of the primer (black broken line). The difference spectrum (red line) showed an absorption maximum at 282 nm. It was consistent with the spectrum of five-fold **H** nucleoside monomers (blue line, $\lambda_{max}$ = 282 nm). This result suggested that the five **H** nucleotides were polymerized with their ligand moiety intact.

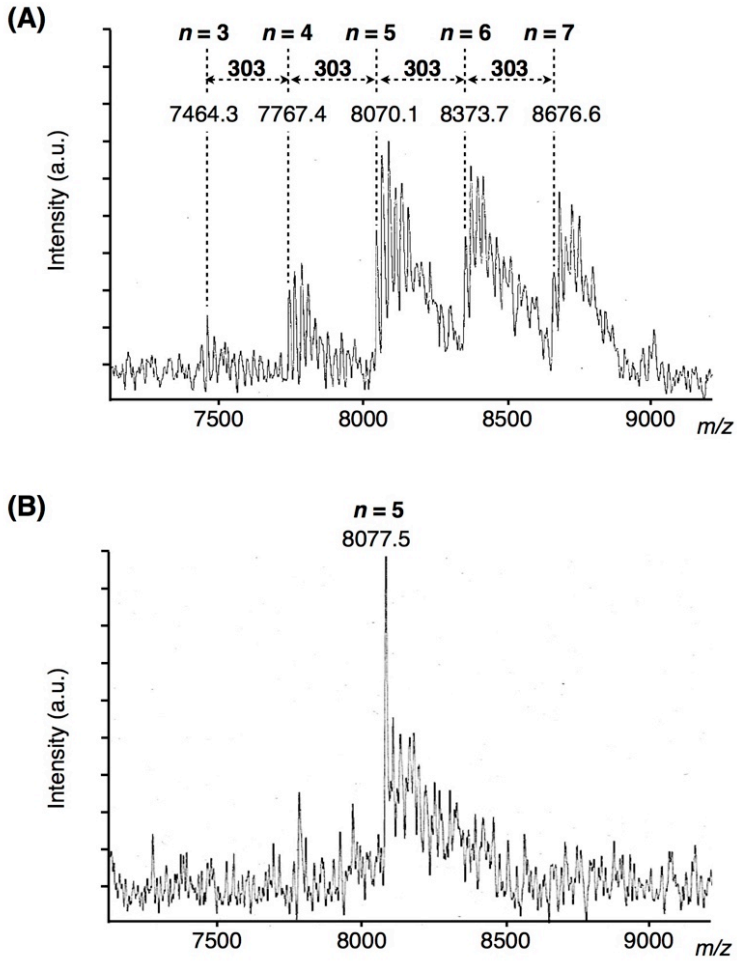


**Fig.3-2-2** Characterization of the reaction products obtained by the TdT-aided extension of a FAM-labeled primer strand using d**H**TP. MALDI-TOF mass spectrometric analysis of **(A)** the reaction mixture and **(B)** the isolated products 5′-FAM-$dT_{20}$-$\mathbf{H}_5$-3′ (**ODN-1**). Sodium adducts were also detected.

**Table 3-2-1** Observed and calculated mass values (*m*/*z*) of the enzymatically synthesized DNAs tailed with **H** nucleotides (5′-FAM-$dT_{20}$-$\mathbf{H}_n$-3′)

| *n* | Observed mass | Calculated mass $(M–H)^-$ |
|---|---|---|
| 3 | 7464.3 | 7469.0 |
| 4 | 7767.4 | 7772.2 |
| 5 | 8070.1 | 8075.4 |
| 6 | 8373.7 | 8378.6 |
| 7 | 8676.6 | 8681.8 |

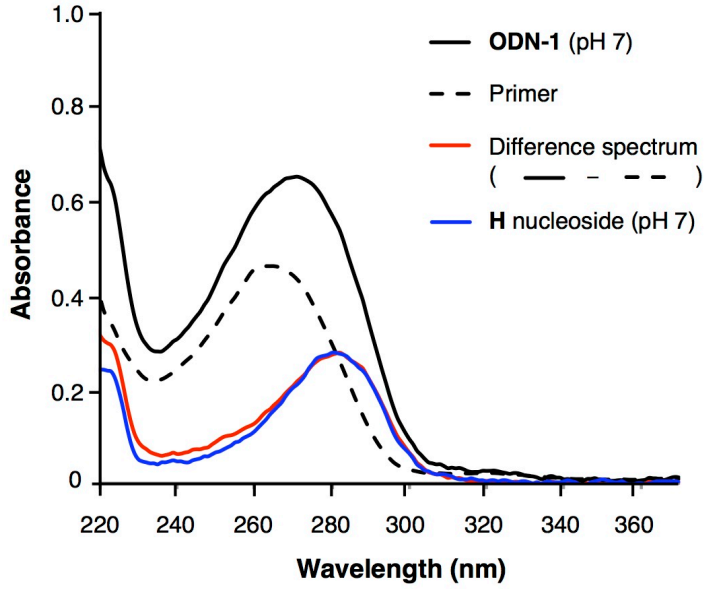


**Fig. 3-2-3** UV absorption spectra of the isolated product, 5′-FAM-dT$_{20}$-**H**$_5$-3′ (**ODN-1**) (36 $\mu$M) (black solid line). A spectrum of the primer (5′-FAM-dT$_{20}$-3′, 36 $\mu$M) (black broken line), difference spectra (red line), a spectrum of **H** nucleoside (180 $\mu$M) (blue line) are overlaid. In 100 mM HEPES buffer (pH 7.0), 500 mM NaCl, $l$ = 0.1 cm, at room temperature. Concentrations of the DNAs were determined based on the absorbance of the FAM moiety at $\lambda$ = 495 nm.

To get further evidence that the ligand moiety remained intact, the UV spectrum of **ODN-1** was additionally analyzed under a basic condition (in 0.1 M NaOH, pH 13) (Fig. 3-2-4). Because the p$K_a$ value of the hydroxy group of hydroxypyridone is 9.8,[7] the **H** nucleoside monomer is fully deprotonated under this condition, and thus exhibited a UV absorption maxima at $\lambda_{max}$ = 308 nm (blue line).

The spectrum of **ODN-1** showed a new absorption band around 310 nm (black line). The difference spectrum (red line) between **ODN-1** and the primer exhibited an absorption maximum at 308 nm, which was well fitted with the spectrum of five-fold **H** nucleoside monomers (blue line). This result revealed that the hydroxyl group of the **H** nucleotides in the DNA strand was deprotonated under a basic condition, consequently confirming that the ligand moieties were intact.

Taken together, UV absorption behaviors conclusively demonstrated that TdT catalyzed the primer extension reaction with **H** nucleotides intact. In the light of the fact that the ligand

moieties on the resulting DNA strands can complex with $Cu^{II}$ ions, the ligand-bearing artificial DNA oligomers appear to be successfully produced by the TdT-catalyzed reaction.

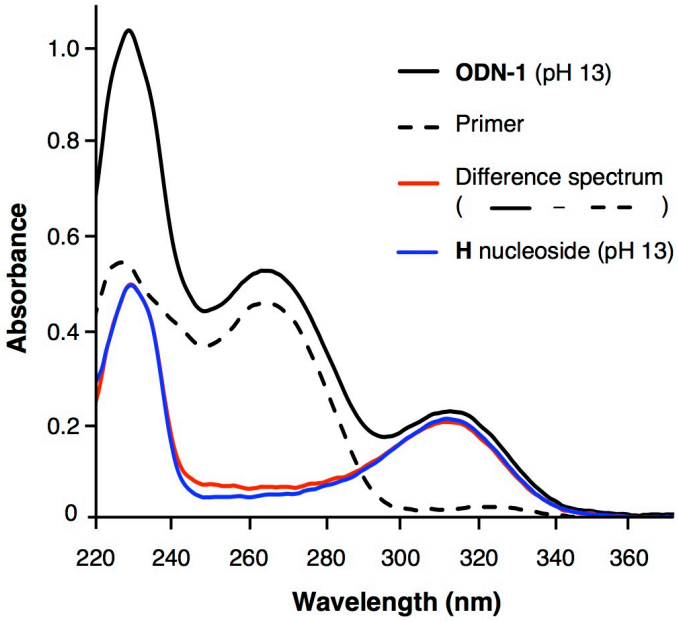


**Fig. 3-2-4** UV absorption spectra of the isolated product, 5′-FAM-$dT_{20}$-$\mathbf{H}_5$-3′ (**ODN-1**) (33 $\mu$M) (black solid line). A spectrum of the primer (5′-FAM-$dT_{20}$-3′, 33 $\mu$M) (black broken line), difference spectra (red line), a spectrum of **H** nucleoside (165 $\mu$M) (blue line) are overlaid. In 0.1 M NaOH (pH 13), $l$ = 0.1 cm, at room temperature. Concentrations of the DNAs were determined based on the absorbance of the FAM moiety at $\lambda$ = 495 nm.

## 3-3. Metal complexation of the enzymatically synthesized DNA

To confirm if the enzymatically synthesized DNA behaves identically with chemically synthesized DNA, I examined metal complexation of the enzymatically synthesized DNA possessing five **H** nucleotides (5′-FAM-dT$_{20}$-**H**$_5$-3′, **ODN-1**) by UV spectroscopic analysis (Figs. 3-3-1, 2).

**ODN-1** was reacted with 2.5 equiv. of Cu$^{II}$ ions (i.e. 0.5 equiv. per **H** nucleotide) in a pH 7.0 HEPES buffer solution. The UV spectrum showed that a new absorption band appeared around 303 nm (black solid line, Fig. 3-3-2). This spectral change indicated that **H**–Cu$^{II}$–**H** base pairs were formed from **H** nucleobases and Cu$^{II}$ ions in a 2:1 ratio.[9]

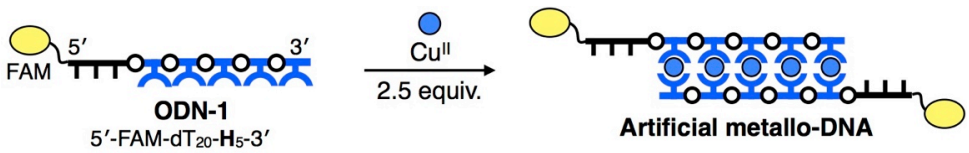


**Fig. 3-3-1** Schematic illustration of construction of artificial metallo-DNA from 5′-FAM-dT$_{20}$-**H**$_5$-3′, **ODN-1**.

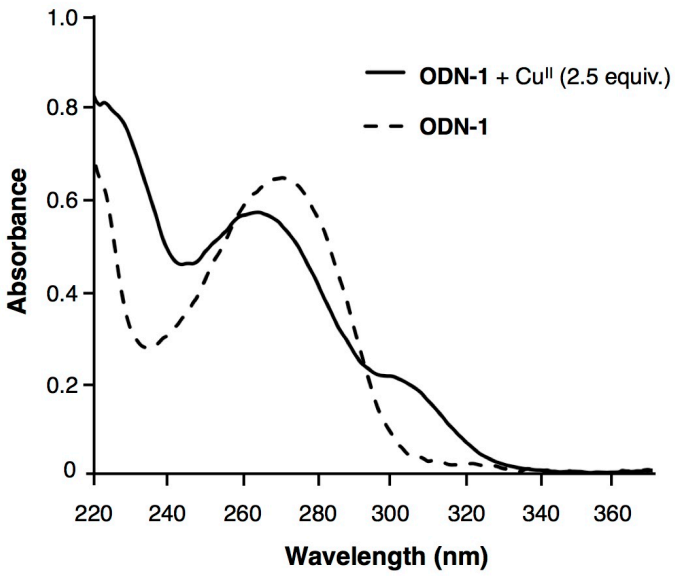


**Fig. 3-3-2** UV absorption spectral changes of the isolated product, 5′-FAM-dT$_{20}$-**H**$_5$-3′ (**ODN-1**) (36 $\mu$M) upon addition of Cu$^{II}$ ions. A spectrum of **ODN-1** with Cu$^{II}$ ions (90 $\mu$M, 2.5 equiv.) (solid line) and without Cu$^{II}$ ions (broken line), in 100 mM HEPES buffer (pH 7.0), 500 mM NaCl, $l$ = 0.1 cm, at room temperature. The concentration of the DNA was determined based on the absorbance of the FAM moiety ($\lambda$ = 495 nm).

Furthermore, a difference spectrum (red line, Fig. 3-3-3) of the complexation product and the primer strand was well fitted with a spectrum of 2.5 equiv. of the **H**–$Cu^{II}$–**H** complex (blue line). This result clearly showed that the **H**–$Cu^{II}$–**H** base pairs were quantitatively formed with the enzymatically synthesized DNA. Thus, this result led to a conclusion that the enzymatically synthesized DNA formed **H**–$Cu^{II}$–**H** base pairs in the same manner as chemically synthesized DNAs possessing **H** nucleotides.[10]

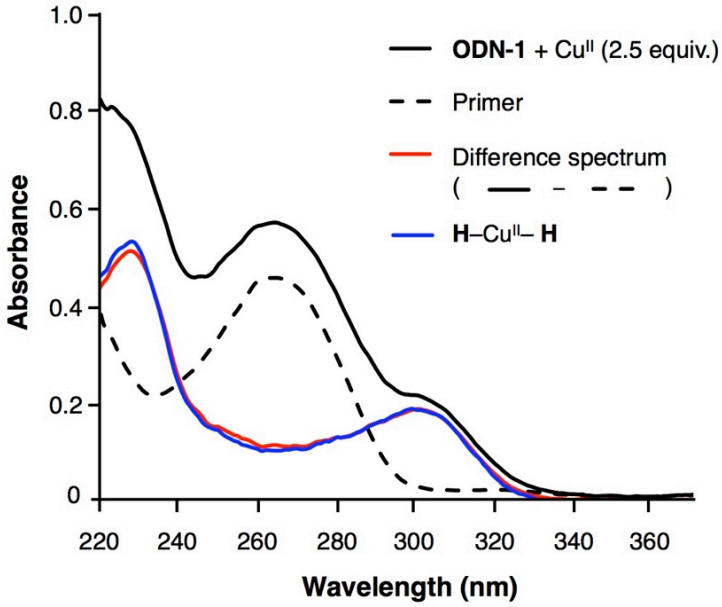


**Fig. 3-3-3** UV absorption spectra of the isolated product, 5′-FAM-$dT_{20}$-$\mathbf{H}_5$-3′ (**ODN-1**) (36 $\mu$M) of $Cu^{II}$ ions (90 $\mu$M, 2.5 equiv.) (black solid line). A spectrum of the primer (5′-FAM-$dT_{20}$-3′, 36 $\mu$M) (black broken line), difference spectra (red line), and the of **H**–$Cu^{II}$–**H** complex (90 $\mu$M) (blue line) are overlaid. In 100 mM HEPES buffer (pH 7.0), 500 mM NaCl, $l$ = 0.1 cm, at room temperature. The concentration of the DNA was determined based on the absorbance of the FAM moiety ($\lambda$ = 495 nm).

## 3-4. Insight into the reaction mechanism of the polymerization of dHTP

It is quite important to discuss detailed reaction mechanisms of enzymatic synthesis of the functionalized DNAs to make it more generalized. First, the TdT-catalyzed polymerization reaction of d**H**TP was compared with that of natural nucleotide triphosphates (dNTPs) (Figure 3-4-1). The reaction was conducted with 20 equiv. of triphosphates at 37 °C. In the case of the reactions with natural triphosphates, all dNTPs were mostly consumed after 24 h. In contrast, only 3–7 **H** nucleotides were incorporated at the 3′-end of the primer in spite of a substantial amount of d**H**TP remained. This result showed that the reaction of d**H**TP progressed but significantly more slowly than those of natural triphosphates.

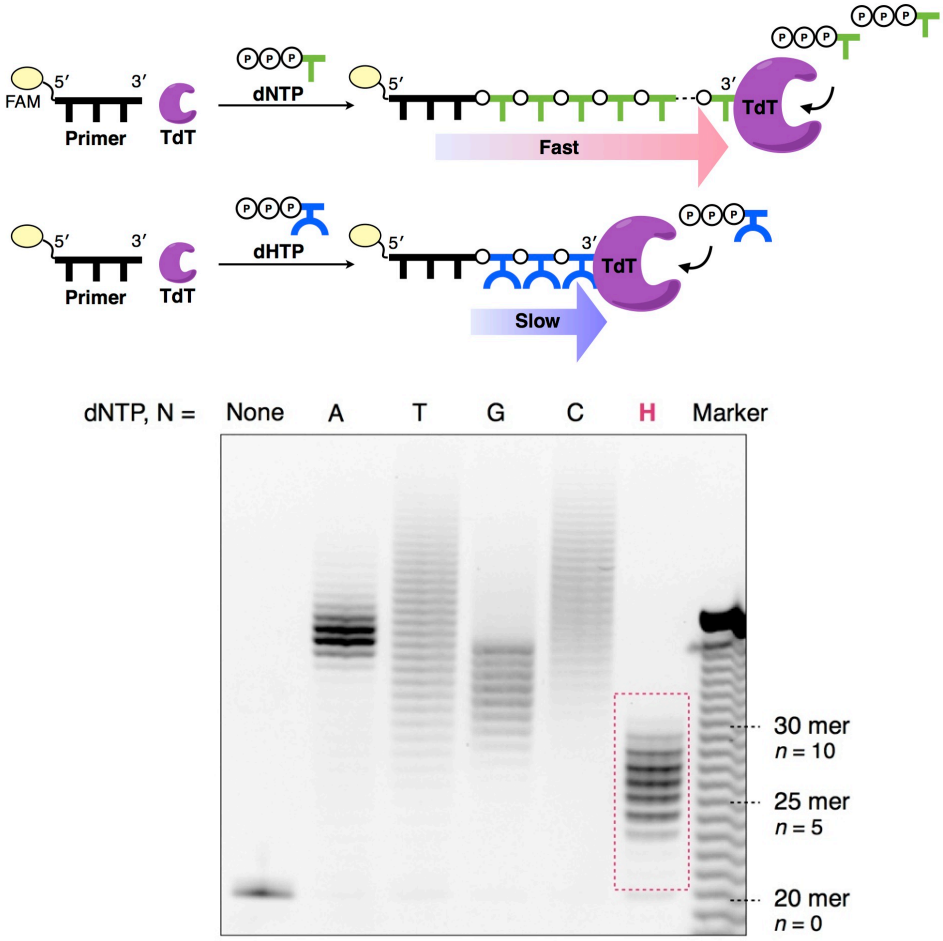


**Fig. 3-4-1** TdT-catalyzed primer extension of d**H**TP and natural nucleotide triphosphates (dNTP, N = A, T, G and C). [5′-FAM-$dT_{20}$-3′ (primer)] = 5.0 $\mu$M, [dNTP (N = A, T, G, C)] = [d**H**TP] = 100 $\mu$M, [TdT] = 2 U/$\mu$L in 20 mM Tris-acetate buffer (pH 7.9), 10 mM $Mg(OAc)_2$, 50 mM KOAc, 37 °C, 24 h. Denaturing PAGE analysis. The bands were detected by FAM fluorescence.

To investigate the details of the incorporation reaction, time course analysis of the enzymatic reaction was carried out. The average extension lengths of the products are plotted against the reaction time in Fig. 3-4-2. For the reaction with the natural triphosphates, the primer was extended by 15–20 nucleotides after 6 h, whereas the reaction with d**H**TP resulted in the extension only by 5 nucleotides even 24 h after. The rate of the d**H**TP polymerization seemed to be slowed down when the extension length reached 5 nucleotides. Even 48 h after no further extension was observed with the **H** oligomer despite the presence of excess amounts of d**H**TP (Fig. 3-4-3).

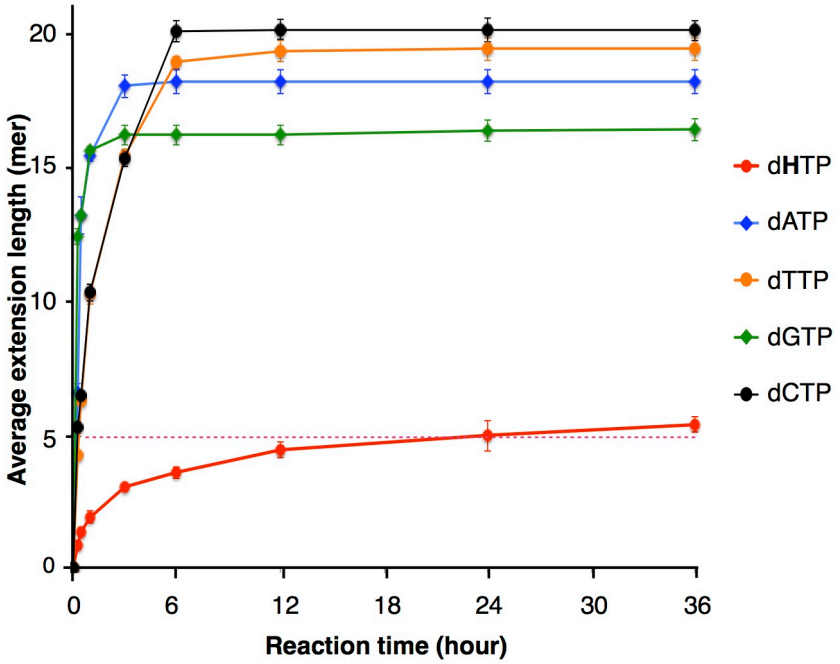


**Fig. 3-4-2** Plots of the average extension length of DNA products against the reaction time (reaction time = 0, 0.25, 0.5, 1, 3, 6, 12, 24, 36 h) using 20 equiv. of nucleotide triphosphates. The averaged values were estimated based on the intensity of the gel images evaluating the results of at least three independent runs with standard errors.

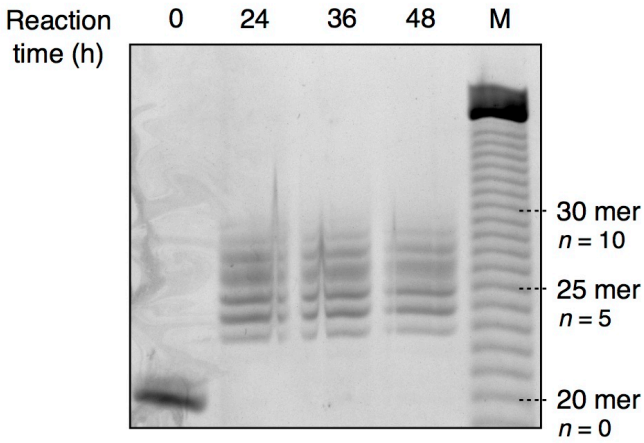


**Fig. 3-4-3** Time-course analysis of the polymerization of d**H**TP. [Primer (5′-FAM-$dT_{20}$-3′)] = 5.0 $\mu$M, [d**H**TP] = 100 $\mu$M (20 equiv.), [TdT] = 2 U/$\mu$L, in 20 mM Tris-acetate buffer (pH 7.9), 10 mM $Mg(OAc)_2$, 50 mM KOAc, 37 °C, 24–48 h. Denaturing PAGE analysis.

Moreover, although the polymerization reaction was examined with increasing concentrations of d**H**TP (40 and 80 equiv.) (Fig. 3-4-4), no further extension was observed, indicating that the concentrations of the triphosphate little affected the extension length of the products. As shown in the time-course analyses (Fig. 3-4-5), the incorporation reaction seemed to stall after elongation with five **H** nucleotides regardless of the d**H**TP concentrations.

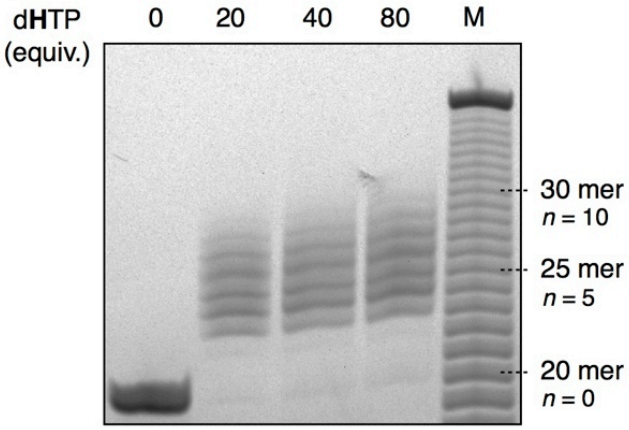


**Fig. 3-4-4** Concentration dependence of the polymerization reaction of d**H**TP. [Primer (5′-FAM-$dT_{20}$-3′)] = 5.0 $\mu$M, [d**H**TP] = 100, 200 and 400 $\mu$M (20, 40 and 80 equiv. respectively), [TdT] = 2 U/$\mu$L, in 20 mM Tris-acetate buffer (pH 7.9), 10 mM $Mg(OAc)_2$, 50 mM KOAc, 37 °C, 24 h. Denaturing PAGE analysis.

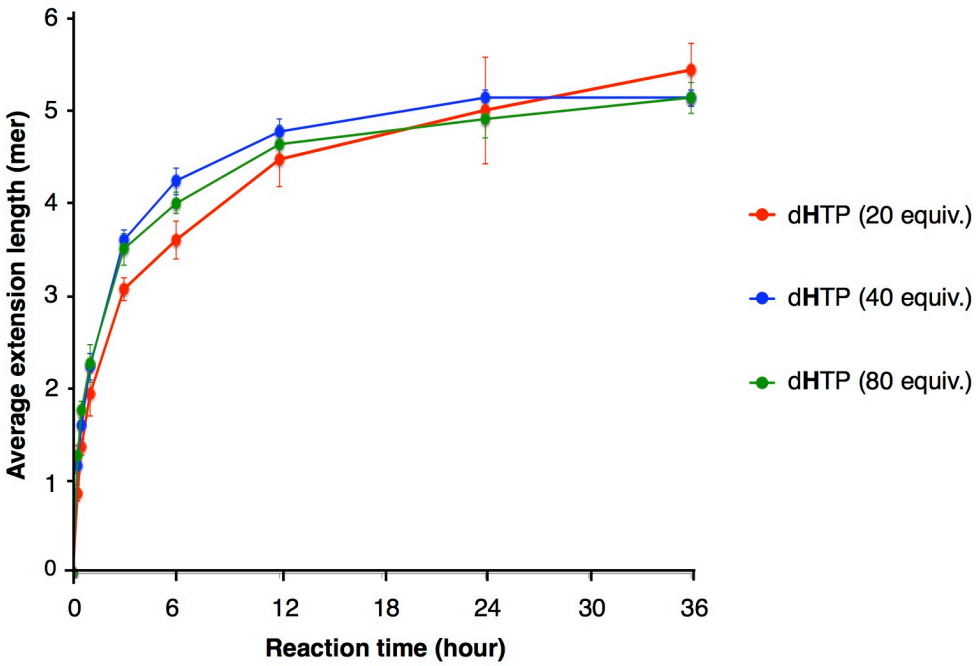


**Fig. 3-4-5** Plots of the average extension length of DNA products against the reaction time (reaction time = 0, 0.25, 0.5, 1, 3, 6, 12, 24, 36 h) using 20, 40 and 80 equiv. of d**H**TP. The averaged values were estimated based on the intensity of the gel images evaluating the results of at least three independent runs with standard errors.

Taken all the results together, it appears that the TdT-catalyzed reaction was halted after about five **H** nucleotides were appended into the DNA primer strands. There are three possible reasons for the termination of the reaction: **(1)** the unnatural hydroxypyridone-bearing nucleotide triphosphate is inherently a poor substrate for TdT enzyme due to the difference in the structure and the electrostatic actions, **(2)** d**H**TPs can form complexes with enzymatic co-factor $Mg^{II}$ ions, which decreases the effective concentration of the substrates and **(3)** the DNA oligomeric products possessing several **H** nucleotides did not act as a primer for the reaction. More detailed explanation is given below.

**(1)** As shown in Fig. 3-4-2, the incorporation of d**H**TP was significantly slower than that of natural nucleotide triphosphates. Since d**H**TP and natural triphosphates have the same triphosphate ($P_3O_9^{4-}$) and sugar backbone structures (Fig. 3-4-6A), the difference is only the nucleobase moiety. Thus, it is apparent that the unnatural nucleobase moiety of d**H**TP (i.e. hydroxypyridone moiety, Fig. 3-4-6B) may cause slowdown of the reaction due to unfavorable interactions with the enzyme.

According to the reported X-ray crystal structure of the TdT binary complex with natural nucleotide (PDB ID code 1KEJ),[8,11] the nucleobase moiety of an incoming nucleotide has favorable π–π stacking and π–cation interactions with the surrounding amino acid residues.

The hydroxypyridone has a methyl group at the 2-position (Fig. 3-4-6B, blue circle) and a hydroxyl group at the 3-position (green circle), which are significant differences between the structures of thymine and hydroxypyridone. So the methyl and hydroxy groups of hydroxypyridone may cause steric constraint and electrostatic interactions with surrounding amino residues to disturb the incorporation of d**H**TP and significantly decrease the rate of the d**H**TP polymerization.

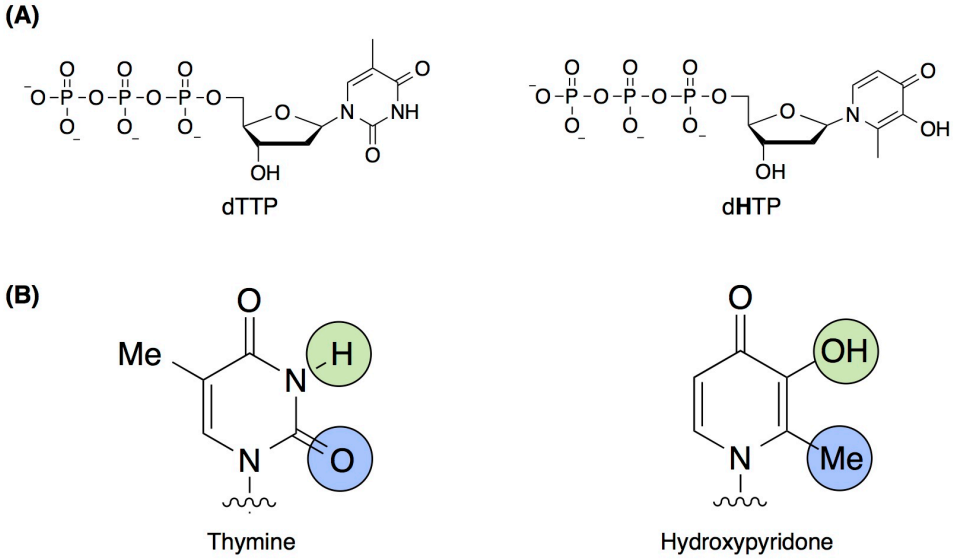


**Fig. 3-4-6** Structural comparisons **(A)** between nucleotide triphosphates, dTTP and d**H**TP and **(B)** between their nucleobase moieties.

**(2)** Another possible reason is that d**H**TPs form complexes with enzymatic co-factor $Mg^{II}$ ions and thereby the effective substrate concentrations are decreased. The complexation behavior of d**H**TP with $Mg^{II}$ ions was estimated by titration experiments with UV spectroscopic analysis (Fig. 3-4-7). The concentration of d**H**TP was set to 100 μM based on the reaction condition. Without $Mg^{II}$ ions, the UV absorption spectrum of d**H**TP has an absorption maximum at 282 nm (blue line). Upon addition of $Mg^{II}$ ions (0.1–100 mM), the absorption band around 282 nm gradually decreased and a new absorption band appeared around 303 nm. Appearance of the band around 303 nm suggested the deprotonation of the

hydroxypyridone hydroxyl group at the 3-position. As the pH value (7.0) was not changed upon addition of $Mg^{II}$ ions, this UV spectral change was apparently caused by the metal complexation of d**H**TPs with $Mg^{II}$ ions. In particular, in the presence of 10 mM $Mg^{II}$ ions (the same as the reaction condition), the absorption around 282 nm was reduced to about two-thirds, while the new absorption around 303 nm increased three-fold (red line). Consequently, under the enzymatic reaction condition (10 mM $Mg^{II}$), a significant amount of d**H**TP formed complexes with $Mg^{II}$ ions and the concentration of metal-free d**H**TP substrate decreased.

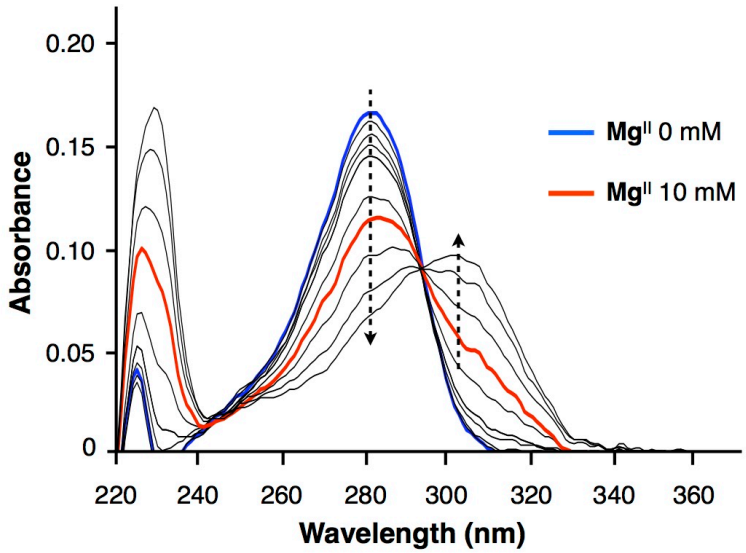


**Fig. 3-4-7** UV absorption changes of d**H**TP (100 $\mu$M) at various concentrations of $Mg^{II}$ ions (0, 0.1, 0.5, 1.0, 2.0, 5.0, 10, 20, 50, 100 mM). A spectrum of the d**H**TP without $Mg^{II}$ (blue line) and that with $Mg^{II}$ (10 mM) (red line) in 25 mM MOPS buffer (pH 7.0), $l$ = 0.1 cm, at room temperature.

**(3)** One more possible reason is that the extended DNAs possessing about five **H** nucleotides at the 3′ ends are no longer recognized by the enzyme, due to the differences in the structure and/or electrostatic actions between natural and unnatural nucleotides. This hypothesis is supported by the fact that TdT enzyme requires at least three nucleotides as a primer.[12] An example of a similar stall of the polymerization was reported with other modified oligonucleotides.[5]

To discuss in more detail, TdT-catalyzed incorporation of nucleotide triphosphates into an unnatural primer possessing five **H** nucleotides was examined (5′-FAM-$dT_{20}$-$\mathbf{H}_5$-3′, **ODN-1**)

(Figs. 3-4-8, 9). In the control experiment with a natural primer strand (5′-FAM-dT$_{20}$-3′) (Fig. 3-4-8), natural triphosphates dTTPs were efficiently incorporated into the primer and almost all the primers were extended at least 0.25 h after. The reaction was almost completed at least in 12 h (see also Fig. 3-4-2).

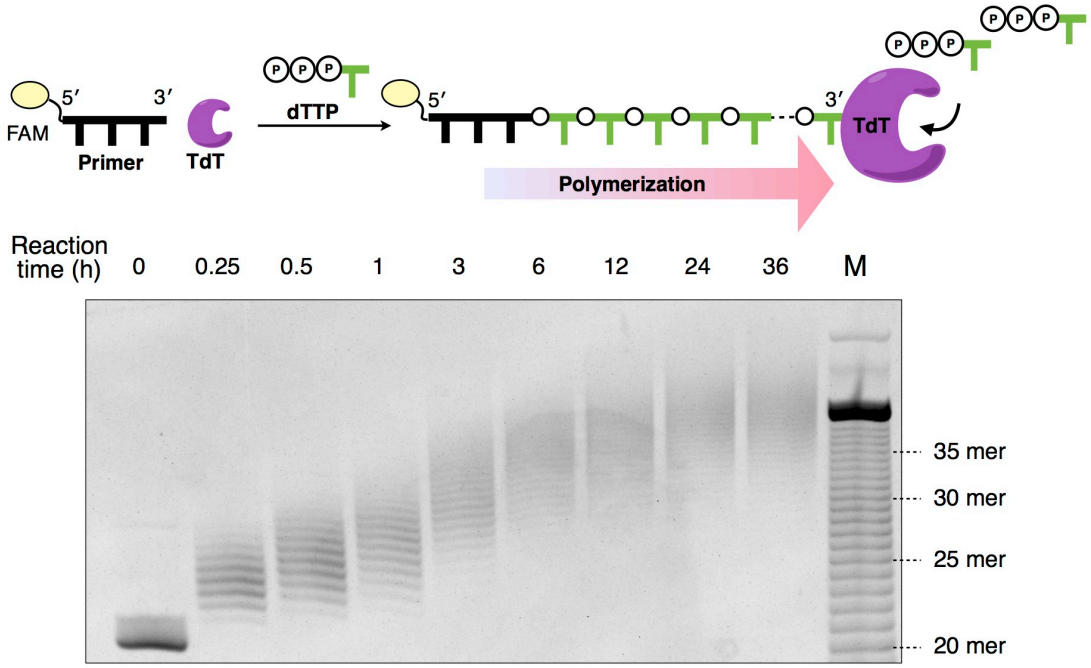


**Fig. 3-4-8** Time-course analyses of TdT-catalyzed incorporation of dTTP into the natural primer (5′-FAM-dT$_{20}$-3′). [Primer] = 5.0 $\mu$M, [dTTP] = 100 $\mu$M (20 equiv.), [TdT] = 2 U/$\mu$L in 20 mM Tris-acetate buffer (pH 7.9), 10 mM Mg(OAc)$_2$, 50 mM KOAc, 37 °C, 0, 0.25, 0.5, 1, 3, 6, 12, 24 and 36 h. Denaturing PAGE analysis. The bands were detected by FAM fluorescence.

On the other hand, the incorporation of the triphosphate (dTTP and d**H**TP) into the unnatural primer (5′-FAM-dT$_{20}$-**H**$_5$-3′, **ODN-1**) hardly proceeded even 36 h after (Fig. 3-4-9).

The TdT-mediated reaction the natural primer proceeded efficiently (Fig. 3-4-8). In contrast, the reaction with the unnatural primer **ODN-1** did not proceed at all regardless of the kind of triphosphates (dTTP and d**H**TP) (Fig. 3-4-9). The enzymatic recognition of DNA primers may be disturbed on the unnatural **H**$_5$ oligomer moiety.

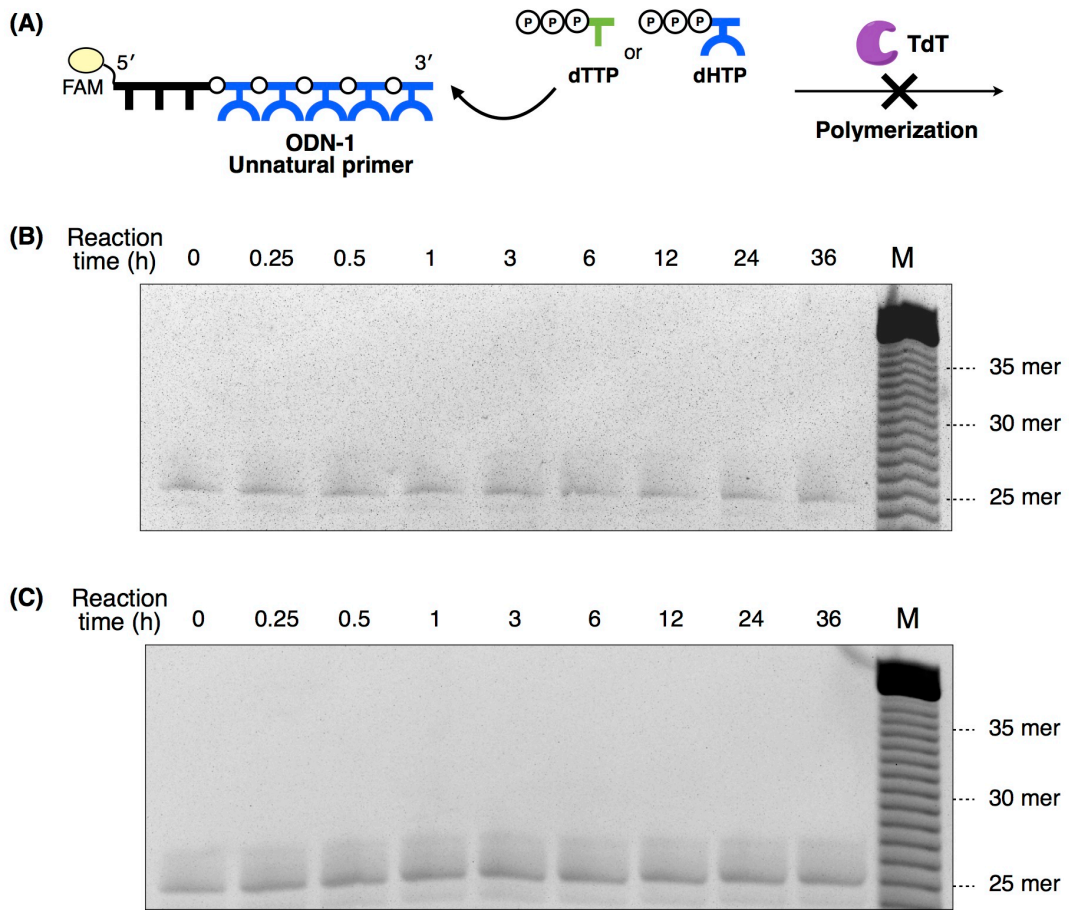


**Fig. 3-4-9** TdT-catalyzed incorporation of nucleotide triphosphates using the unnatural primer (5′-FAM-dT$_{20}$-**H**$_5$-3′, **ODN-1**). **(A)** Schematic representation of the reaction. Time-course analyses of the incorporation reaction of **(B)** dTTP and **(C)** d**H**TP into **ODN-1**. [Primer] = 5.0 $\mu$M, [dTTP and d**H**TP] = 100 $\mu$M (20 equiv.), [TdT] = 2 U/$\mu$L in 20 mM Tris-acetate buffer (pH 7.9), 10 mM Mg(OAc)$_2$, 50 mM KOAc, 37 °C, 0, 0.25, 0.5, 1, 3, 6, 12, 24 and 36 h. Denaturing PAGE analysis. The bands were detected by FAM fluorescence.

In general, a DNA primer is recognized by TdT though the interactions with surrounding amino acid residues that constitute the active site of TdT, as is the case for recognition of nucleotide triphosphates.[8,11,13] As reported on X-ray structural analysis of the TdT-DNA complex,[8,11,13] DNA strands form a B-type DNA conformation in the active site. Thus, it can be inferred that the unnatural **H**$_5$ DNA oligomer did not form B-type conformation, probably because hydroxyl and methyl groups of **H** nucleotides provided steric hindrance and/or electrostatic repulsion with adjacent nucleobases and the surrounding amino residues (see also Fig. 3-4-6B). Consequently, the unnatural DNA weakened its affinity to the TdT enzyme, and the DNA was eventually dissociated from the enzyme to terminate the DNA synthesis.

In addition, as shown in Fig. 3-4-7, **H** nucleotides can form complexes with $Mg^{II}$ ions. Therefore, it is likely that the $\mathbf{H_5}$ DNA oligomers form complexes with $Mg^{II}$, which may induce a folded DNA structure. As TdT has a steric gate to discriminate single-stranded DNAs from double-stranded DNAs,[11,13] TdT hardly recognizes the possibly folded DNA structures. Therefore, the folding of the $\mathbf{H_5}$ oligomer in the presence of $Mg^{II}$ ions may reduce the binding affinity to the enzyme, which results in the stall of DNA synthesis.

Indeed, similar phenomena were previously observed with the formation of G-quadruplex (complexation of guanines with potassiums).[14] Therefore, similarly to this report, the unnatural primer **ODN-1** may be rejected by the enzyme.

## 3-5. Optimization of the reaction condition for the synthesis of longer artificial DNA strands

In the previous sections, I demonstrated that TdT-mediated polymerization is an excellent method to obtain artificial DNA strands with several **H** nucleotides, and also discussed why the polymerase reaction was stalled. The synthesis of longer ligand-bearing DNA strands has been strongly desired in terms of the application for the construction of DNA-based metal nanowires. To overcome the limitation of the TdT-catalyzed polymerization of d**H**TP, there are two possible strategies: **(I)** changing the enzymatic co-factor (divalent metal ions) to alter the fidelity and efficiency of TdT polymerase and **(II)** increasing the concentration of DNA primers to facilitate the binding of DNA strands with the enzyme to promote the processive DNA synthesis. More detailed explanation is given below.

**(I)** The effect of metal co-factors on the polymerization reaction was examined to facilitate further elongation of **H** nucleotides. It was reported that the co-factors directly change the fidelity and efficiency of enzymatic reactions.[8,15] Thus, the polymerization of d**H**TPs was expected to further progress by changing the type of metal co-factors.

The TdT-catalyzed reaction was carried out in the presence of conventional co-factors, namely $Mg^{II}$, $Co^{II}$ and $Mn^{II}$ ions (Fig. 3-5-1).[8,15] In the reaction with natural dTTP (Fig. 3-5-1A), the polymerization of 5–20 dTTPs was observed after 24 h regardless of the kinds and the concentrations of metal ions. By contrast, the polymerization reaction with d**H**TP was significantly affected by the metal co-factors (Fig. 3-5-1B). Compared with a reaction under a usual reaction condition (10 mM $Mg^{II}$), the reaction was significantly slower to extend only 3-5 d**H**TPs in the presence of 10 mM $Co^{II}$ or $Mn^{II}$ ions.

To confirm whether or not complexation between d**H**TP and these metal ions may decrease the effective concentration of substrates to inhibit the enzymatic reaction (cf. section **3-4**, **(2)**), the concentration of these metal ions was then decreased. In the presence of 1.0 mM $Co^{II}$ or 0.1 mM $Mn^{II}$, the polymerization reaction proceeded more efficiently and yielded DNA strands tailed with about 5–10 d**H**TPs (Fig. 3-5-1B). Moreover, in the presence of 1.0

mM $Mg^{II}$ ions (about tenth concentration of usual reaction conditions), the reaction was a little improved and 5–7 d**H**TPs were polymerized.

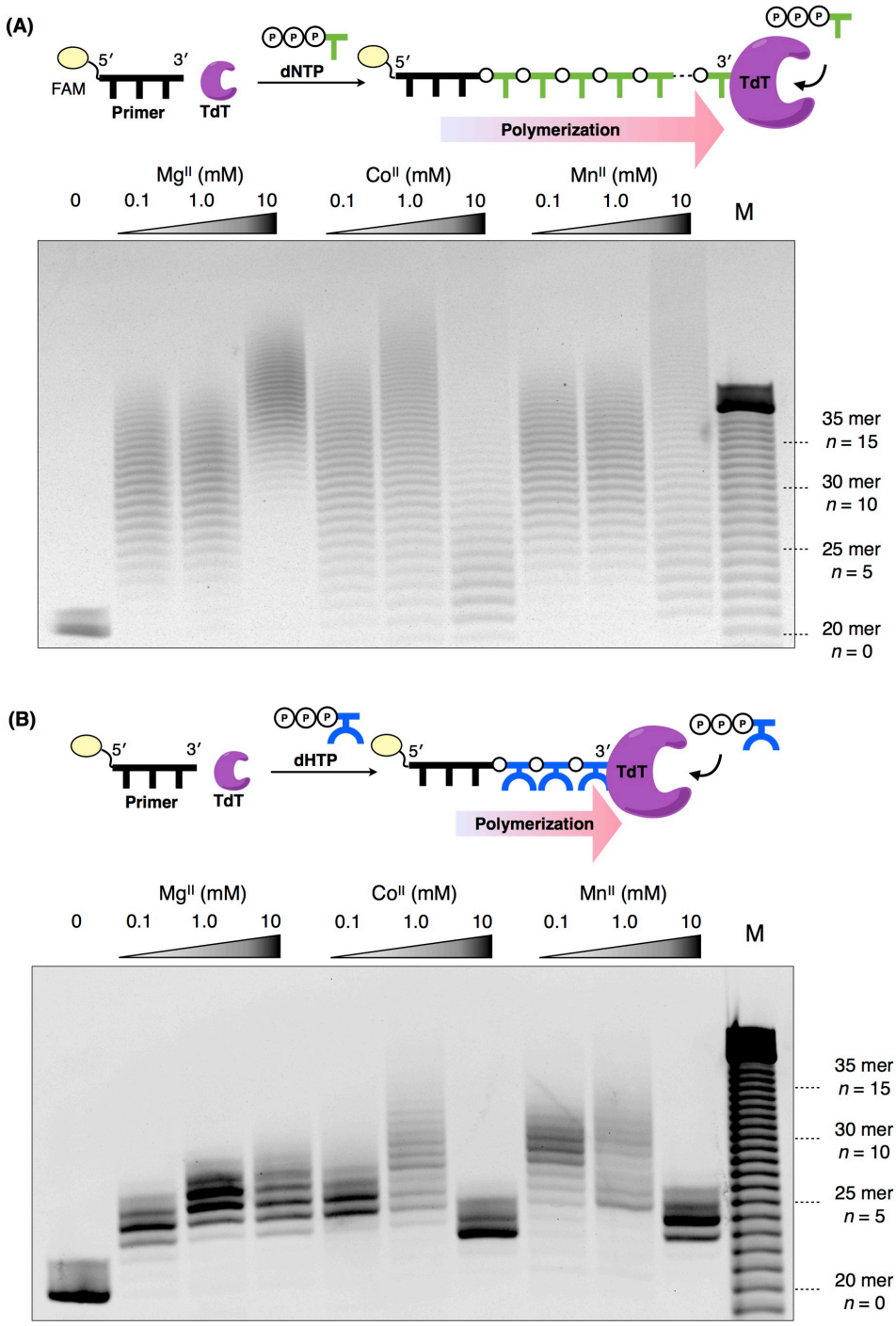


**Fig. 3-5-1** Effects of divalent metal cations on TdT catalyzed reaction of **(A)** natural dTTP and **(B)** artificial d**H**TP. [Primer (5′-FAM-$dT_{20}$-3′)] = 5.0 $\mu$M, [dTTP and d**H**TP] = 100 $\mu$M (20 equiv.), [TdT] = 2 U/$\mu$L, [$MCl_2$ (M = Mg, Co, Mn)] = 0.1, 1.0 10 mM in 20 mM Tris-acetate buffer (pH 7.9), 50 mM KOAc, 37 °C, 24 h. Denaturing PAGE analysis. The bands were detected by FAM fluorescence.

The concentration effects of $Mg^{II}$ ions on the reaction were further investigated (Fig. 3-5-2). Regardless of the concentrations of $Mg^{II}$ ions, about 20 dTTP was polymerized by TdT. In other words, the polymerization reaction of dTTP was little affected by the concentrations of $Mg^{II}$ ions. In contrast, with a decrease in the concentration of $Mg^{II}$ ions, the reaction of d**H**TP significantly proceeded. In particular, in the presence of 2.0 mM $Mg^{II}$ ions, 10–15 d**H**TP were polymerized.

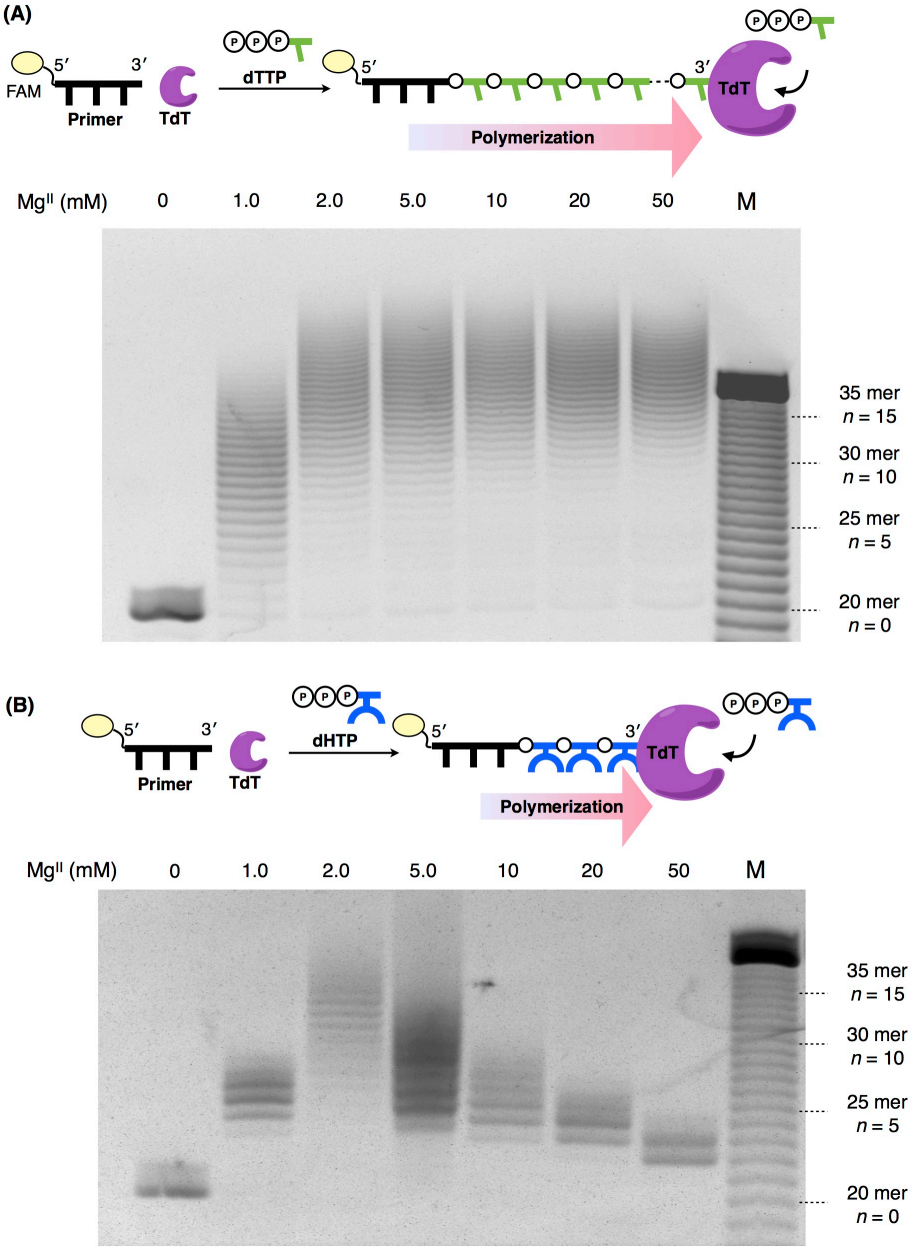


**Fig. 3-5-2** Effects of the concentrations of $Mg^{II}$ ions on TdT-catalyzed polymerization of **(A)** natural dTTP and **(B)** artificial d**H**TP. [Primer (5′-FAM-$dT_{20}$-3′)] = 5.0 $\mu$M, [dTTP and d**H**TP] = 100 $\mu$M (20 equiv.), [TdT] = 2 U/$\mu$L, [$MgCl_2$] = 0, 1.0, 2.0, 5.0, 10, 20, 50 mM, 37 °C, 24 h. Denaturing PAGE analysis. The bands were detected by FAM fluorescence.

Taken together, these results suggest that, by changing the type of metal co-factors or adjusting concentrations of the metal co-factors, TdT-mediated polymerization of d**H**TP can be promoted. Based on the denaturing PAGE analysis in Fig. 3-5-2, the best condition of the concentration of $Mg^{II}$ ions for the polymerization was determined to be 2.0 mM.

**(II)** Secondly, in order to promote further DNA extension, the concentration of the DNA primer was increased to facilitate the DNA binding with the enzyme (Fig. 3-5-3). As discussed in section **3-4 (3)**, the artificial DNA products seemed difficult to be recognized by TdT. Thus, increasing the DNA concentration was thought to be effective to force the DNAs to bind the enzyme and consequently facilitates the polymerization reaction.

The reaction was carried out using 25 μM of the DNA primer (5′-FAM-$dT_{20}$-3′), which was a five-fold concentration of the standard reaction condition. The primer was incubated with 20 equiv. of the triphosphate (500 μM) in the presence of TdT enzyme (2 U/μM) in the same buffer solution at 37 °C for 24 h. Then, the extended DNA products were analyzed by denaturing PAGE (Fig. 3-5-3).

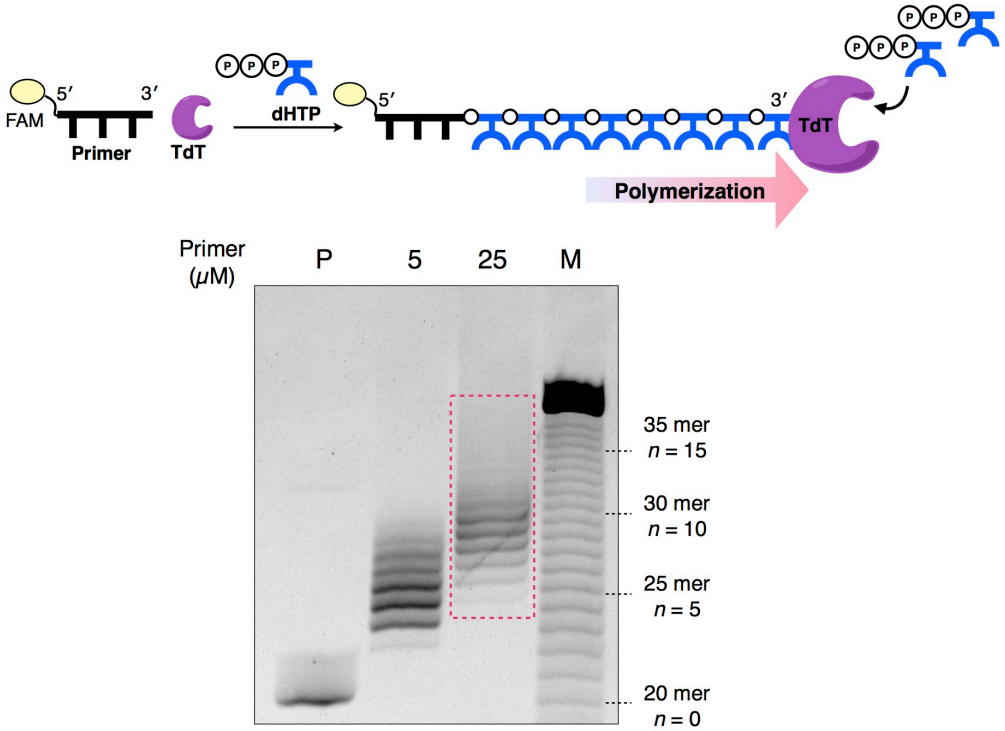


**Fig. 3-5-3** Primer extension reactions with different concentrations of the primer. [Primer (5′-FAM-$dT_{20}$-3′)] = 5.0, 25 μM, [d**H**TP] = 100, 500 μM, [TdT] = 2 U/μL in 20 mM Tris-acetate buffer (pH 7.9), 10 mM $Mg(OAc)_2$, 50 mM KOAc, 37 °C, 24 h. The bands were detected by FAM fluorescence. P: primer, M: ladder marker.

The gel image exhibited that the longer DNA was formed compared to the previous reaction (red square, Fig. 3-5-3). The average extension length of the DNA was roughly estimated to be about 10 mer based on the band intensities, which was twice as long as the products obtained under the standard condition (5 μM primer). This result proved that the polymerization of d**H**TP further proceeded with the high concentration of the DNA primer.

After removal of residual d**H**TP and enzymes, the reaction products were identified utilizing MALDI-TOF mass spectrometry (Fig. 3-5-4A). The mass spectrum of the reaction mixture exhibited a series of signals, which were ascribable to the DNA oligomers possessing 5–11 **H** nucleotides (5′-FAM-$dT_{20}$-$\mathbf{H}_n$-3′ ($n$ = 5–11)). Thus the mass spectrometric analysis also confirmed the further elongation of the DNA with **H** nucleotides.

UV absorption spectroscopic analysis also showed evidence of the further tailing of **H** nucleotides (Fig. 3-5-4B). The difference spectrum (red line) of the products and the primer was well fitted with the spectrum of tenfold **H** nucleoside monomers (blue line). This result suggests that TdT polymerized about 10 d**H**TP in average.

Thus, the increase in the DNA concentration is effective for further elongation of the artificial DNAs with **H** nucleotides.

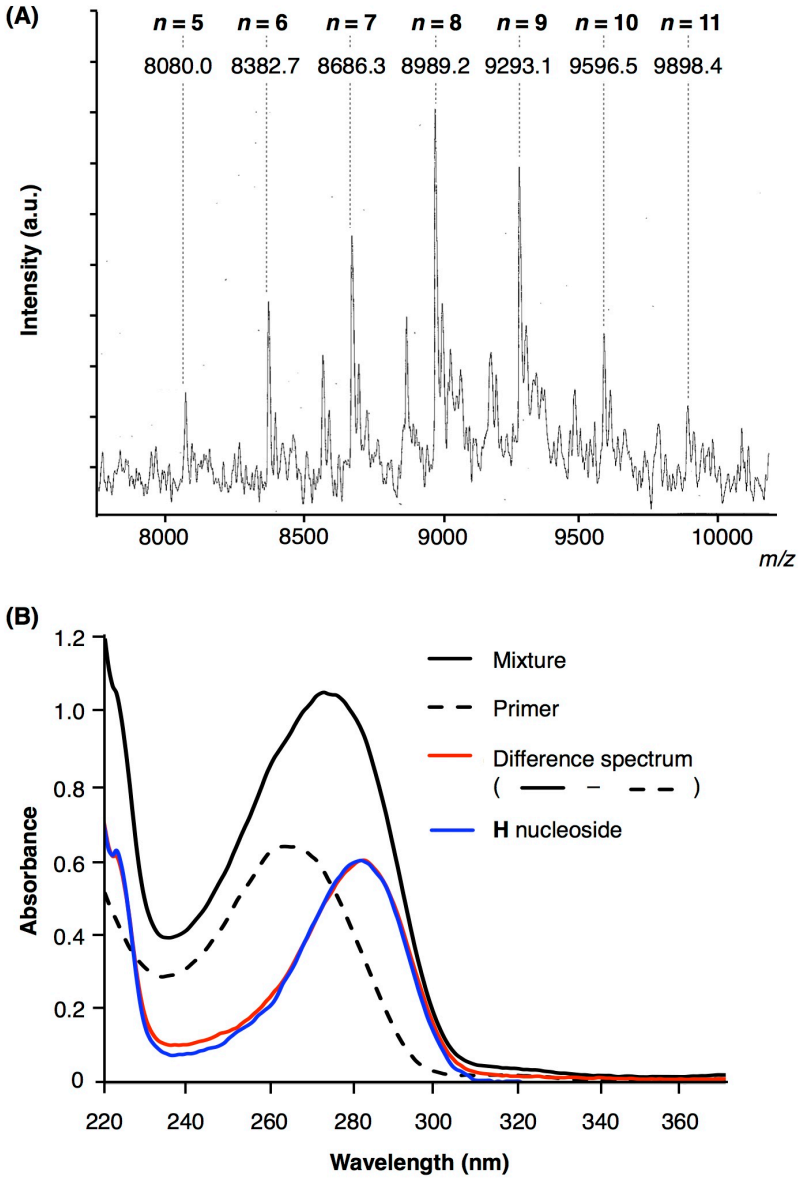


**Fig. 3-5-4 (A)** MALDI-TOF mass spectrometric analysis of the reaction mixture. **(B)** UV absorption spectra of the reaction mixture (36 $\mu$M) (black solid line). A spectrum of the primer (36 $\mu$M) (black broken line), difference spectra (red line), a spectrum of **H** nucleoside (360 $\mu$M) (blue line) are overlaid. In 100 mM HEPES buffer (pH 7.0), 500 mM NaCl, $l$ = 0.1 cm, at room temperature. Concentrations of the DNAs were determined based on the absorbance of the FAM moiety at $\lambda$ = 495 nm.

## 3-6. Conclusion

In this **Chapter 3**, I described TdT-catalyzed synthesis of ligand-bearing artificial DNAs. In conclusion, sequential polymerization of d**H**TP proceeds to generate ligand-bearing artificial DNAs, whose ligand moieties remained intact. The metal-mediated base pairs (**H**–$Cu^{II}$–**H**) were quantitatively formed in the enzymatically synthesized ligand-bearing artificial DNAs in a fashion similar to chemically synthesized DNAs to produce the artificial metallo-DNA duplex.[10,19]

I found that the incorporation of d**H**TP was stalled after tailing with about 5 **H** nucleotides, as TdT-catalyzed polymerization did not proceed with the artificial DNA possessing 5 **H** nucleotides (**ODN-1**). This result lead to a conclusion that the artificial DNA tailed with **H** nucleotides did not act as the DNA primer, which result is one of the explanations for the termination of the DNA synthesis. Furthermore, the concentrations of metal co-factors, primers and substrates was optimized to realize the synthesis of longer ligand-bearing DNA strands, which would provide an important clue to its application for DNA-based metal nanowires.

Our group has developed not only the **H** nucleoside but also other ligand-bearing nucleosides including mercaptopyridone- (**M**),[16] hydroxypyridinethione- (**S**)[16] and 5-hydroxyuracil-bearing nucleosides ($\mathbf{U^{OH}}$),[17] which form metal-mediated base pairs with appropriate metal ions (for example, $Ni^{II}$, $Pt^{II}$, $Pd^{II}$ and $Gd^{III}$) (Fig. 3-6-1). As these ligand-bearing nucleotides are similar to the **H** nucleotide in terms of size and shape, TdT-catalyzed DNA-synthesis would be applicable for other ligand-bearing nucleotides.

Considering that enzymatic polymerization allows post-synthetic and site-selective modification of DNA constructs, the method developed in this study would be applied for the functionalization of DNA-based supramolecular structures such as DNA origami, DNA polyhedra and DNA-peptide conjugates. This aspect will be discussed in **Chapter 4**.

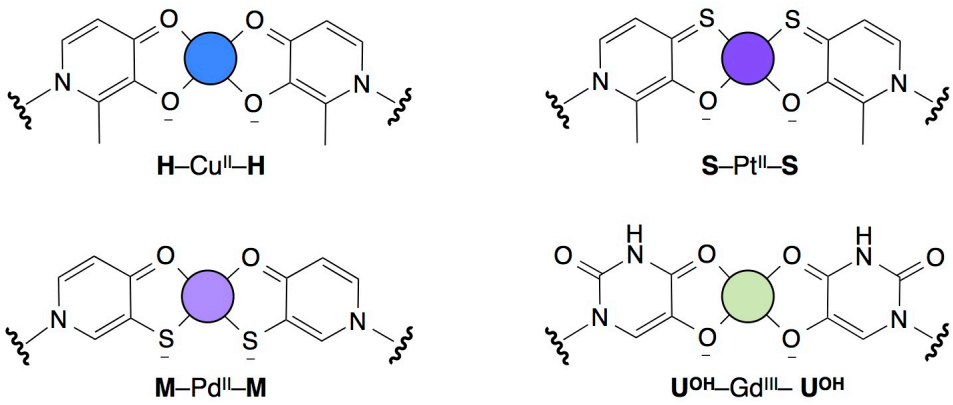


**Fig. 3-6-1 Schematic illustration for other metal-mediated base pairs. (refs. 16, 17, 19)**

## 3-7. Experimental

### Materials and methods

Natural DNA primer strands including 6-carboxyfluorescein (FAM)-labeled ones were purchased from Japan Bio Service Co., Ltd. in HPLC purification grade. Terminal deoxynucleotidyl transferase (TdT) and Terminal Transferase Reaction Buffer was purchased from New England Biolabs, Inc. The FAM-labeled single-stranded DNA ladder marker was prepared by the treatment of a FAM-labeled $T_{38}$ oligomer with DNase I (Promega). $MgCl_2 \cdot 6H_2O$ (98% purity), $CoCl_2 \cdot 6H_2O$ (99.5%) and $MnCl_2 \cdot 4H_2O$ (99%) were purchased from Wako Pure Chemical Industries. $CuSO_4 \cdot 5H_2O$ (99.9%) was purchased from Soekawa Chemical Co. EDTA was purchased from Nacalai Tesque. 3-Hydroxypicolinic acid was purchased from Sigma-Aldrich. HEPES and MOPS were purchased from Dojindo. The other reagents (Tris, KCl, NaCl, NaOH, ammonium citrate, glycerol, bromophenol blue, boric acid and acetic acid) were purchased from Wako Pure Chemical Industries. Matrix assisted laser desorption ionization-time-of-flight (MALDI-TOF) mass spectra were recorded on Bruker ultrafleXtreme. UV spectra were measured using Thermo Scientific NanoDrop 2000 spectrophotometer with a path length of 0.1 cm. Denaturing polyacrylamide gel electrophoresis (PAGE) was carried out with 21% polyacrylamide gel with 7 M urea in a TBE buffer (90 mM Tris, 90 mM boric acid, 50 mM EDTA, pH 8.3). The gels were analyzed using Alpha imager mini (LMS) and a blue-LED (470 nm) transilluminator (Optocode).

### A typical procedure for the enzymatic reactions

A FAM-labeled DNA primer (5′-FAM-$dT_{20}$-3′) and triphosphates were combined on ice in 1 × Terminal Transferase Reaction Buffer (20 mM Tris-acetate (pH 7.9), 50 mM KOAc and 10 mM $Mg(OAc)_2$). After addition of TdT, the mixture was incubated at 37 °C for 24 h. The final concentration of each component was as follows: 2 U/μL TdT, 5 μM primer and 100 μM triphosphates (20 equiv.). The reaction was quenched by a 5:2:6 mixture of 500 mM EDTA, a loading solution (30% glycerol, 0.25% bromophenol blue) and 10 M urea. The

mixture was immediately heated at 95 °C for 5 min. The products were analyzed by denaturing PAGE. The band intensities were quantified using ImageJ (NIH).

### Time-course analysis of the enzymatic reactions using the natural DNA primer

The DNA primer (5 μM, 5′-FAM-d$T_{20}$-3′) was incubated with natural triphosphates (dNTP, N = A, T, G, C) (100 μM) or d**H**TP (100, 200 and 400 μM) in the presence of TdT (2 U/μL) in the 1 × reaction buffer for 0.25, 0.5, 1, 3, 6, 12, 24 and 36 h at 37 °C. The reaction was quenched by the typical procedure. The products were analyzed by denaturing PAGE. The number-average molecular length of products was estimated based on the band intensities. The results were plotted against the reaction time. The standard error represented as the error bar. The experiments were carried out at least three times independently.

### Mass spectral analysis of the reaction mixture

The reaction mixture (5′-FAM-d$T_{20}$-$\mathbf{H}_n$-3′, $n$ = 3, 4, 5...) was roughly purified and desalted, and then characterized by MALDI-TOF mass spectrometry (Fig. 3-2-2A, Fig. 3-6-4A). The enzymatic reaction was carried out with a total volume of 50 μL. After incubation at 37 °C for 24 h, the reaction was quenched by 500 mM EDTA (50 μL), and then the mixture was heated at 95 °C for 5 min. The resulting solution was then subjected to a reverse-phase column chromatography (Poly-Pak Packing (Glen Research), $H_2O$:MeCN = 1:0–8:2). After isopropanol precipitation, the sample was desalted by gel filtration chromatography (Sephadex G-25 Fine, GE Healthcare) and by the treatment with a cation-exchange resin (Dowex 50W×8, 50–100 mesh, The DOW Chemical Company) as an $NH_4^+$-form. MALDI-TOF MS measurements were conducted using a mixture of 3-hydroxypicolinic acid and ammonium citrate as matrix.

### UV absorption spectral analysis of the reaction mixture

UV spectral analysis was performed to confirm the incorporation of **H** nucleotides (Fig. 3-6-4B). The desalted mixture (5′-FAM-d$T_{20}$-$\mathbf{H}_n$-3′, $n$ = 3, 4, 5...) was dissolved in 100 mM HEPES buffer (pH 7.0) containing 500 mM NaCl and subjected to the UV measurements at

room temperature. The concentration of the DNA was determined based on the absorbance of the FAM moiety ($\lambda$ = 495 nm, $\varepsilon_{495}$ = 3.75 × $10^4$ $M^{-1}$ $cm^{-1}$ at pH 7.0)

### Mass and UV absorption spectral analysis of the ODN-1

One of the reaction products possessing 5 **H** nucleotides (5′-FAM-$dT_{20}$-$\mathbf{H}_5$-3′, **ODN-1**) was isolated from the gel and characterized by MALDI-MS analysis (Fig. 3-2-2B) and UV absorption spectroscopy (Figs. 3-2-3, 4). The enzymatic reaction was carried out under concentrated conditions ([primer] = 25 μM, [d**H**TP] = 500 μM, [TdT] = 2 U/μL) with a total volume of 240 μL. After incubation at 37 °C for 24 h, the reaction was quenched by EDTA (240 μL, 500 mM). The resulting solution was immediately heated at 95 °C for 5 min and then subjected to a denaturing PAGE. After running the gel, **ODN-1** was extracted from gel slices using Model 422 Electro-Eluter (Bio-Rad). The extracts were purified by a reverse-phase column chromatography (Poly-Pak™ Packing (Glen Research), $H_2O$:MeCN = 1:0–8:2) and by isopropanol precipitation.

Prior to mass measurements, the sample was desalted by gel filtration chromatography and by the treatment with a cation-exchange resin (Dowex 50W×8, 50–100 mesh, The DOW Chemical Company) as an $NH_4^+$-form. The measurement was conducted using a mixture of 3-hydroxypicolinic acid and ammonium citrate as matrix.

The sample for UV measurement was desalted by gel filtration chromatography (Sephadex G-25 Fine, GE Healthcare) and then dissolved in a pH 7 buffer (100 mM HEPES buffer (pH 7.0), 500 mM NaCl) or a pH 13 solution (0.1 M NaOH). The concentration of the oligonucleotide was determined based on the absorbance of the FAM moiety ($\lambda$ = 495 nm, $\varepsilon_{495}$ = 3.75 × $10^4$ $M^{-1}$ $cm^{-1}$ at pH 7.0 and $\varepsilon_{495}$ = 7.50 × $10^4$ $M^{-1}$ $cm^{-1}$ at pH 13).[18]

### Metal complexation of the enzymatically synthesized DNA (ODN-1)

The isolated product **ODN-1** (36 μM) was mixed with 2.5 equiv. of $CuSO_4$ (90 μM) in a 100 mM HEPES buffer (pH 7.0) containing 500 mM NaCl. After incubation at 25 °C for 1 h, the UV spectra were measured at room temperature.

### Time-course analysis of the enzymatic reactions using the unnatural DNA primer (ODN-1)

The unnatural DNA primer (5 μM, **ODN-1**) was incubated with 20 equiv. of d**H**TP and TdT (2 U/μL) in the 1 × reaction buffer at 37 °C for 0.25, 0.5, 1, 3, 6, 12, 24 and 36 h. After the reaction was quenched by the typical procedure, the reaction mixture was analyzed by denaturing PAGE.

### Investigation of the effects of the metal co-factors on the polymerization reaction

The natural primer (5 μM, 5′-FAM-$dT_{20}$-3′) and 20 equiv. of triphosphates (100 μM, dTTP or d**H**TP) were mixed with TdT (2 U/μL) in a handmade reaction buffer containing 20 mM Tris and 50 mM KCl (the pH was adjusted to 7.9 using acetic acid) and various concentrations of divalent metal ions as follows: $MnCl_2$ (0.1, 1.0 and 10 mM) or $CoCl_2$ (0.1, 1.0 and 10 mM) or $MgCl_2$ (0.1, 1.0, 2.0, 5.0, 10, 20 and 50 mM). The mixture was incubated at 37 °C. After 24 h, the reaction was quenched by the typical procedure. The reaction mixtures were analyzed by denaturing PAGE. The band intensities were quantified using ImageJ (NIH).

### Investigation of the enzymatic synthesis with the high concentration of the DNA primer

The DNA synthesis was carried out by the typical procedure in the presence of the natural primer (25 μM), 20 equiv. of d**H**TP (100 μM) and TdT (2 U/μL).

### Titration experiment of dHTP with $Mg^{II}$ ions

The triphosphate d**H**TP (100 μM) was mixed with various concentrations of $MgCl_2$ (1.0, 2.0, 5.0, 10, 20, 50 and 100 mM) in a 25 mM MOPS buffer (pH 7.0). After incubation at 25 °C for 1 h, the UV spectra were measured at room temperature. The concentration of d**H**TP was determined based on the absorbance at 260 nm under application of the extinction coefficient of the unmodified **H** nucleoside ($\varepsilon_{260} = 5.34 \times 10^3\ M^{-1}\ cm^{-1}$).[19]

## 3-8. References


1 Y. Gavrieli, Y. Sherman and S. A. Ben-Sasson, *J. Cell Biol.*, 1992, **119**, 493–501.

2 V. Tjong, H. Yu, A. Hucknall, S. Rangarajan and A. Chilkoti, *Anal. Chem.*, 2011, **83**, 5153–5159.

3 (a) A. Anne, B. Blanc and J. Moiroux, *Bioconjugate Chem.* 2001, **12**, 396-405; (b) A. Anne, C. Bonnaudat, C. Demaille and K. Wang, *J. Am. Chem. Soc.*, 2007, **129**, 2734–2735; (c) P. Horáková, H. Macíčková-Cahová, H. Pivoňková, J. Špaček, L. Havran, M. Hocek and M. Fojta, *Org. Biomol. Chem.*, 2011, **9**, 1366–1371.

4 M. Hollenstein, *Org. Biomol. Chem*., 2013, **11**, 5162–5172.

5 (a) Y. Cho and E. T. Kool, *ChemBioChem*, 2006, **7**, 669–672; (b) S. K. Jarchow-Choy, A. T. Krueger, H. Liu, J. Gao and E. T. Kool, *Nucleic Acids Res*., 2011, **39**, 1586–1594; (c) M. Hollenstein, F. Wojciechowski and C. J. Leumann, *Bioorg. Med. Chem. Lett*., 2012, **22**, 4428–4430.

6 A. J. Berdis and D. McCutcheon, *ChemBioChem*, 2007, **8**, 1399–1408.

7 Ali El-Jammal, P. L. Howell, M. A. Turner, N. Li and D. M. Templeton, *J. Med. Chem*., 1994, **37**, 461-466

8 (a) J. D. Fowler and Z. Suo, *Chem. Rev*., 2006, **106**, 2092–2110; (b) E. A. Motea and A. J. Berdis, *Biochim. Biophys. Acta*, 2010, **1804**, 1151–1166.

9 K. Tanaka, A. Tengeiji, T. Kato, N. Toyama, M. Shiro and M. Shionoya, *J. Am. Chem. Soc*., 2002, **124**, 12494–12498.

10 K. Tanaka, A. Tengeiji, T. Kato, N. Toyama and M. Shionoya, *Science*, 2003, **299**, 1212–1213.

11 M. Delarue, J. B. Boule, J. Lescar, N. Expert-Bezancon, N. Jourdan, N. Sukumar, F. Rougeon and C. Papanicolaou, *EMBO J*., 2002, **21**, 427–439.

12 K. I. Kato, J. M. Goncalves, G. E. Houts and F. J. Bollum, *J. Biol. Chem.*, 1967, **242**, 2780–2789.

13 J. Gouge, S. Rosario, F. Romain, P. Beguin and M. Delarue, *J. Mol. Biol.*, 2013, **425**, 4334–4352

14 L. Oganesian, I. K. Moon, T. M. Bryan and M. B. Jarstfer, *EMBO J.*, 2006, **25**, 1148–1159

15 (a) M. R. Deibel Jr. and M. S. Coleman, *J. Biol. Chem.*, 1980, **255**, 4206–4212; (b) L. M. Chang and F. J. Bollum, *J. Biol. Chem.*, 1990, **265**, 17436–17440.

16 Y. Takezawa, K. Tanaka, M. Yori, S. Tashiro, M. Shiro and M. Shionoya, *J. Org. Chem.*, 2008, **73**, 6092–6098.

17 Y. Takezawa, K. Nishiyama, T. Mashima, M. Katahira and M. Shionoya, *Chem. – Eur. J.*, 2015, **21**,14713–14716.

18 (a) K. Kuzelov, D. Grebenova and Z. Hrkal, *Cytometry A.*, 2007, **71A**, 605–611; (b) R. Fischer, K. Köhler, M. Fotin-Mleczek and R. Brock, *J Biol Chem.*, 2004, **279**, 12625–12635; (c) T. B. Updegrove, J. J. Correia, Y. Chen, C. Terry and R. M. Wartell, *RNA*, 2011, **17**, 489–500.

19 K. Tanaka, A. Tengeiji, T. Kato, N. Toyama, M. Shiro and M. Shionoya, *J. Am. Chem. Soc.*, 2002, **124**, 12494–12498.

# Chapter 4

## Post-synthetic Modification of DNA Duplexes and Metal-mediated Assembly of the DNAs

## 4-1. Introduction

As overviewed in section **1-3** of **Chapter 1**, DNA has been widely utilized as a molecular scaffold to array functional components such as metallic nanoparticles and biomolecules.[1–13] The resulting DNA nanoconjugates exhibit structure-specific unique properties such as photonic, catalytic and dynamic properties, depending on the spatial configuration of the individual components. Therefore, the structural regulation of DNA nanoconjugates has been challenging for the last decade.

To achieve this, artificial-metallo DNAs are excellent candidates (**Chapter 1**, section **1-4**). The metallo-DNAs can endow specific physiochemical properties to the DNA structures (geometry, dynamics and stability etc.).[14] Furthermore, geometry of coordination structures in metallo-base pairs varies with the innate characteristics of metal ions and ligands. Thus, metallo-DNAs possibly provide key structural motifs to regulate self-assembly modes of DNA nanostructures.

There is a report that DNA nanostructures can be modified by enzyme post-synthetically and site-selectively.[15] For example, TdT-mediated DNA synthesis was utilized for the modification of DNA block copolymer nanoparticles[16] and DNA origami nanostructures.[17] Thus, post-synthetic incorporation of ligand-bearing artificial nucleotides by TdT is a powerful tool to endow DNA hybrid materials with metal-responsive properties.

In **Chapter 3**, I successfully synthesized ligand-bearing artificial DNA possessing hydroxypyridone nucleotides (**H**) by utilizing TdT enzyme. Furthermore, the obtained artificial DNA strands quantitatively formed artificial metallo-DNAs through the formation of metallo-base pairs (**H**–$Cu^{II}$–**H**) (Fig. 3-3-3 and Fig. 4-1-1A). Subsequently, in **Chapter 4**, I will discuss the enzymatic modification of DNA nanostructures with the artificial metallo-DNA structures toward future application to regulate DNA assembly. To verify the usability of the enzymatic synthesis, a simple DNA duplex was used as a model structure of the targeted DNA nanoarchitectures (Fig. 4-1-1B).

TdT polymerase is known to start a reaction from 3′-protruding end (2–4 mer) of the duplex efficiently, but this enzyme inefficiently recognizes a 3′-blunt end of the duplex as the primer.[18] In fact, TdT has been utilized for site-selective labeling of the 3′-protruding end of

DNA duplexes in medical studies.[19] Therefore, I investigated the TdT-catalyzed incorporation of d**H**TP using a DNA duplex with a 2 mer protruding end. Subsequently, metal-mediated assembly of modified DNA duplex was studied to investigate their metal-responsiveness (Fig. 4-4-1B).

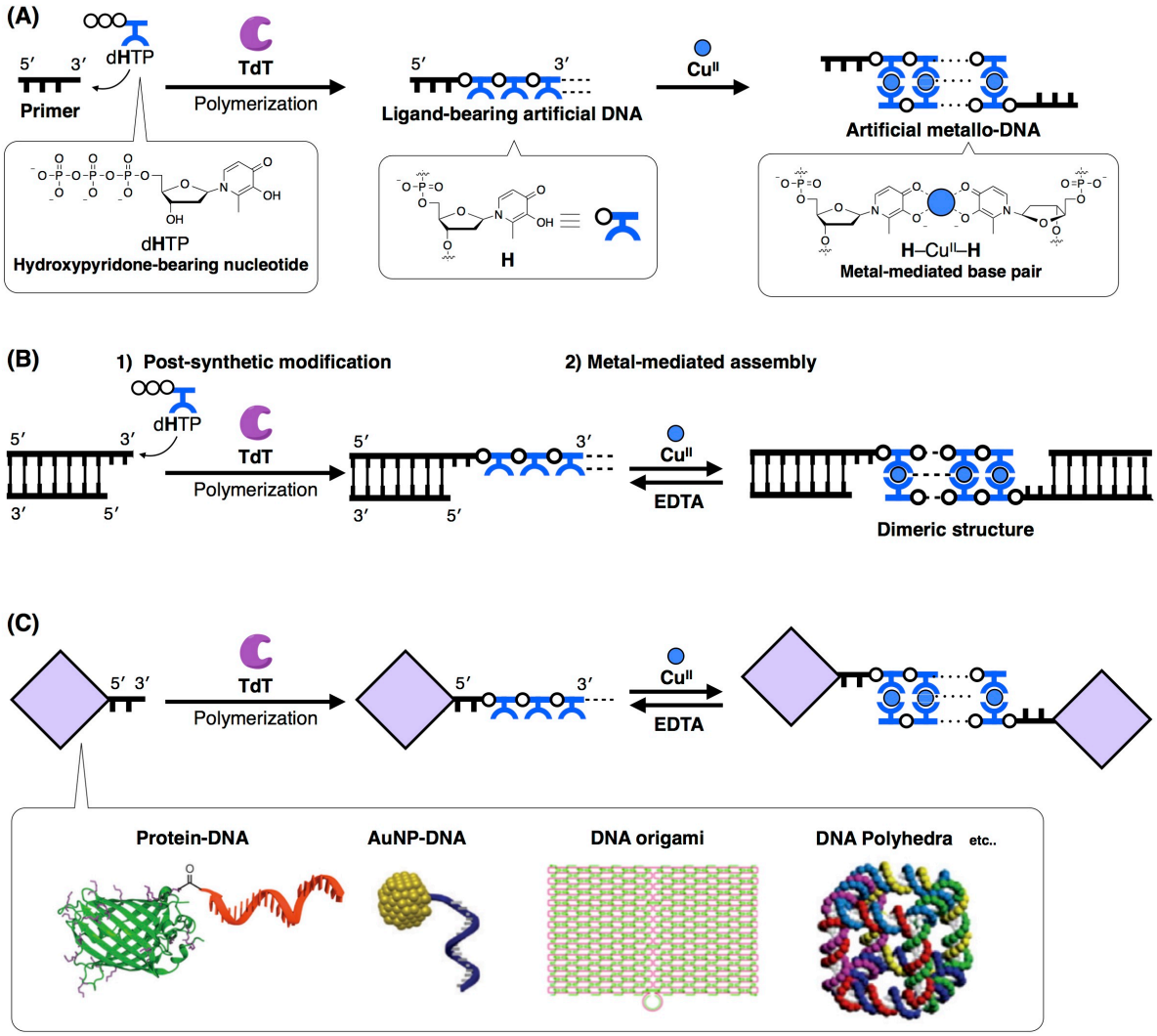


**Fig. 4-1-1**. Schematic representation for **(A)** TdT-mediated synthesis of an artificial metallo-DNA, **(B)** post-synthetic modification of a simple DNA duplex and metal-mediated assembly of a duplex and **(C)** post-synthetic modification of DNA nanoconjugates. Protein-DNA conjugates (ref. 20), AuNP-DNA conjugates (ref. 8), DNA origami structures (ref. 21) and DNA polyhedral (ref. 22) are taken as examples. Their figures are reproduced with ref. 8 and ref. 20–22. Copyright 1996 Nature Publishing Group. Copyright 2006 Nature Publishing Group. Copyright 2010 Annual Reviews. Copyright 2014 Nature Publishing Group.

By utilizing the metal-mediated assembly, the DNA-nanoconjugates (i.e. protein and metallic nanoparticle, Fig. 4-1-1C) will be ordered with well-controlled spatial configuration to regulate distance-dependent interactions and substance transport in response to metal ion

stimuli, in light of the fact that DNA nanostructures (i.e. DNA origami and polyhedra, Fig. 4-1-1C) are promising scaffolds to array biomolecular and inorganic functional components at nanometer scale.

I expected that the enzymatic synthesis of **H** oligomers would be applied to post-synthetic and site-selective modification of the DNA-based nanoconjugates to endow a metal-responsive property leading to future supramolecular nanodevices and nanomachines.

## 4-2. Metal complexation study of the enzymatically synthesized DNA mixture

One of the practical advantages of TdT-catalyzed DNA synthesis is its ability to accept post-synthetic modification of DNA-based materials. However, TdT-catalyzed reaction normally generates some distribution in the chain-length of product oligomers (**Chapter 3**, Fig. 3-2-1). In **Chapter 3**, I confirmed that the isolated artificial DNA possessing five **H** nucleotides (5′-FAM-$dT_{20}$-$\mathbf{H}_5$-3′, **ODN-1**) quantitatively formed metal-mediated **H**–$Cu^{II}$–**H** base pairs to produce a metallo-DNA duplex. In order to increase simplicity and convenience of the enzymatic synthesis toward further applications, the formation of metallo-DNA duplex with the ligand-bearing DNA mixture (5′-FAM-$dT_{20}$-$\mathbf{H}_n$-3′, $n$ = 3, 4, 5...) was investigated without isolation of each oligomer.

The mixture of the enzymatically-synthesized DNA strands possessing about 4.3 **H** nucleotides on average was combined with 2.2 equiv. of $Cu^{II}$ ions (i.e. 0.5 equiv. per **H** nucleotide) in a pH 7.0 buffer. As shown in Fig. 4-2-1, a characteristic absorption band newly appeared around 303 nm (black solid line), indicating that the **H**–$Cu^{II}$–**H** complex was formed (i.e. a 2:1 complex of the **H** nucleosides and a $Cu^{II}$ ion).

A difference spectrum (red line, Fig. 4-2-2) of the complexation product and the primer strand was consistent with a spectrum of 2.2 equiv. of the **H**–$Cu^{II}$–**H** complex (blue line). This result suggests that the metal-mediated **H**–$Cu^{II}$–**H** base pairs were quantitatively formed to provide a metallo-DNA duplex structure in the same manner as the isolated **H**-oligomers **ODN-1**.

This result suggests that DNA strands tailed with **H** nucleotides quantitatively formed a mixed metal-mediated duplexes. Then, further experiment was carried out without the isolation of individual **H** oligomers.

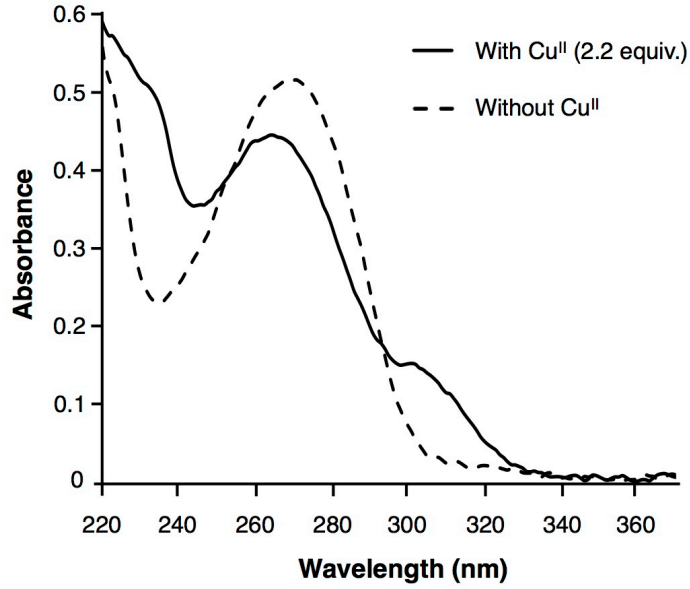


**Fig. 4-2-1** UV absorption spectral changes of the reaction mixture (30 $\mu$M) upon addition of Cu$^{II}$ ions. A spectrum with Cu$^{II}$ ions (65 $\mu$M, 2.2 equiv.) (solid line) and without Cu$^{II}$ ions (broken line), in 100 mM HEPES buffer (pH 7.0), 500 mM NaCl, $l$ = 0.1 cm, at room temperature. The concentration of the DNA was determined based on the absorbance of the FAM moiety ($\lambda$ = 495 nm).

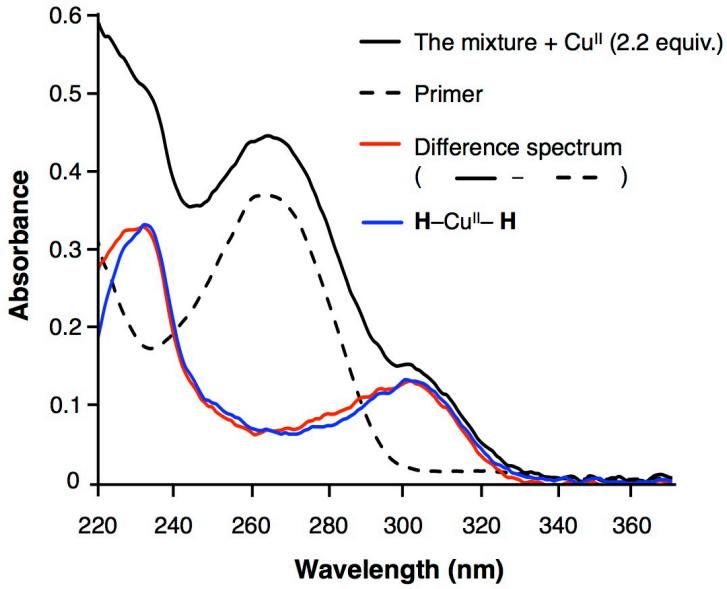


**Fig. 4-2-2** UV absorption spectra of the reaction mixture (30 $\mu$M) by addition of Cu$^{II}$ ions (black solid line). A spectrum of the primer (30 $\mu$M) (black broken line), difference spectra (red line) and a spectrum of the of **H**–Cu$^{II}$–**H** complex (65 $\mu$M) (blue line) are overlaid. In 100 mM HEPES buffer (pH 7.0), 500 mM NaCl, $l$ = 0.1 cm, at room temperature. The concentration of the DNA was determined based on the absorbance of the FAM moiety ($\lambda$ = 495 nm).

## 4-3. Post-synthetic modification of DNA duplexes by TdT

### 4-3-a. Enzymatic modification of DNA duplexes with H nucleotides

As mentioned in **4-1** and **4-2**, the post-synthetic incorporation of artificial ligand-bearing nucleotides by TdT would be a powerful tool to endow DNA hybrid materials with metal-responsive properties. In this section, the enzymatic modification with **H** nucleotides examined using a simple DNA duplex, consisting of a 22-mer primer (**ODN-2**) and a complementary 20-mer strand (**ODN-3**) (Table 4-3-1).

**Table 4-3-1** Sequences of DNA strands used for the duplex modification.

| Name | Length | Sequence |
|---|---|---|
| **ODN-2** | 22 mer | 5′-FAM-GAA GGA ACG TAC ACT CGC AGT T-3′ |
| **ODN-3** | 20 mer | 5′-CTG CGA GTG TAC GTT CCT TC-3′ |
| **ODN-4** | 20 mer | 5′-FAM-GAA GGA ACG TAC ACT CGC AG-3′ |

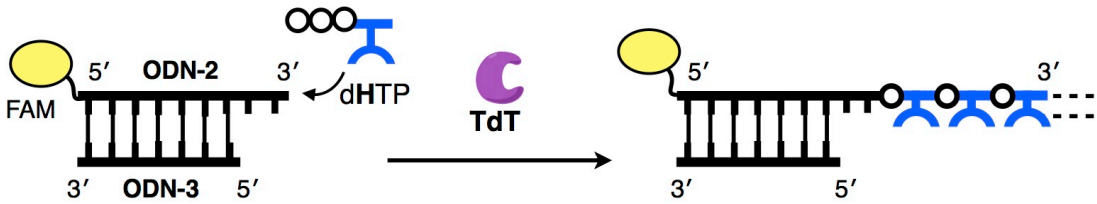


**Fig. 4-3-1** Schematic illustration of enzymatic modification of a DNA duplex with 3'-protruding end.

The duplex (**ODN-2·ODN-3**) has a 3′-protruding end (2 mer) as the starting point of the TdT-catalyzed reaction (Fig. 4-3-1). After incubation for 24 h with 20 equiv. of d**H**TP, the reaction products were analyzed by denaturing polyacrylamide gel electrophoresis (PAGE) (Fig. 4-3-2). Prior to the gel electrophoresis, the duplexes were dissociated to individual single-stranded DNAs. Since the bands on the gel were detected by the fluorescence of the FAM label moiety, only the FAM-labeled primer strands (**ODN-2** and extended strands) were observed. The result showed that the triphosphate d**H**TP was efficiently appended to the primer (lane 2) and the resulting DNA product was tailed with 3–9 **H** nucleotides in a manner similar to the single-stranded primer (Fig. 3-2-1B, **Chapter 3**). The average number of the tailed **H** nucleotides was estimated to be ca. 5 based on the intensities of the gel images (Fig.

4-3-2). This result was almost consistent with the number estimated with UV absorption spectrum (ca. 5.5, Fig. 4-3-3).

Accordingly, the TdT-catalyzed enzymatic synthesis is expected to be applied for the incorporation of about 5 **H** nucleotides to the 3′-protruding end of the DNA duplex.

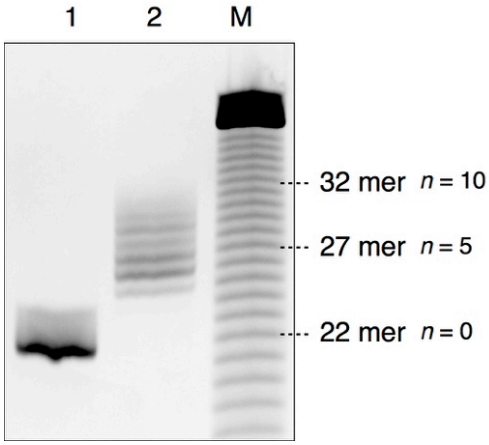


**Fig. 4-3-2** Denaturing PAGE analysis of the reaction products after TdT-catalyzed duplex modification with **H** nucleotides. (Lane 1) Starting material (duplex **ODN-2**·**ODN-3**), (lane 2) the reaction products, (M) single-stranded DNA ladder marker. Since the bands were detected by the fluorescence of the FAM moiety, only the FAM-labeled strands (**ODN-2** and extended ones) were observed. [**ODN-2**·**ODN-3**] = 5.0 $\mu$M, [d**H**TP] = 100 $\mu$M, [TdT] = 2 U/$\mu$L in 20 mM Tris-acetate buffer (pH 7.9), 10 mM $Mg(OAc)_2$, 50 mM KOAc, 37 °C, 24 h.

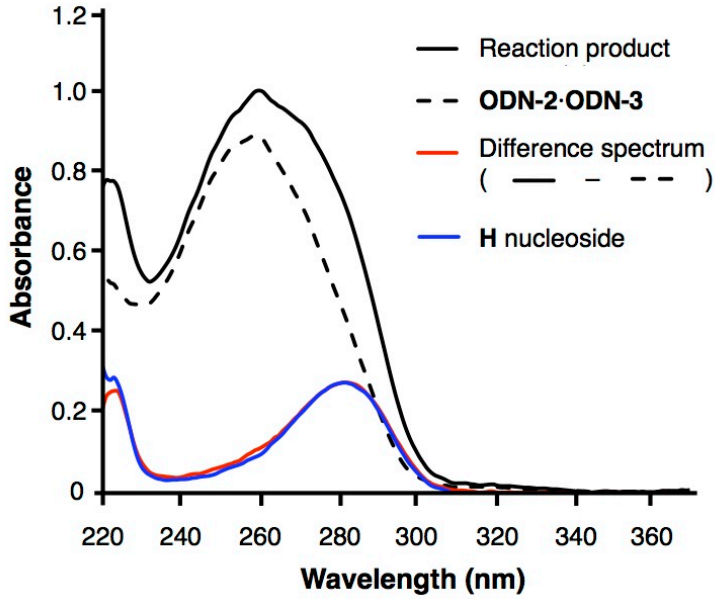


**Fig. 4-3-3** UV absorption spectrum of the modified DNA duplexes. (Black solid line) the reaction product (32 $\mu$M), (black broken line) the starting material (duplex **ODN-2**·**ODN-3**) (32 $\mu$M), (red line) a difference spectrum, (blue line) **H** nucleoside monomer (175 $\mu$M) in 100 mM HEPES buffer (pH 7.0), 500 mM NaCl, $l$ = 0.1 cm, at room temperature. The concentration of the DNA was determined based on the absorbance of the FAM moiety ($\lambda$ = 495 nm).

### 4-3-b. Metal complexation study of the modified DNA duplexes

With the **H**-modified duplex in hand, I examined metal-mediated assembly of the DNA duplex (Fig. 4-3-4).

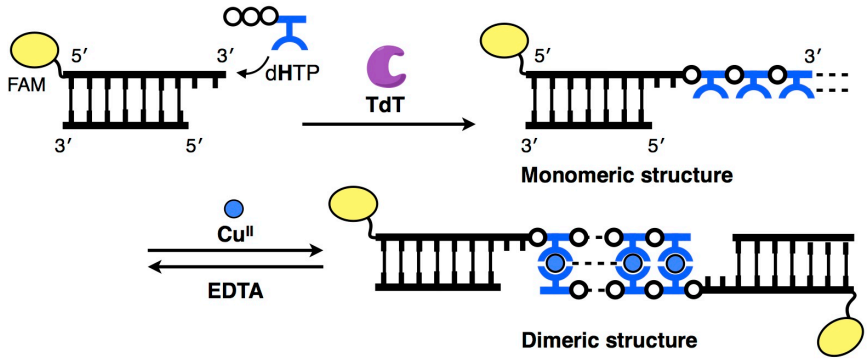


**Fig. 4-3-4** Schematic illustration of enzymatic modification of a DNA duplex and metal-triggered assembly of the duplexes.

As shown in Fig. 4-3-5, when 2.8 equiv. of $Cu^{II}$ ions were added (i.e. 0.5 equiv. per **H** nucleotide), the UV spectral changes showed that absorption band newly appeared around 303 nm (black solid line). This indicated the formation of the **H**–$Cu^{II}$–**H** complex, i.e. a 2:1 complex of the **H** nucleosides and a $Cu^{II}$ ion. A difference spectrum (red line) of the complexation product and the original duplex (**ODN-2·ODN-3**) was well fitted with a spectrum of 2.8 equiv. of the **H**–$Cu^{II}$–**H** complex (blue line). This result confirmed that the metal-mediated **H**–$Cu^{II}$–**H** base pairs were quantitatively formed in the same manner as Fig. 4-2-3.

The assembly of the DNA duplexes was monitored by native PAGE analysis. Upon addition of $Cu^{II}$ ions, the band on the gel image shifted to a higher molecular weight (Fig. 4-3-6, lane 3). The shift corresponds approximately to twice as much as the molecular weight of the metal-free duplex (described as a "monomeric structure" in Fig. 4-3-4). This indicates that a dimeric structure was formed through the metal-mediated **H**–$Cu^{II}$–**H** base pairing.

Subsequently, 31 equiv. of EDTA was added to the sample solution to remove $Cu^{II}$ ions. The corresponding band appeared at the original position on the gel, clearly indicating that the original monomeric duplex **ODN-2·ODN-3** tailed with **H** nucleotides was regenerated (lane 4).

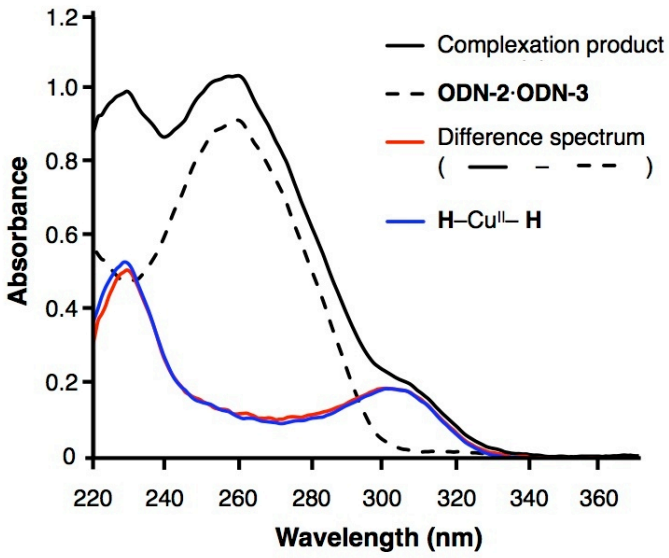


**Fig. 4-3-5** UV absorption spectrum of the complexation product. (Black solid line) the complexation product (32 $\mu$M duplex + 90 $\mu$M $Cu^{II}$), (black broken line) the original duplex (**ODN-2·ODN-3**) (32 $\mu$M), (red line) a difference spectrum, (blue line) **H**–$Cu^{II}$–**H** complex (175 $\mu$M **H** nucleotide + 90 $\mu$M $Cu^{II}$) in 100 mM HEPES buffer (pH 7.0), 500 mM NaCl, $l$ = 0.1 cm, at room temperature. The concentration of the DNA was determined based on the absorbance of the FAM moiety ($\lambda$ = 495 nm).

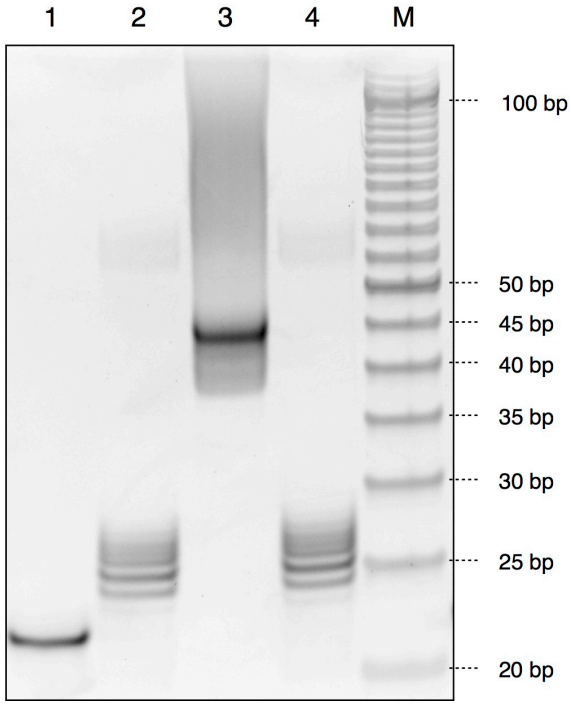


**Fig. 4-3-6** Native PAGE analysis of the resulting structures. (Lane 1) the starting duplex (**ODN-2·ODN-3**), (lane 2) after the enzymatic reaction, (lane 3) after addition of 2.8 equiv. of $Cu^{II}$ ions, (lane 4) after subsequent addition of 31 equiv. of EDTA and (lane M) double-stranded DNA markers. The bands of lanes 3–4 were detected by FAM fluorescence. The FAM-free marker was stained by SYBR Gold. **ODN-2**: FAM-5′-GAA GGA ACG TAC ACT CGC AGT T-3′ (22 mer), **ODN-3**: 5′-CTG CGA GTG TAC GTT CCT TC-3′ (20 mer). The condition of the enzymatic reaction is described with Fig. **4-3-2**.

In contrast, the unmodified duplex (**ODN-2·ODN-3**), not possessing **H** nucleotides, showed almost no changes upon addition of $Cu^{II}$ ions on the UV spectra and even on the gel images (Fig. 4-3-7). These results confirmed that the metal-mediated assembly of DNA duplexes was caused by the metal complexation of the tailed **H** nucleotides.

Collectively, the assembly and disassembly of DNA duplexes mediated by metal coordination were clearly demonstrated with the enzymatically synthesized ligand-bearing DNA duplexes.

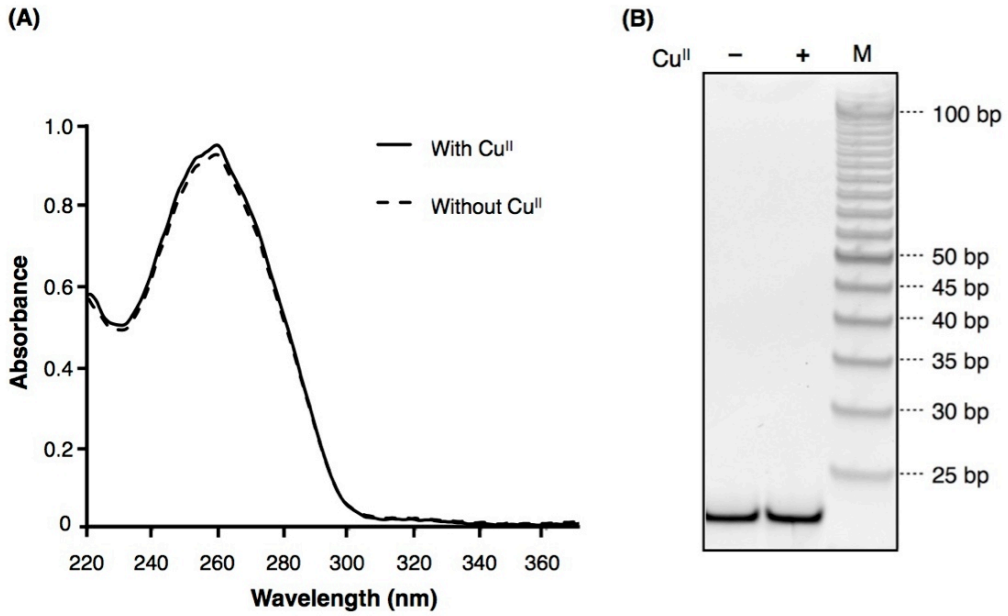


**Fig. 4-3-7** Metal complexation studies with the unmodified DNA duplex (**ODN-2·ODN-3**). [Duplex] = 32 $\mu$M, [$CuSO_4$] = 0, 90 $\mu$M in 100 mM HEPES buffer (pH 7.0), 500 mM NaCl. **(A)** UV spectral analysis. (Solid line) with $Cu^{II}$ ions, (broken line) without $Cu^{II}$ ions, $l$ = 0.1 cm, at room temperature. **(B)** Native PAGE analysis. (M) Double-stranded DNA markers.

### 4-3-c. Site-selectivity of the TdT-catalyzed modification of DNA duplexes

TdT polymerase is known to add nucleotide triphosphates only to the 3′-protruding end. To confirm the site-selective tailing with **H** nucleotides, an enzymatic reaction was carried out with a blunt-end 20-bp duplex **ODN-4·ODN-3** as a control experiment (the sequences are shown in Table 4-3-1). This duplex has no 3′-protruding ends as a starting point of the TdT reaction.

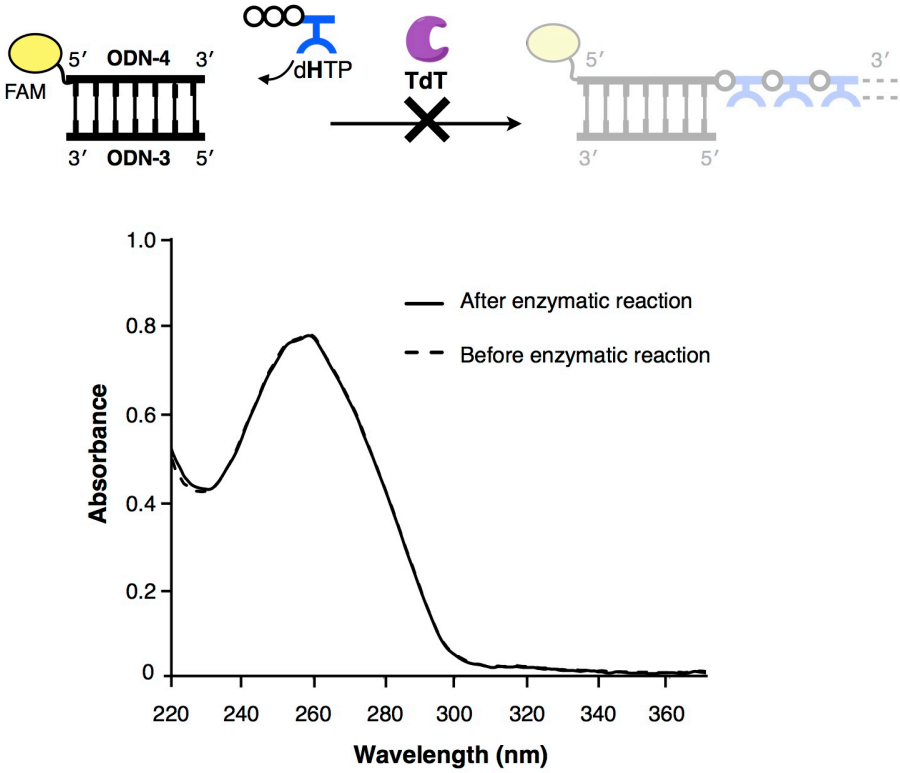


**Fig. 4-3-8** Enzymatic reaction using a blunt-end DNA duplex (**ODN-4·ODN-3**). The reaction condition was the same as Fig. 4-3-2. UV spectral analysis (solid line) after (broken line) and before enzymatic reaction, $l$ = 0.1 cm, at room temperature.

UV absorption spectra of the duplex showed almost no changes between before and after the enzymatic reaction (Fig. 4-3-8), indicating that no **H** nucleotides were added to the duplex by TdT polymerase. The native PAGE analysis evidently showed that the blunt-end duplex was not modified by the enzyme (Fig. 4-3-9, lanes 1 and 2). Furthermore, subsequent treatment with $Cu^{II}$ ions and EDTA did not lead to the assembly of DNA duplexes (lanes 3 and 4). These results clearly demonstrated that the

TdT appended the **H** nucleotides at the 3′-protruding end of DNA duplexes site-selectively.

Accordingly, I expect that the TdT-mediated reactions with **H** nucleotides would be a promising tool to incorporate **H** nucleotides site-selectively into the 3′-protruding moiety of high-dimensional DNA nanostructures such as DNA origami. By utilizing the reaction, metal responsive properties (as mentioned in section **4-1**) will be endowed with the DNA-based nanomaterial.

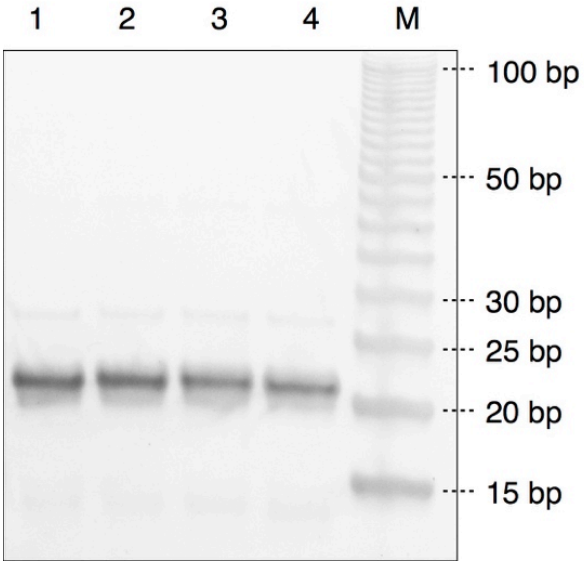


**Fig. 4-3-9** Control experiments using a blunt-end DNA duplex (**ODN-4**·**ODN-3**). Native PAGE analysis. (Lane 1) the starting duplex (**ODN-4**·**ODN-3**), (lane 2) after enzymatic reaction, (lane 3) after addition of $Cu^{II}$ ions, (lane 4) after subsequent addition of EDTA and (lane M) double-stranded DNA markers. The bands were detected by FAM fluorescence. The conditions of the enzymatic reaction and the metal complexation are the same as for Fig. 4-3-6.

## 4-4. Stability of the DNA-based dimeric structure

Because the TdT-mediated polymerization products have distribution of a molecular length as shown above, it is not easy to add precise concentration of $Cu^{II}$ ions to **H**-modified DNA duplexes ("monomeric structure"). Thus, the stability of the complexation products ("dimeric structure") in the presence of excess $Cu^{II}$ ions was investigated by the titration experiment (Fig. 4-4-1).

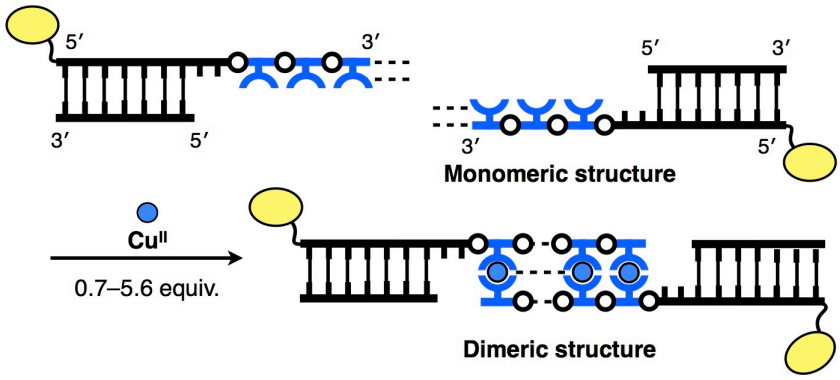


**Fig. 4-4-1** Schematic illustration of titration experiment with **H**-modified duplexes.

To **H**-modified DNA duplexes possessing ca. 5.5 **H** in average (Fig. 4-4-2A), 0.7–2.8 equiv. of $Cu^{II}$ ions were added (i.e. 0.1–0.5 equiv. per **H** nucleotide). Native PAGE analysis showed that the band on the gel image moved from lower position (monomeric structure) to upper position (dimeric structure) upon $Cu^{II}$ addition (lane 1–5, Fig. 4-4-2A). The population of the dimeric structures increased in a linear fashion in the range of 0 to 2.8 equiv of $Cu^{II}$ ions (Fig. 4-4-2B). With 2.8 equiv. of $Cu^{II}$ ions, the monomeric structure was completely converted to the dimeric structure (lane 5, Fig. 4-4-2A). When 3.4–5.6 equiv. of $Cu^{II}$ ions were added, the band of the dimeric structure no longer changed in the presence of excess amounts of $Cu^{II}$ ions (i.e. 0.6–1.0 equiv. per **H** nucleotide). This stoichiometric complexation behavior was almost the same as the metal complexation of chemically-synthesized $\mathbf{H}_5$ oligomers (5′-G$\mathbf{H}_n$C-3′, $n$ = 1–5).[23] This result further supports the quantitative formation of **H**–$Cu^{II}$–**H** base pairs.

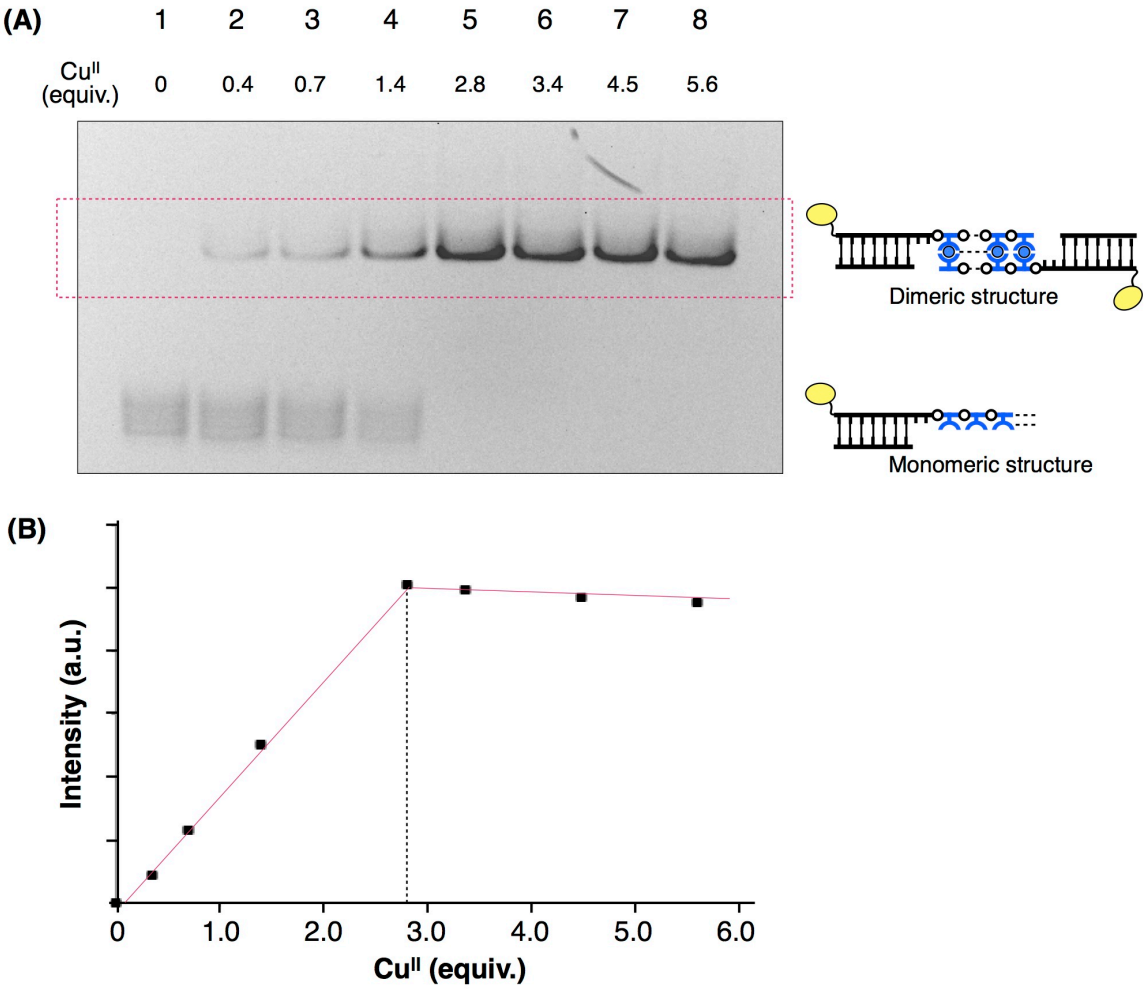


**Fig. 4-4-2 (A)** Native PAGE analysis of the stability of the dimeric structure after titration of $Cu^{II}$ ions to the monomeric structure (3 $\mu$M) in 10 mM HEPES buffer (pH 7.0), 50 mM NaCl. (Lane 1) before addition of $Cu^{II}$ ions, (lane 2) after addition of 0.4 equiv., (lane 3) 0.7 equiv., (lane 4) 1.4 equiv., (lane 5) 2.8 equiv., (lane 6) 3.4 equiv., (lane 7) 4.5 equiv., (lane 8) 5.6 equiv. of $Cu^{II}$ ions. The bands were detected by FAM fluorescence. **(B)** Plot of the intensity of the bands against the ratio of [$Cu^{II}$] to [DNA duplex].

The amount of EDTA required for the disassembly of the dimeric structure was then estimated by titration experiments. Different amounts of EDTA were added to the $Cu^{II}$-mediated dimer. After incubation for 1 h, the samples were subjected to native PAGE analysis (Fig. 4-4-3). Addition of 2.8 equiv. of EDTA (i.e. 1.0 equiv. per **H**–$Cu^{II}$–**H** base pair) little affected the dimeric structure (lane 2). Excess amount of EDTA (~28 equiv.) was required to regenerate the monomeric structure (lane 5).

The **H**–$Cu^{II}$–**H** base pairs might be reinforced cooperatively by interactions of surrounding base pairs (i.e. hydrogen bonding, π-π stacking etc.) in the hydrophobic environment inside

the DNA duplex. Thus, excess EDTA (i.e. 10 equiv. per **H**–$Cu^{II}$–**H** base pair) was needed to remove $Cu^{II}$ ions from the metal-mediated base pairs.

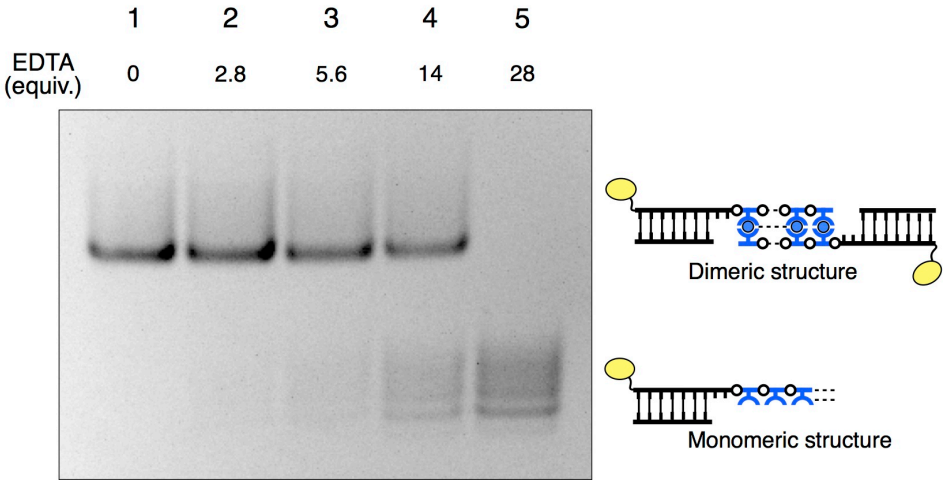


**Fig. 4-4-3** Native PAGE analysis of the regeneration of the monomeric structure after titration of EDTA to the dimer (3 $\mu$M) in 10 mM HEPES buffer (pH 7.0), 50 mM NaCl. (Lane 1) before addition of EDTA, (lane 2) after addition of 2.8 equiv., (lane 3) 5.6 equiv., (lane 4) 14 equiv and (lane 5) 28 equiv. The bands were detected by FAM fluorescence.

Taken together, I found that the dimeric structure possessing the **H**–$Cu^{II}$–**H** base pairs are stable even in the presence of excess amounts of $Cu^{II}$ ions, and that the complexation structure was completely dissociated by addition of EDTA. This result revealed the metal-responsive behaviors of DNA containing **H**–$Cu^{II}$–**H** base pairs.

Considering that the **H**–$Cu^{II}$–**H** base pairs quantitatively formed without isolation of individual **H** oligomers, I expect it will be easy to conduct metal-responsive assembly of DNA-based functionalized molecules by utilizing the enzymatic modification method established here.

## 4-5. Conclusion

To demonstrate the usability of the enzymatic synthesis of artificial metallo-DNAs, firstly, I have investigated the TdT-catalyzed incorporation of d**H**TP into the 3′-end of DNA duplexes. This study revealed that only a protruding-end duplex can be tailed with artificial **H** nucleotides. This result suggests that the site-selective modification of DNA nanostructures with ligand-bearing nucleotides by TdT polymerase possibly endow them with metal-responsive properties.

By subsequent addition of $Cu^{II}$ ions, modified DNA duplexes possessing **H** nucleotides self-assembled to form their dimeric structures quantitatively through metal-mediated **H**–$Cu^{II}$–**H** base pairing. The dimeric structures were dissociated to regenerate the monomeric DNA duplexes by excess amounts of EDTA. This result suggests that the enzymatically modified DNA duplexes formed stable complex structures in response to metal ion stimuli.

From this result of the modification method established here, I expect construction of metal-responsive nanodevices driven by changing geometry and spatial configuration of functional components on the DNA scaffolds.

## 4-6. Experimental

### Materials and methods

Natural DNA primer strands including 6-carboxyfluorescein (FAM)-labeled ones were purchased from Japan Bio Service Co., Ltd. in HPLC purification grade. Terminal deoxynucleotidyl transferase (TdT) was purchased from New England Biolabs, Inc. The FAM-labeled single-stranded DNA ladder marker was prepared by the treatment of a FAM-labeled $T_{38}$ oligomer with DNase I (Promega). The double-stranded marker (10–100 bp) was purchased from Thermo Fisher Scientific and detected after staining with SYBR Gold dye (Thermo Fisher Scientific). Matrix assisted laser desorption ionization-time-of-flight (MALDI-TOF) mass spectra were recorded on Bruker ultrafleXtreme. UV spectra were measured using Thermo Scientific NanoDrop 2000 spectrophotometer with a path length of 0.1 cm. Denaturing polyacrylamide gel electrophoresis (PAGE) was carried out with 21% polyacrylamide gel with 7 M urea. Native PAGE was performed with 20% gel in an EDTA-free buffer (90 mM Tris, 90 mM boric acid, 50 mM NaCl, pH 8.3) at 10–15 °C. The gels were analyzed using Alpha imager mini (LMS) and a blue-LED (470 nm) transilluminator (Optocode).

### Metal complexation of the enzymatically synthesized DNA mixture

A ligand-bearing DNA mixture (32 μM, 5′-FAM-$dT_{20}$-$\mathbf{H}_n$-3′, $n$ = 3, 4, 5...) (cf. section **3-2**, **Chapter 3**) was mixed with 2.2 equiv. of $CuSO_4$ (65 μM) in a 100 mM HEPES buffer (pH 7.0) containing 500 mM NaCl. After incubation at 25 °C for 1 h, UV absorption was measured at room temperature. The concentration of the DNA was determined based on the absorbance of the FAM moiety ($\lambda$ = 495 nm, $\varepsilon_{495}$ = 3.75 × $10^4$ $M^{-1}$ $cm^{-1}$ at pH 7.0).

### Post-synthetic modification of DNA duplexes with H nucleotides by TdT

Enzymatic modification of simple DNA duplexes with **H** nucleotides was investigated using **ODN-2**·**ODN-3** (see Table 4-3-1 for the sequences). Prior to the

reaction, two DNA strands in the reaction buffer was heated at 85 °C for 5 min, followed by slow cooling to 4 °C (–1 °C/min) to form a duplex. After addition of d**H**TP and TdT, the mixture was incubated at 37 °C for 24 h. The total volume was 20 μL and the final concentration of each component was as follows: 2 U/μL TdT, 5 μM duplex, 100 μM d**H**TP (20 equiv.). The reaction was quenched by EDTA (20 μL, 500 mM) on ice. After isopropanol precipitation, the products were desalted by gel filtration chromatography (Sephadex G-25 Fine, GE Healthcare).

The reaction products were then analyzed by native PAGE as well as denaturing PAGE. Prior to the denaturing PAGE analysis, the sample was mixed with an equal volume of 10 M urea and heated at 95 °C for 5 min to denature the duplexes. The average extension length was estimated based on the integrated intensity of the bands.

UV spectral analysis was further performed to verify the incorporation of **H** nucleotides. The desalted reaction products were dissolved in a 100 mM HEPES buffer (pH 7.0) solution containing 500 mM NaCl and subjected to the UV measurements at room temperature. The concentration of the DNA was determined based on the absorbance of the FAM moiety ($\lambda$ = 495 nm, $\varepsilon_{495} = 3.75 \times 10^4$ $M^{-1}$ $cm^{-1}$ at pH 7.0).

### Control experiments to investigate site-selectivity of the modification

A blunt-end 20-bp duplex **ODN-4·ODN-3** (see Table 4-3-1 for the sequences) was subjected to the same procedure as mentioned above.

### Metal complexation of the modified DNA duplexes

The DNA duplexes tailed with **H** nucleotides (32 μM) were mixed with 2.8 equiv. of $CuSO_4$ (90 μM) in a HEPES buffer (pH 7.0) containing 500 mM NaCl. After incubation at 25 °C for 1 h, the UV spectra were measured at room temperature. The complexation product was further analyzed by native PAGE. Subsequently, the sample

was treated with excess EDTA (1 mM) to remove $Cu^{II}$ ions and then analyzed by native PAGE.

### Titration experiment of $Cu^{II}$ ions with the enzymatically modified duplex

The DNA duplexes tailed with **H** nucleotides (3 μM) were mixed with different concentrations of $CuSO_4$ (1, 2, 4, 8, 10, 14 and 17 μM) in a 10 mM HEPES buffer (pH 7.0) containing 50 mM NaCl. After incubation at 25 °C for 1 h, the complexation products were analyzed by native PAGE. The band intensities were quantified using ImageJ (NIH).

### Titration experiment of EDTA with the complexation product

The DNA duplexes tailed with **H** nucleotides (3 μM) were mixed with 2.8 equiv. of $CuSO_4$ (8 μM) in a 10 mM HEPES buffer (pH 7.0) solution containing 50 mM NaCl. After incubation at 25 °C for 1 h, the complexation product was mixed with different concentrations of EDTA (90, $1.8 \times 10^2$, $4.5 \times 10^2$, $9.0 \times 10^2$ μM). After incubation at 25 °C for 1 h, the mixtures were analyzed by native PAGE.

## 4-7. References


1. A. Kuzuya, M. Kimura, K. Numajiri, N. Koshi, T. Ohnishi, F. Okada and M. Komiyama, *ChemBioChem*, 2009, **10**, 1811–1815.

2. N. V. Voigt, T. Tørring, A. Rotaru, M. F. Jacobsen, J. B. Ravnsbæk, R. Subramani, W. Mamdouh, J. Kjems, A. Mokhir, F. Besenbacher and K. V. Gothelf, *Nat. Nanotechnol*., 2010, **5**, 200–203.

3. N. Stephanopoulos, M. H. Liu, G. J. Tong, Z. Li, Y. Liu, H. Yan and M. B. Francis, *Nano Lett*., 2010, **10**, 2714–2720.

4. M. Langecker, V. Arnaut, T. G. Martin, J. List, S. Renner, M. Mayer, H. Dietz and F. C. Simmel, *Science*, 2012, **338**, 932–936.

5. A. Kuzyk, R. Schreiber, Z. Fan, G. Pardatscher, E.-M. Roller, A. Hogele, F. C. Simmel, A. O. Govorov and T. Liedl, *Nature*, 2012, **483**, 311–314.

6. J. Zheng, P. E. Constantinou, C. Micheel, A. P. Alivisatos, R. A. Kiehl and N. C. Seeman, *NanoLett*., 2006, **6**, 1502–1504.

7. J. Fu, Y. R. Yang, A. Johnson-Buck, M. Liu, Y. Liu, N.G. Walter, N. W. Woodbury and H. Yan, *Nat. Nanotechnol*., 2014, **9**, 531−536.

8. A. P. Alivisatos, K. P. Johnson, X. G. Peng, T. E. Wilson, C. J. Loweth, M. P. Bruchez and P. G. Schultz, *Nature*, 1996, **382**, 609–611.

9. A. J. Mastroianni, S. A. Claridge and A. P. Alivisatos, *J. Am. Chem. Soc*., 2009, **131**, 8455–8459.

10. H. Y. Li, S. H. Park, J. H. Reif, T. H. LaBean and H. Yan, *J. Am. Chem. Soc*., 2004, **126**, 418–419.

11. Y. Y. Pinto, J. D. Le, N. C. Seeman, K. Musier-Forsyth, T. A. Taton and R. A. Kiehl, *NanoLett*., 2005, **5**, 2399–2402.

12. (a) C. K. McLaughlin, G. D. Hamblin and H. F. Sleiman, *Chem. Soc. Rev*., 2011, **40**, 5647–5656; (b) H. Li, T. H. LaBean and K. W. Leong, *Interface Focus*, 2011, **1**, 702–724; (c) A. Kuzuya and Y. Ohya, *Polymer Journal*, 2012, **44**, 452–460.

13. Y. R. Yang, Y. Liu and H. Yan*, Bioconjugate Chem.*, 2015, **26**, 1381−1395.

14. (a) Y. Takezawa and M. Shionoya, *Acc. Chem. Res.*, 2012, **45**, 2066–2076; (b) P. Scharf and J. Müller, *ChemPlusChem*, 2013, **78**, 20–34.

15. (a) S. Keller and A. Marx, *Chem. Soc. Rev.*, 2011, **40**, 5690–5697; (b) D. Yang, M. R. Hartman, T. L. Derrien, S. Hamada, D. An, K. G. Yancey, R. Cheng, M. Ma, and D. Luo, *Acc. Chem. Res.*, 2014, **47**, 1902−1911

16. (a) F. E. Alemdaroglu, J. Wang, M. Börsch, R. Berger and A. Herrmann, *Angew. Chem., Int. Ed.*, 2008, **47**, 974–976; (b) J. Wang, F. E. Alemdaroglu, D. K. Prusty, A. Herrmann and R. Berger, *Macromolecules*, 2008, **41**, 2914–2919.

17. A. H. Okholm, H. Aslan, F. Besenbacher, M. Dong and J. Kjems, *Nanoscale*, 2015, **7**, 10970–10973.

18. A. M. Michelson and S. H. Orkin, *J. Biol. Chem.*, 1982, **257**, 14773–14782.

19. (a) D. P. Steensma, M. Timm and T.E. Witzig, *Methods Mol. Med.*, 2003, **85**, 323–332; (b) W. Gorczyca, J. Gong and Z. Darzynkiewicz, *Cancer Res.*, 1993, **53**, 1945–1951.

20. C. B. Rosen, L. B. K. Anne, J. S. Nielsen, D. H. Schaffert, C. Scavenius, A. H. Okholm, N. V. Voigt, J. J. Enghild, J. Kjems and T. Tørring, *Nat. Chem.*, 2014, **6**, 804−809.

21. P. W. K. Rothemund, *Nature*, 2006, **440**, 297–302.

22. N. C. Seeman, *Annu. Rev. Biochem.*, 2010, **79**, 65–87.

23. K. Tanaka, A. Tengeiji, T. Kato, N. Toyama and M. Shionoya, *Science*, 2003, **299**, 1212–1213.

# Chapter 5

# Conclusion

The present thesis describes the enzymatic synthesis of artificial metallo-DNAs utilizing template-independent DNA polymerases (TdT) (Fig. 5-1).

The synthetic strategy using TdT is as follows: **(1)** TdT catalyzes the polymerization of the hydroxypyridone-bearing nucleotide triphosphate (d**H**TP) into a DNA primer to extend the ligand-bearing artificial DNA possessing hydroxypyridone-bearing nucleotide(s) (**H**), and **(2)** subsequently the enzymatically synthesized DNA forms metal-mediated base pairs (**H**–$Cu^{II}$–**H**) to provide an artificial metallo-DNA duplex.

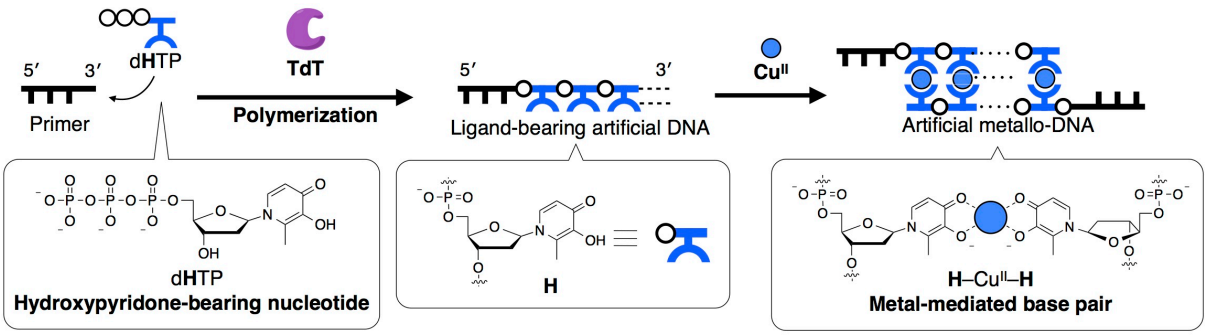


**Fig. 5-1** Schematic representation for enzymatic synthesis of artificial metallo-DNAs utilizing template-independent DNA polymerases (TdT).

The results are summarized as follows.

In **Chapter 2**, the synthesis of a triphosphate derivative of the hydroxypyridone-bearing nucleotide (d**H**TP) is described. The 5′-phosphorylation of a hydroxypyridone-bearing nucleoside produced d**H**TP via conventional Eckstein method. The reaction afforded not only a triphosphate d**H**TP but also a nucleoside monophosphate. Utilizing the charge difference, d**H**TP was successfully purified and isolated from the mixture using anion-exchange column chromatography. Compared with the previous work, the isolation and purification methods of d**H**TP were improved in this study to provide highly pure **H**TP for enzymatic reactions.

In **Chapter 3**, I demonstrated the enzymatic synthesis of the ligand-bearing artificial DNA for metal-mediated base pairing. The enzymatic incorporation of d**H**TP into a single-stranded primer was investigated using a template-independent DNA polymerase, TdT. PAGE analysis of the products revealed that TdT catalyzed the sequential polymerization of d**H**TP,

which provided the artificial DNAs tailed with **H** nucleotides. One of the main products possessing 5 **H** nucleotides (**ODN-1**) was isolated and identified by MALDI-TOF mass spectrometry. UV absorption analysis under neutral and basic conditions evidently showed that the **H** nucleotides on the **ODN-1** were deprotonated. These results established that **(1)** the ligand-bearing DNA can be synthesized by TdT enzyme and **(2)** the ligand moieties of the DNA stayed intact and thus will be able to complex with $Cu^{II}$ ions.

Subsequently, the complexation behavior of **ODN-1** with $Cu^{II}$ ions was examined in a neutral buffer. The UV spectral changes upon $Cu^{II}$ addition revealed that **ODN-1** quantitatively formed metal-mediated **H**–$Cu^{II}$–**H** base pairs to provide artificial metallo-DNA duplexes. This behavior was the same as a chemically synthesized **H** oligomer, which was previously reported. Thus, it was found that the enzymatically synthesized DNA can form metallo-DNA duplexes.

Meanwhile, I found that the TdT-catalyzed polymerization of d**H**TP stalled when about 5 **H** nucleotides were incorporated, which inhibited the synthesis of longer ligand-bearing DNAs. One hypothesis is that artificial DNA possessing several **H** nucleotides at the 3′-end have a low affinity to the enzyme and therefore halted the further elongation. The enzymatic reaction using **ODN-1** possessing 5 **H** nucleotides as a primer demonstrated that TdT polymerizes neither dTTP nor d**H**TP. In conclusion, **H**-tailed products did not act as the primer for further elongation to result in the termination of the polymerization.

The synthesis of longer ligand-bearing DNA strands has been in strong demand in terms of the application for the construction of DNA-based metal nanowires. Therefore, the reaction condition was optimized to facilitate further incorporation of d**H**TP. As a result, it was found that the reaction proceeded further with the high concentration of the DNA primer. PAGE, UV absorption and mass analyses confirmed that about 10 **H** nucleotides were polymerized to elongate the artificial DNA by TdT enzyme. It is most likely that increasing the concentration forced the DNA to bind the enzyme and consequently facilitated the reaction progress. Thus, the limitation in the length of the product was overcome and so the

synthesis of much longer ligand-bearing artificial DNAs would be realized by the synthetic method developed here.

In **Chapter 4**, post-synthetic modification of DNA duplexes with **H** nucleotides was discussed to verify the usability of the TdT-mediated enzymatic reactions (Fig. 5-2).

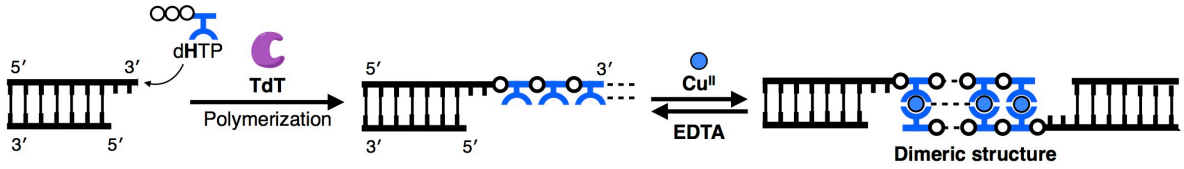


**Fig. 5-2** Schematic representation for post-synthetic modification of DNA duplexes and metal-mediated assembly of the enzymatically modified duplexes.

I carried out the reaction with simple DNA duplexes possessing a 3′-protruding end. PAGE analysis of the products revealed that only 3′-protruding end was tailed with about 5 **H** nucleotides. This result showed that the 3′-protruding end is essential to append **H** nucleotides to the DNA duplex. Therefore, it is expected that the TdT-catalyzed reaction will be usable for post-synthetic modification of the 3′-protruding end selectively on the DNA-based material.

Subsequently, $Cu^{II}$-mediated assembly of the modified duplexes was investigated. Without isolation of individual oligomers, the modified DNA duplex possessing 5 **H** nucleotides in average was mixed with $Cu^{II}$ ions. UV absorption and PAGE analyses showed that the duplexes formed dimeric structures through quantitative **H**–$Cu^{II}$–**H** base pairing. By removal of $Cu^{II}$ ions with EDTA, original DNA duplexes were regenerated from the dimeric structures. These results revealed that the modified duplex assembled and disassembled in response to addition and removal of $Cu^{II}$ ions. Moreover, for $Cu^{II}$-mediated assembly, the enzymatically modified duplexes did not require isolation of individual oligomer.

The enzymatic DNA synthetic method developed here allows post-synthetic and site-selective modification of DNA duplexes. This method has great potential to endow metal-responsive functions with DNA-based materials that can regulate the stability and

dynamics of DNA scaffolds, and thereby contribute to construction of DNA-based nanodevices and machines.

Furthermore, the enzymatic method would be expanded to other artificial ligand-bearing nucleotides with different metal affinity. The resulting metal-mediated base pairs will have different geometry, kinetics and dynamic functions through coordination bonding. As a result, it will diversify physicochemical properties of the DNA nanoarchitectures.

Therefore, I believe that the enzymatic synthesis developed in this study will open the door to future applications of artificial metallo-DNA in the field of DNA nanotechnology.

## A list of publications

(1) “鋳型非依存性 DNA ポリメラーゼを利用した金属配位子型人工 DNA オリゴマーの合成”, T. Kobayashi, *Bull. Jpn. Soc. Coord. Chem.* **2015**, *65*, 88–90.

(2) “Enzymatic Synthesis of Ligand-bearing DNAs for Metal-mediated Base Pairing Utilising a Template-independent Polymerase”, T. Kobayashi, Y. Takezawa, A. Sakamoto and M. Shionoya, *Chem. Commun.* **2016**, *in press.*

## Acknowledgement

During the voyage of discovery in the academia, I always walked with an absolute dream in science. I vividly remember the first day that I succeeded in the enzymatic synthesis (on November 12th, 2013) and rejoiced with my professors.

I would like to express my deepest appreciation to my supervisor Professor Mitsuhiko Shionoya and Assistant Professor Yusuke Takezawa. Since I moved from Tokyo Institute of Technology to the University of Tokyo, they always gave me sophisticated guidance and suggestions. I was deeply affected by their kindness. I am glad that I belong to the TAKEZAWA team in SHIONOYA Laboratory in the doctoral course.

I am also grateful to Associate Professor Shohei Tashiro for his valuable comments and kind help. I wish to thank Assistant Professor Hitoshi Ube for useful advice and instruction. Beyond our specialty, we lively discussed with each other about progress, novelty and advantages of our research. Consequently, I greatly enjoyed my life in this laboratory.

I am thankful to Mr. Yoshimitsu Hori for his assistance with MALDI-MS measurements. When I found out the signals of my desired compound for the first time, I danced and cried with joy in the experimental room.

I sincerely appreciate Professor Timothy J. Wright and Professor Evelyn J. Reinbold for training me in English communication and writing. Actually, when I was a first-year student in the doctoral course, I could not write or speak English very well at all. However, as a result of their intensive programs, I was able to complete this doctoral thesis and discuss about my research in English. I would like to grow up more to be a fine international scientist in the future.

I thank Mr. Hiroto Tamashima, Mr. Tomoya Ohyama, Mr. Yuji Kikuchi, Mr. Eiichi Watanabe and all of present and past members in IWASAWA KUSAMA laboratory (Tokyo Institute of Technology). When I belonged to Tokyo Institute of Technology, they kindly

trained and helped me in all the time of my research. I learned not only techniques, but also attitude to scientific research for the first time.

I thank all of present and past members in SHIONOYA Laboratory for their encouragement. My spirit bounded with hopeful joy, while I studied and interested with them during the three years. I am glad that I was able to meet them.

On the 20th anniversary of SHIONOYA Laboratory, I am honored to receive a doctorate in science at the University of Tokyo.

***Nothing gives me greater pleasure to spend the time with wonderful people.***

Finally, I would like to close by deeply thanking my mother, father, grandmothers, grandfathers and all my relatives who were always with me during my life in the academia.

Teruki Kobayashi

小林輝樹